AD NUMBER

AD888693

LIMITATION CHANGES

TO:

Approved for public release; distribution is unlimited.

FROM:

Distribution authorized to U.S. Gov't. agencies only; Administrative/Operational Use; OCT 1971. Other requests shall be referred to Aeronautical Systems Div., Wright-Patterson AFB, OH 45433.

AUTHORITY

ASD ltr 4 Aug 1977

RESULTS OF A 0.1-SCALE B-1 INLET MODEL TEST AT TRANSONIC AND SUPERSONIC MACH NUMBERS

F. J. Graham
ARO, Inc.

October 1971

PROPULSION WIND TUNNEL FACILITY
ARNOLD ENGINEERING DEVELOPMENT CENTER
AIR FORCE SYSTEMS COMMAND
ARNOLD AIR FORCE STATION, TENNESSEE

NOTICES

When U. S. Government drawings specifications, or other data are used for any purpose other than a definitely related Government procurement operation, the Government thereby incurs no responsibility nor any obligation whatsoever, and the fact that the Government may have formulated, furnished, or in any way supplied the said drawings, specifications, or other data, is not to be regarded by implication or otherwise, or in any manner licensing the holder or any other person or corporation, or conveying any rights or permission to manufacture, use, or sell any patented invention that may in any way be related thereto.

Qualified users may obtain copies of this report from the Defense Documentation Center.

References to named commercial products in this report are not to be considered in any sense as an endorsement of the product by the United States Air Force or the Government.

RESULTS OF A 0.1-SCALE B-1 INLET MODEL TEST AT TRANSONIC AND SUPERSONIC MACH NUMBERS

F. J. Graham
ARO, Inc.

FOREWORD

The work reported herein was done at the request of the Aeronautical Systems Division (ASD), Air Force Systems Command (AFSC), for North American Rockwell Corporation, Los Angeles, California, under Program Element 64215F, System 139A, Task 01A.

The results of the test were obtained by ARO, Inc. (a subsidiary of Sverdrup & Parcel and Associates, Inc.), contract operator of the Arnold Engineering Development Center (AEDC), AFSC, Arnold Air Force Station, Tennessee, under Contract F40600-72-C-0003. The tests were conducted from June 23 to July 20, 1971, under ARO Project No. PT0177. The manuscript was submitted for publication on September 3, 1971.

This technical report has been reviewed and is approved.

George F. Garey
Lt Colonel, USAF
AF Representative, PWT
Directorate of Test

Joseph R. Henry
Colonel, USAF
Director of Test

ABSTRACT

Results are presented of a wind tunnel investigation of a 0.1-scale model of the left-hand dual inlet air induction system of the B-1 aircraft. The test was conducted from Mach number 0.55 to 2.2 over an angle-of-attack range from -4 to 13 deg and yaw angles of -8 to 5 deg. Inlet performance in terms of compressor-face total-pressure recovery, total-pressure distortion, and turbulence index is presented as a function of inlet mass-flow ratios for various inlet geometries and model attitudes. The total-pressure recovery of the mixed-compression inlet was very good, but the total-pressure distortion at critical mass-flow ratios was higher than normally desired for satisfactory turbine engine operation. Best performance was realized with ramp and throat height schedules determined from previous testing. Effects of angle of attack and yaw were seen as general sidewash effects. The addition of canard-type fins had negligible effect on inlet performance.

CONTENTS

APPENDIXES

I. ILLUSTRATIONS

Figure

NOMENCLATURE

D_2	Compressor-face total-pressure distortion, $(p_{t_2})_{max} - (p_{t_2})_{min}/(\bar{p}_{t_2})$
FBL	Fuselage buttock line, in.
FRP	Fuselage reference plane
FS	Fuselage station, in.
FWL	Fuselage waterline, in.
I	Inboard inlet of the left-hand dual air induction system
M_A	Inlet first-ramp Mach number

MFR_{BP} Bypass door mass-flow ratio: ratio of the mass flow bypassed overboard through the bypass doors to the inlet capture mass flow. The inlet capture mass flow is defined as the captured stream tube for the inlet projected area with the model at 0-deg angle of attack and yaw

MFR_2 Engine mass-flow ratio: ratio of compressor-face station mass flow to inlet capture mass flow

M_∞ Free-stream Mach number

NBL Nacelle buttock line, in.

NRP Nacelle reference plane

NS Nacelle station, in.

NWL Nacelle waterline, in.

N_2 Compressor-face total-pressure recovery: the average compressor-face total pressure ratioed to free-stream total pressure, $(\bar{p}_{t_2}/p_{t_\infty})$

O Outboard inlet of the left-hand dual air induction system

p_{rms} Compressor-face root-mean-square value of total pressure, psf

$\bar{p}_{rms}$ Area weighted average compressor-face root-mean-square value of total pressure, psf

p_{t_2} Compressor-face total pressure, psfa

$\bar{p}_{t_2}$ Area weighted average compressor-face total pressure, psfa

p_{t_∞} Free-stream total pressure, psfa

R_B Inlet second ramp (first movable ramp)

TI_2 Turbulence index; average root-mean-square value of total-pressure oscillations at the compressor face normalized by the average compressor-face total pressure, $\bar{p}_{rms}/\bar{p}_{t_2}$

TH Inlet throat height, in.

TU Throat height a. which the inlet unstarts at each Mach number and model attitude, in.

α Model angle of attack (angle between the fuselage reference line and the relative wind projected into the plane of symmetry), nose up is positive, deg

ψ Model angle of yaw (angle between the plane of symmetry and the relative wind), nose right is positive, deg

SECTION I
INTRODUCTION

At the request of North American Rockwell Corporation (NARC), a series of development tests on the B-1 aircraft air induction system was initiated under the sponsorship of the Aeronautical Systems Division (ASD), Air Force Systems Command (AFSC). This series included testing in both of the 16-ft Propulsion Wind Tunnels, Transonic (16T) and Supersonic (16S), with a 0.10-scale model through the Mach number range from 0.55 to 2.20.

The primary purpose of the tests reported herein was to determine the steady- and unsteady-state performance of the B-1 inlet by evaluating the effects of angle of attack, angle of yaw, and various model configurations at subsonic and supersonic Mach numbers.

Representative data presented herein are in the form of inlet total-pressure recovery, total-pressure distortion, and turbulence index as a function of inlet mass-flow ratios.

SECTION II
APPARATUS

2.1 TEST FACILITY

Tunnels 16T and 16S are closed-circuit, continuous flow tunnels which can be operated in the Mach number range from 0.2 to 1.6 and 1.5 to 4.75, respectively. A complete description of their physical facilities and operating characteristics is presented in Ref. 1.

2.2 TEST ARTICLE

The test article was a 0.10-scale model of the North American Rockwell Corporation B-1 Air Vehicle (Fig. 1, Appendix I). The axial location of the model and model support systems is shown in Figs. 2a and b for Tunnels 16S and 16T, respectively. Photographs of the model installation in Tunnels 16S and 16T are shown in Figs. 3a and b, respectively.

The test model simulated the air vehicle fuselage forebody, 65-deg-sweep stub wings, and the left-hand, two-engine nacelle (Fig. 3a). Provisions were made for installing "soft-ride" fins (Figs. 3b and 4) near the front of the forebody.

Both inlets were of the mixed compression type in design and duplicated the air vehicle internal lines to the engine face station. Although of opposite hand, the inlets were geometrically similar. The nacelle external lines were duplicated to a point just aft of the sideplate and cowl leading edges, as well as in the region of the bypass doors on the cowl side.

The ramp side of each inlet consisted of a fixed first ramp and remotely controlled movable second, third, fourth (throat), and fifth (diffuser) ramps (Fig. 5). Because of the linkage arrangement, the third ramp was slaved to the second and fourth ramps, and the diffuser ramp was slaved and positioned by the trailing edge of the fourth ramp.

Boundary-layer control (BLC) was provided for each inlet by porous internal surfaces on the second, third, and fourth ramps, the upper and lower sideplates, and the cowl. The BLC system was compartmented into four separate bleed zones such that bleed air would not flow from one zone into adjacent zones. The bleed zones and percentage of porosity of the various surfaces are shown in Fig. 6. Bleed air from Zone I exited on the wing upper surface, Zones II and III exited through the lower sideplate, and Zone IV exited through the cowl. Bleed Zone I had a fixed exit which was manually adjustable from fully open to closed, but Zones II, III, and IV had remotely variable exit areas. The remotely variable exits were of the choked plug variety actuated by direct-current drive motors.

Each inlet had two remotely variable bypass doors (Fig. 5) for matching inlet-supply with engine-demand airflow. The two doors were linked together to utilize one hydraulic actuator per inlet.

Simulated engine airflow was controlled with flow throttling vanes located just downstream of each engine-face station. The throttling vanes were followed by a transition section (including flow-straightening screens) and an ASME-type airflow metering section. The flow throttling vanes were hydraulically actuated independently and were remotely operated with closed-loop servocontrols.

The wing-nacelle boundary-layer diverter was set at a basic height of 0.70 in. (Fig. 7) measured from the leading edge of the upper sideplate to the wing moldline at the cowl-sideplate junction. Diverter height could be varied by installing or removing shims. Additional test article details may be found in Ref. 2.

2.3 INSTRUMENTATION

The model was heavily instrumented with steady- and unsteady-state pressure instrumentation. The steady-state pressure instrumentation was located on the wing surface, internal cowl surface, ramp surfaces, in the boundary-layer bleed control plenums and metering tubes, the internal and external surfaces of the bypass doors, the simulated engine faces, and in the main duct metering tubes, Figs. 8 and 9. The unsteady-state instrumentation consisted of flush-mounted transducers on the wing, ramp, and cowl surfaces and total-pressure probes on the simulated engine face, Figs. 8 and 9.

The simulated engine face steady and unsteady pressures were measured with dual-purpose probes as shown in Fig. 8. The array consisted of eight five-tube rakes on equal-area centers.

All steady-state transducer outputs were scanned into an on-line computer system which reduced the raw data to engineering units, computed pertinent parameters, and tabulated and plotted the results. Test results were continually monitored in this fashion. Details of the AEDC standard 16-ft tunnel recording system are given in Ref. 1.

High-frequency pressure fluctuations were measured by user-furnished 25-psid pressure transducers and were recorded on constant bandwidth FM multiplex recording systems.

The signals from the simulated engine face dynamic transducers were also paralleled to true rms/dc converters to obtain unsteady (rms) pressure levels.

Model angle of attack relative to the tunnel centerline was measured by means of a model-mounted pendulum angle sensor. Model yaw angle and model component positions were sensed with potentiometers.

SECTION III
PROCEDURE

After the tunnel free-stream total pressure and Mach number were established (Fig. 10), the model was positioned to the desired angle of attack and yaw. Model variables such as second-ramp angle (RB, I, O), throat ramp position (TH, I, O), bypass door position (U), and mass-flow controls were varied to study the desired effect. At most test conditions, inlet pressure data were obtained for a range of engine mass-flow ratios from subcritical to supercritical for Mach number 1.7 and lower (unstarted inlet), and from peak recovery to supercritical (started inlet), or from buzz to supercritical (unstarted inlet), for Mach number 2.2. Mass-flow variation was controlled by positioning the flow control vanes located aft of the simulated engine face. Onset of inlet buzz was determined from the output of dynamic pressure transducers located in the inlet duct and on the simulated engine face.

For Mach numbers 1.4, 1.7, and 2.2, the local Mach number on the first ramp of each inlet was determined for various angles of attack and yaw (Table I, Appendix II). These values of local Mach number were used to schedule the second-ramp angle and throat ramp position as determined from previous testing in the NAR trisonic wind tunnel (see Figs. 11 and 12 and Ref. 3).

SECTION IV
RESULTS AND DISCUSSION

Test results are presented for a 0.1-scale inlet model of the North American Rockwell B-1 aircraft. Inlet performance in terms of compressor-face total-pressure recovery (N_2), total-pressure distortion (D_2), and turbulence index (TI_2) is presented as a function of engine mass-flow ratio (MFR_2) or bypass mass-flow ratio (MFR_{BP}) for the test variables. The only configuration variable was the addition of the soft-ride fins (Fig. 3b) to the forward fuselage. Except for the bypass data presented, the bypass area was sealed. The boundary-layer bleed exits were held constant at fixed areas for the data presented herein.

Only the significant aspects of the steady- and unsteady-state pressure data are presented in this report. Complete analysis of the unsteady-state data is a long-term task and beyond the scope of this report.

4.1 EFFECT OF MODEL VARIABLES

4.1.1 Effect of Second-Ramp Angle

The effect of the second-ramp angle on inlet performance at M_∞ = 0.85, 1.7, and 2.2 for a representative cruise angle of attack is shown in Figs. 13, 14, and 15, respectively.

Increasing the second-ramp angle at M_∞ = 0.85, Fig. 13, produced negligible effects until a "critical" angle was reached where a loss in supercritical mass flow was noticed. The value of this "critical" angle decreased as throat height increased. At the scheduled throat height of 2.8 in., the outboard inlet was more sensitive to the effect in addition to having a slightly lower recovery. This reduction in mass-flow ratio was caused by shifting the minimum (choked) area of the inlet from the throat ramp to the area of the third ramp at the higher values of second-ramp angle and throat height.

At M_∞ = 1.7, Fig. 14, the inlet was operated unstarted (external compression). Increasing the second-ramp angle again reduced the supercritical mass-flow ratios by spilling flow over the cowl lip but increased performance for the subcritical mass-flow ratios. There was essentially no difference between inboard and outboard inlet performance.

With inlet started (mixed compression) operation at M_∞ = 2.2, Fig. 15, a loss in mass-flow ratio and performance was noted as the ramp angle was increased to more than 12.5 deg. Peak performance for both inlets occurred with the second-ramp angle at about 10 deg where the inboard inlet showed a slight superiority.

For the conditions presented, the scheduled second-ramp angle at the scheduled throat height exhibited equal or better performance characteristics than the off-schedule second-ramp angles. However, the total-pressure distortion near critical mass-flow ratios was 10 percent or greater for all conditions.

4.1.2 Effect of Throat Height

Throat height effects at M_∞ = 0.85, 1.7, and 2.2 for a representative cruise angle of attack are shown in Figs. 16, 17, and 18, respectively.

Decreasing the throat height at M_∞ = 0.85 and 1.7 for any given second-ramp angle did not produce any significant effects except for the expected reduction in supercritical mass-flow ratio. The scheduled throat heights and second-ramp angles again exhibited the best performance characteristics. At M_∞ = 2.2, an increase of the percentage of unstart throat height from 105 percent to 117 percent resulted in a loss in peak recovery of approximately 3 percent.

The total-pressure distortion was 10 percent or greater for all conditions near critical mass-flow ratios. The turbulence index (TI_2) was nominally less than 2 percent near the critical mass-flow ratio.

4.1.3 Effect of Bypass Door Variation

Data in Figs. 19 and 20 represent the effects of bypass door flow on the inlet performance. The data shown represent the conditions of peak recovery at M_∞ = 2.2. At M_∞ = 1.4, the peak recovery points with the bypass doors open were compared to the recovery point at 95 percent of supercritical mass flow with the bypass doors closed.

Each inlet was affected in a similar manner at both Mach numbers. At M_∞ = 1.4, the inlet performance was not significantly affected by bypass mass flow. At M_∞ = 2.2, the maximum inlet performance was obtained with the bypass doors closed.

4.2 EFFECT OF SOFT-RIDE FINS

The effect of soft-ride fins is shown in Figs. 21 and 22 for M_∞ = 0.85 and 1.4, respectively. There was a slight reduction in the supercritical mass flow for both inlets at M_∞ = 0.85, α = 3 deg. The inboard inlet exhibited the same characteristics at M_∞ = 1.4, α = 0 deg, but the outboard inlet was not affected. Performance at subcritical and critical mass-flow ratios was essentially not affected.

4.3 GENERAL PERFORMANCE

The general performance of the inlet system is shown as functions of angle of attack, Figs. 23 through 26, angle of yaw, Figs. 27 through 30, and Mach number, Fig. 31. All second-ramp angles were according to the schedules as shown in Figs. 11 and 12. At M_∞ = 2.2, a TH/TU = 105 percent, which is a relatively high performance throat height, was used for comparative purposes.

4.3.1 Effect of Angle of Attack and Yaw

With the inlets located beneath the wing of this sweptwing configuration, variations in free-stream angle of attack and yaw were felt by the inlet as perturbations on the wing flow field in deference to the more direct effects felt by exposed inlets. For subsonic Mach numbers (M_∞ = 0.85, Fig. 12), high angles of attack produced a loss in performance of the leeward (outboard) inlet, but performance of the windward (inboard) inlet was virtually unaffected. At supersonic Mach numbers, a different phenomenon was noted. An omen of this phenomenon can be seen in Table I; the high outwash along the lower surface of the wing at high angles of attack greatly reduced the inboard first-ramp Mach number but left the outboard value relatively unchanged. Thus the variations in inlet performance shown in Figs. 24, 25, and 26 were to be expected: (1) an increase in supercritical mass-flow ratios and an improvement in performance of the inboard inlet as angle of attack increased (ramp Mach number decreased) and (2) little change in the outboard inlet performance; some decrease was noted at M_∞ = 1.4 where the first-ramp Mach number increased slightly, and some increase at M_∞ = 2.2 where a small decrease in ramp Mach number was noted.

Table I also portrays the affect of the angle of yaw. For angles of attack less than 3 deg, performance was essentially the same for both inlets with a reflection effect in

which the performance at positive yaw angles for the inboard inlet was the same as for the outboard inlet at negative angles of yaw (Figs. 27a, 28a, 29a, and 30a). At the higher angles of attack of 9 to 18 deg (Figs. 27b, 28b, 29b, and 30b), the effect of yaw variation upon the inboard inlet was small when compared to the outboard inlet. The outwash at those conditions affected the leeward (outboard) inlet more at negative yaw angles than the windward (inboard) inlet at positive yaw angles. The difference diminished as M_∞ increased.

4.3.2 Effect of Mach Number

Figure 31 shows the variation in inlet performance for the Mach number range from 0.55 to 2.2, ψ = 0 deg, for a representative angle of attack at the scheduled second-ramp angles and throat heights.

The overall trends were those expected for a well-designed mixed-compression inlet with the lowest peak recovery of about 92 percent at critical mass-flow ratio at M_∞ = 2.2. In general, the total-pressure distortion was 10 percent or higher for critical mass-flow ratios. As expected, the turbulence index for both inlets increased as mass-flow ratio increased but was less than 2 percent for critical mass-flow ratios. Figure 32 presents typical compressor-face pressure profiles for critical and supercritical mass-flow ratios at M_∞ = 2.2. As the mass-flow ratio increased from critical to supercritical, the low pressure region behind the ramp side of both inlets increased in magnitude and area. For the supercritical conditions, the areas of higher total-pressure recovery were also areas of higher turbulence.

SECTION V
CONCLUSIONS

Based on results obtained during this test, the following conclusions are made:

1. Equal or better inlet performance characteristics were obtained with the scheduled second-ramp angles and throat heights than with the off-schedule values.

2. High second-ramp angles induced choking ahead of the throat ramp at a Mach number of 0.85 for large throat heights and caused flow spillage at Mach numbers of 1.7 and 2.2.

3. Increasing the throat height for any given second-ramp angle increased the supercritical mass-flow ratio for Mach numbers from 0.85 to 1.7 (unstarted inlet) but as the throat height was increased at a Mach number of 2.2 (started inlet) a loss in total-pressure recovery resulted.

4. Increasing the bypass mass flow at a Mach number of 2.2 resulted in a loss in inlet performance. Only small effects were noted at a Mach number of 1.4.

5. Installation of soft-ride fins produced negligible effects on inlet performance.

6. Effects of angle of attack and yaw on inlet performance were attributed to sidewash effects characteristic of sweptwing aircraft.

7. For supercritical operation, the areas of higher inlet turbulence on the engine face occurred in areas of higher total-pressure recovery.

8. For a representative cruise angle of attack and 0-deg angle of yaw, the lowest total-pressure recovery at critical mass-flow ratio was 92 percent at a Mach number of 2.2 with scheduled second-ramp angles and throat heights.

9. The inlet total-pressure distortion was 10 percent or greater at critical mass-flow ratios. This is higher than normally desired for satisfactory turbine engine operation.

REFERENCES

1. Test Facilities Handbook (Ninth Edition). "Propulsion Wind Tunnel Facility, Vol. 4." Arnold Engineering Development Center, July 1971.

2. "Pretest Information for the 0.10-Scale B-1 Inlet Development Model II in the AEDC Propulsion Wind Tunnel - 16S, 16T, Test 5." NA-70-550-2, April 16, 1971.

3. "Inlet Development Model II in Trisonic Wind Tunnel, Test 4." TIS-0721-1-017, April 1, 1971.

APPENDIXES

I. ILLUSTRATIONS

II. TABLE

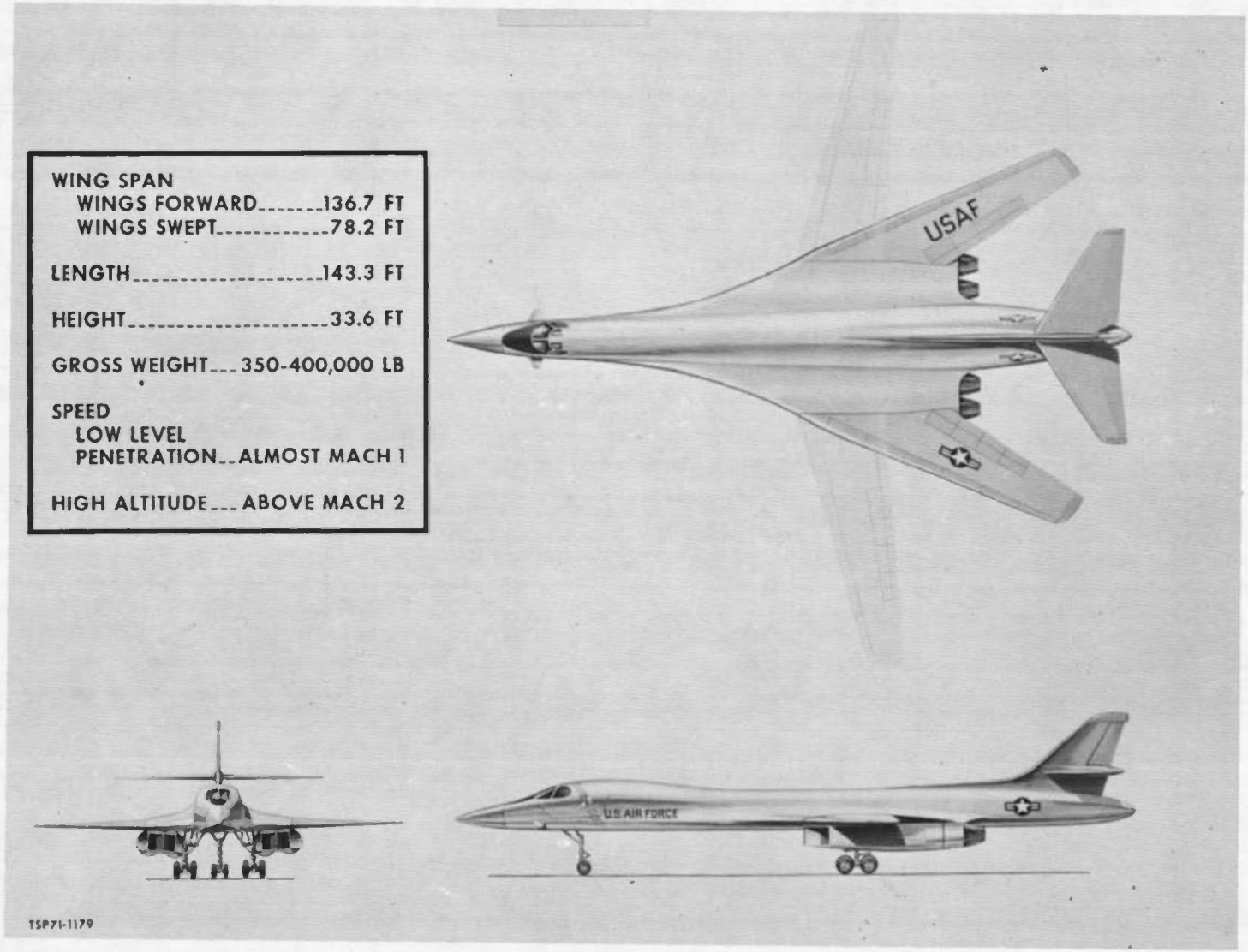

Fig. 1 General Arrangement of the B-1 Aircraft

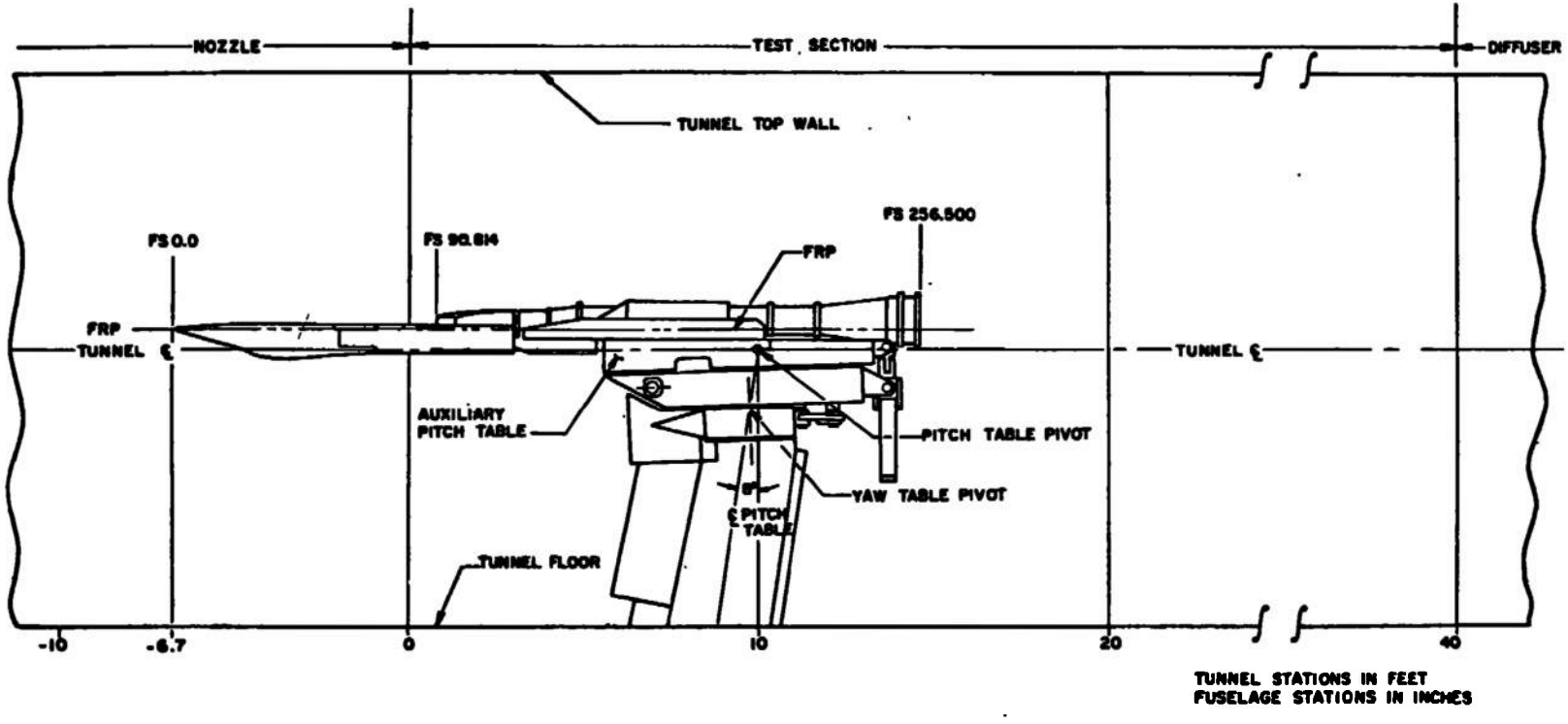

a. Tunnel 16S

Fig. 2 Model Location in the Test Section

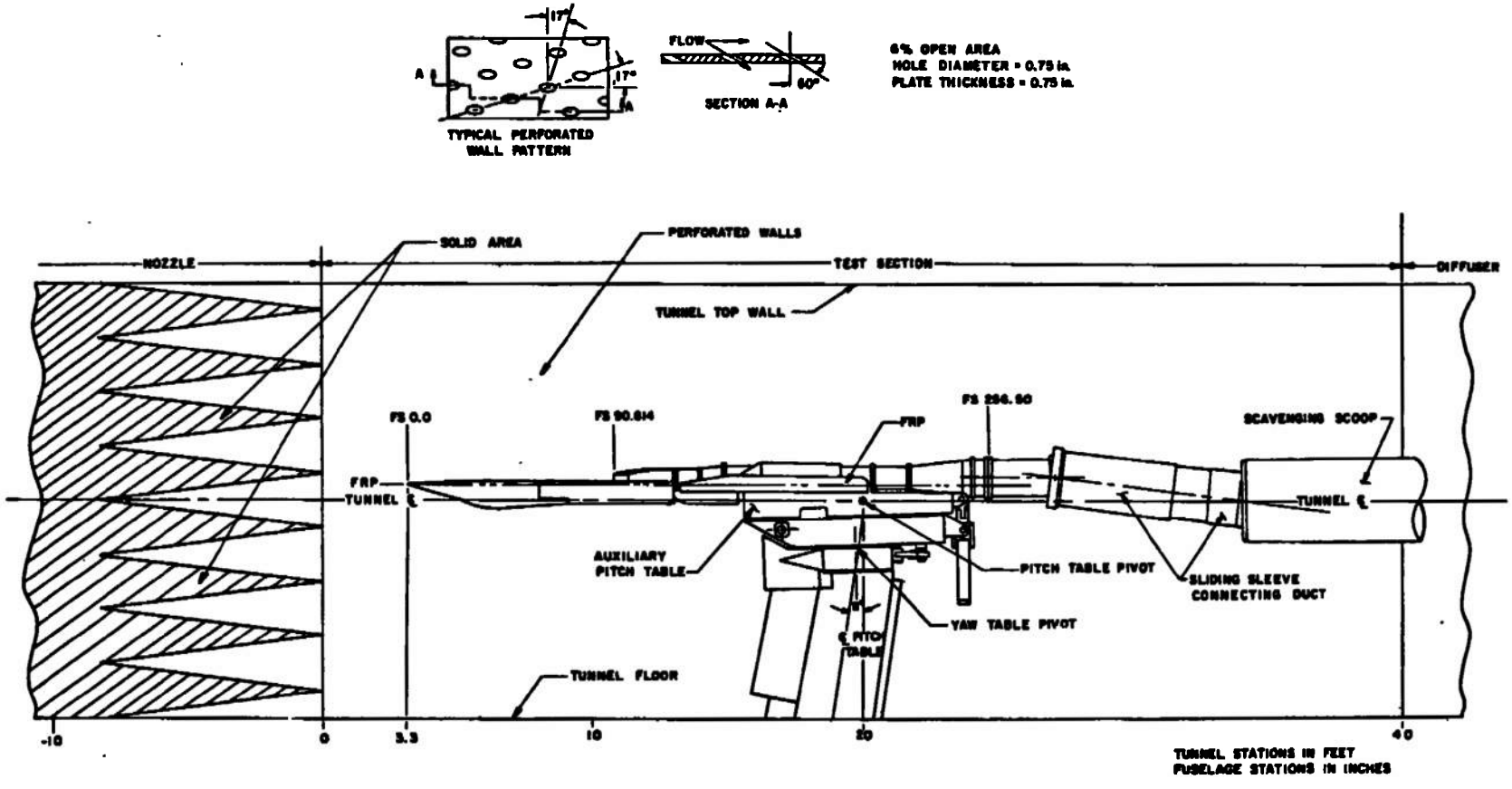

b. Tunnel 16T

Fig. 2 Concluded

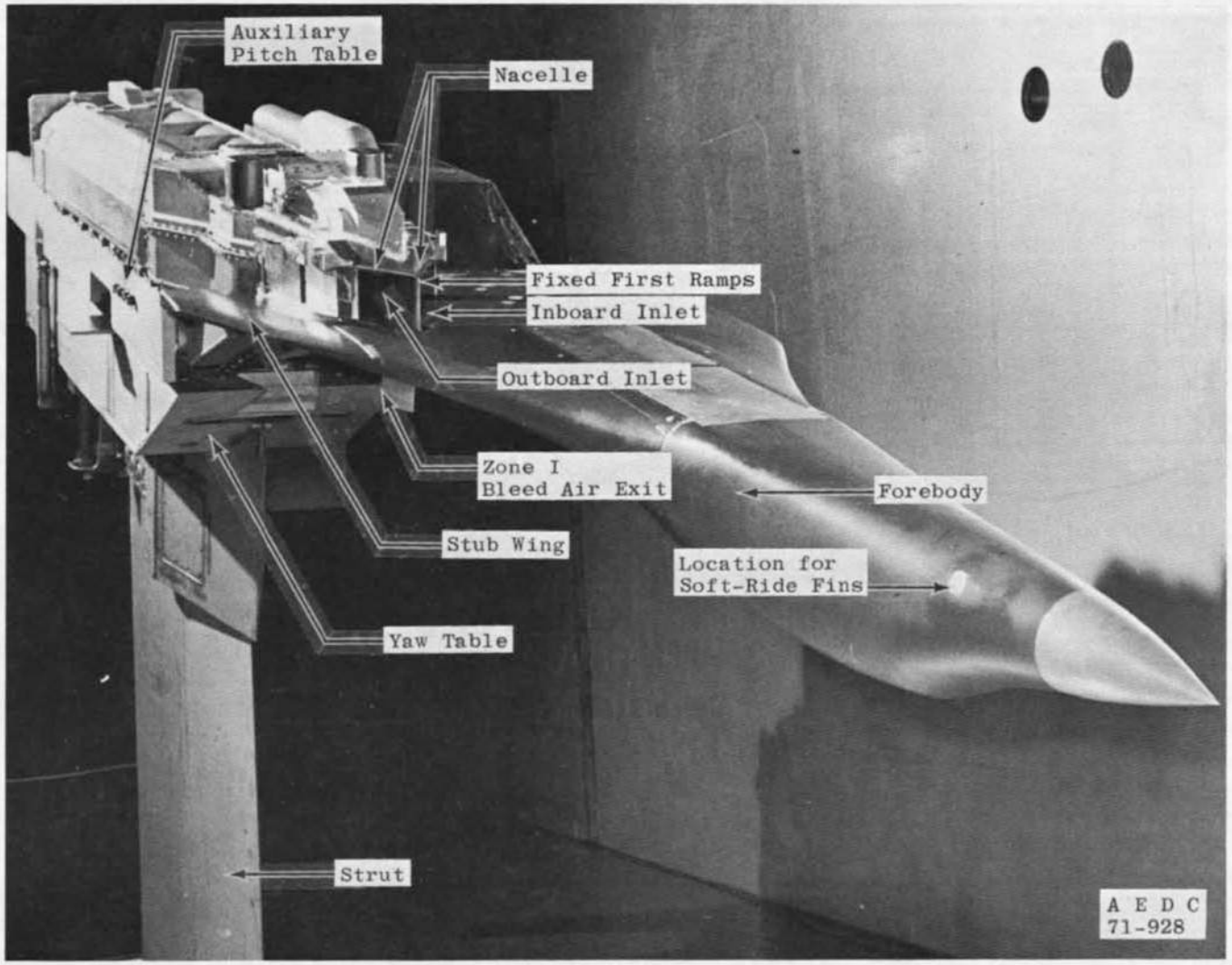

a. Tunnel 16S

Fig. 3 Model Installation

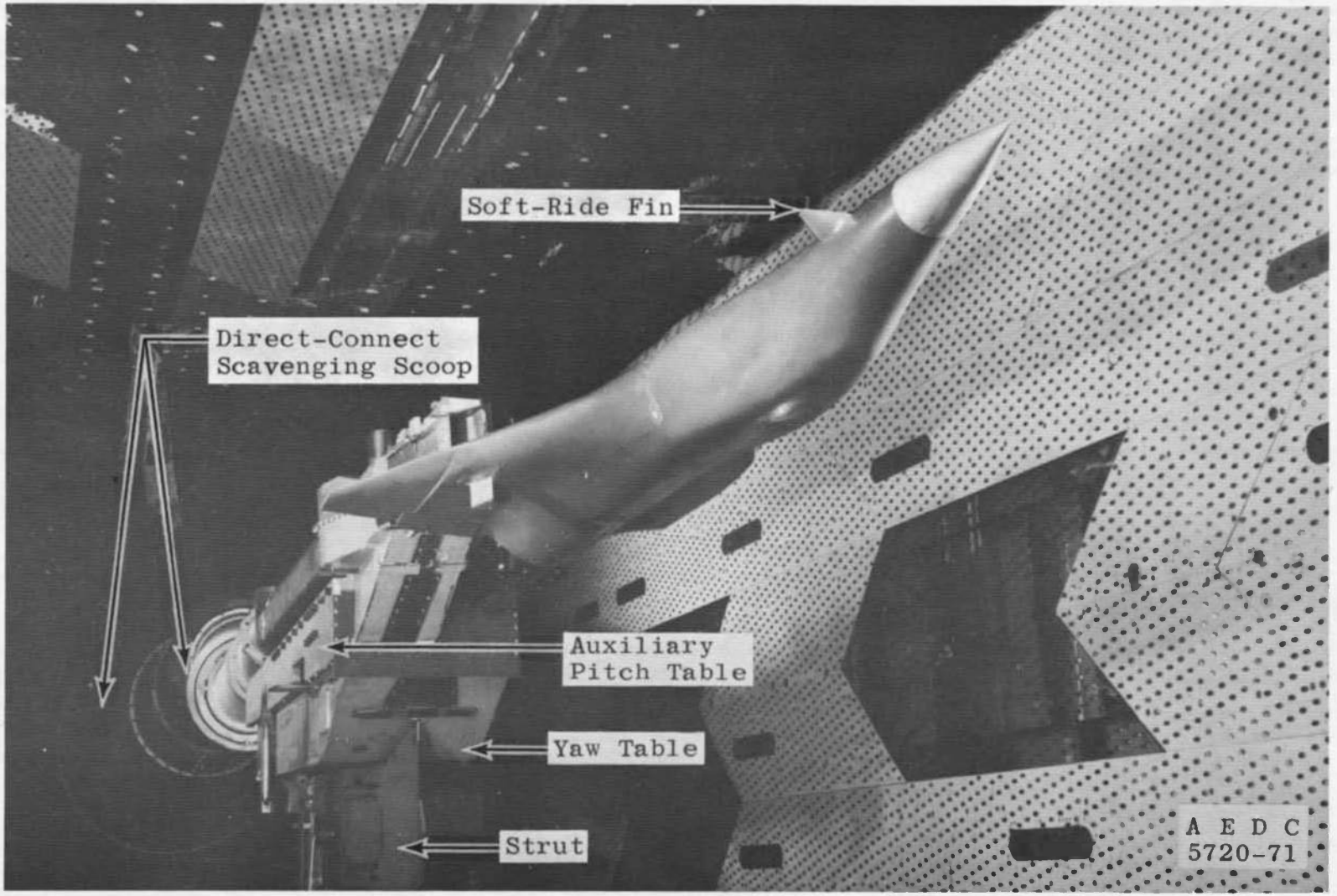

b. Tunnel 16T
Fig. 3 Concluded

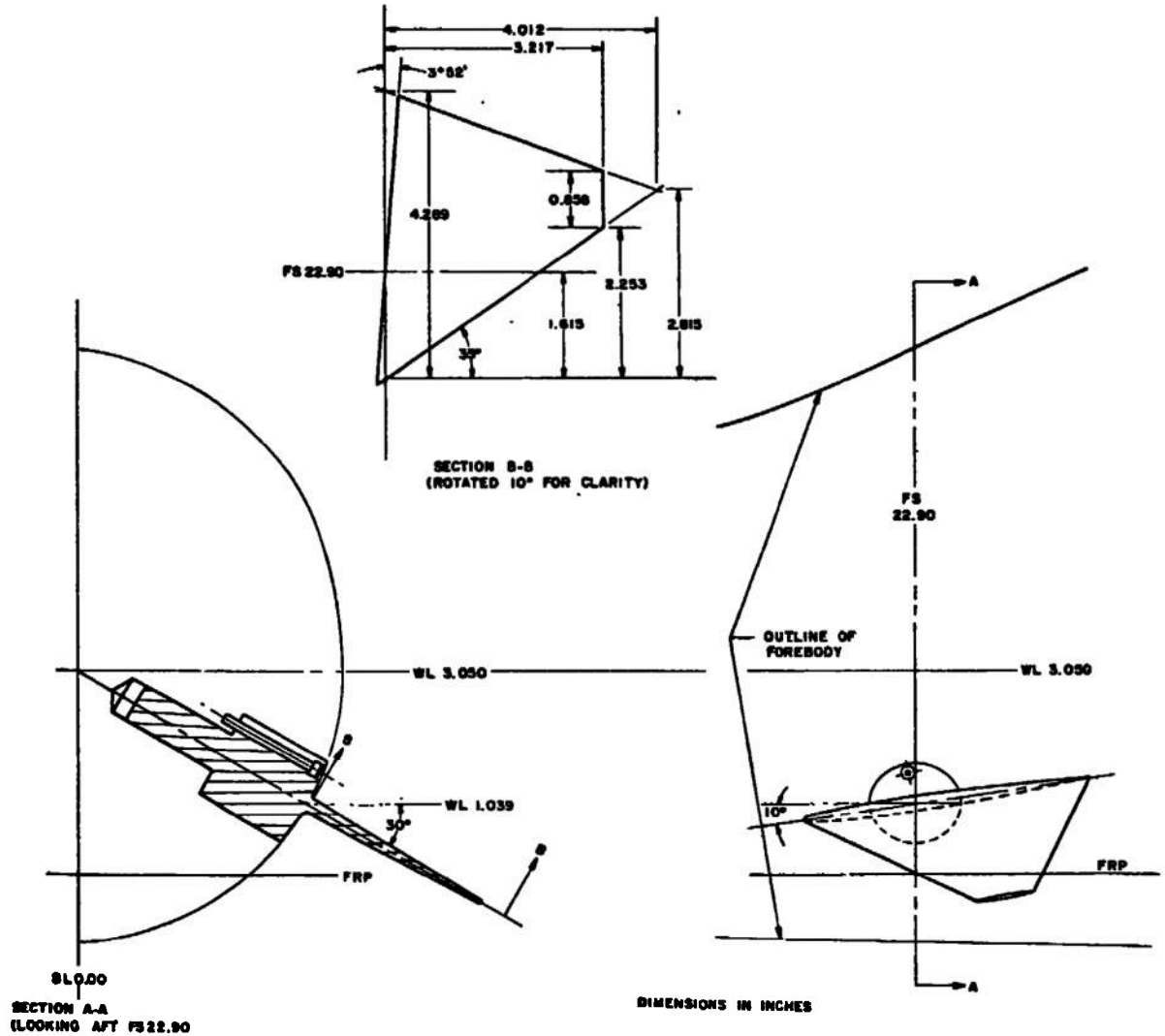

Fig. 4 Details of the Soft-Ride Fins

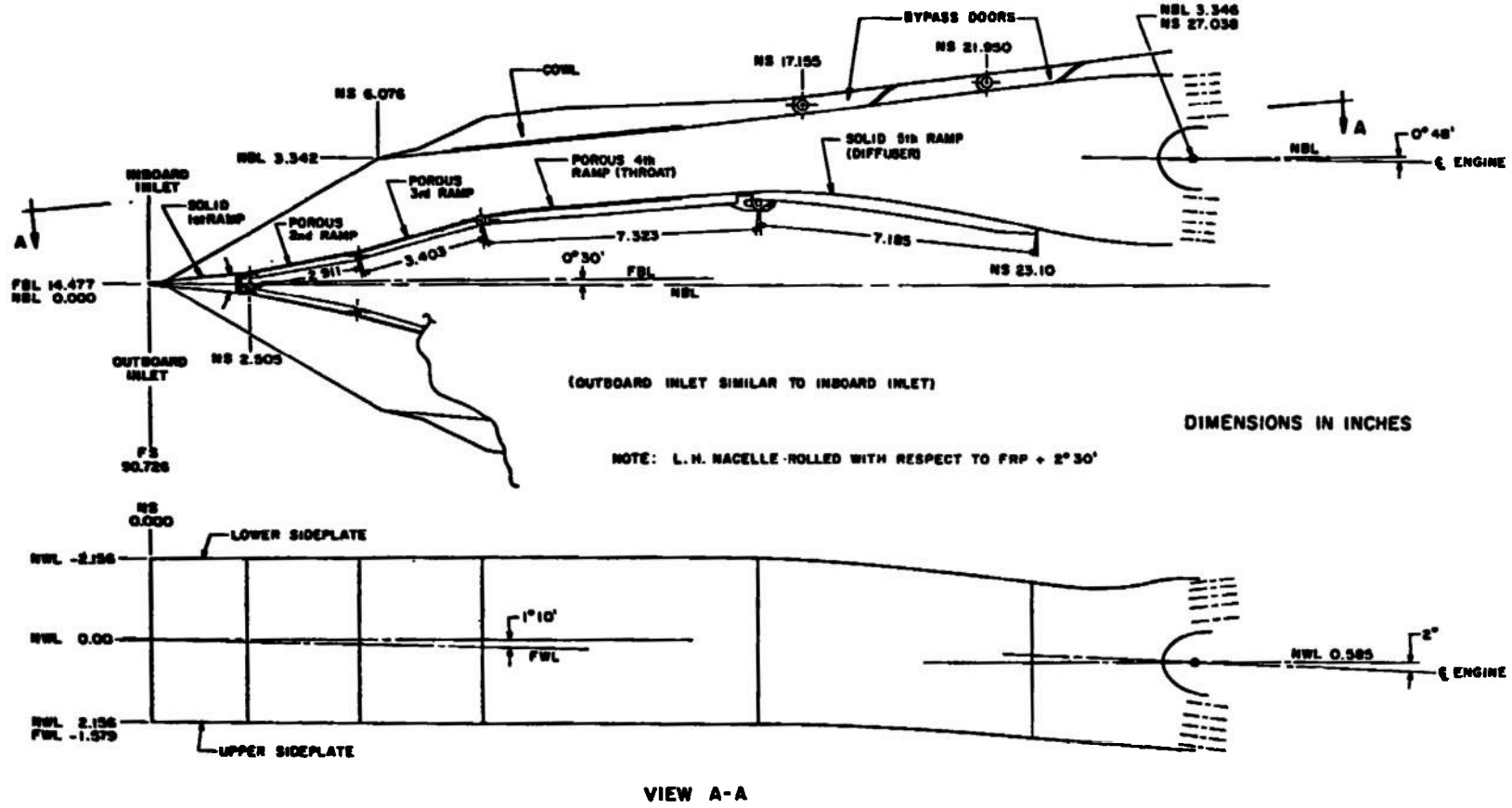

VIEW A-A

Fig. 5 Schematic of the Inlet Nacelles

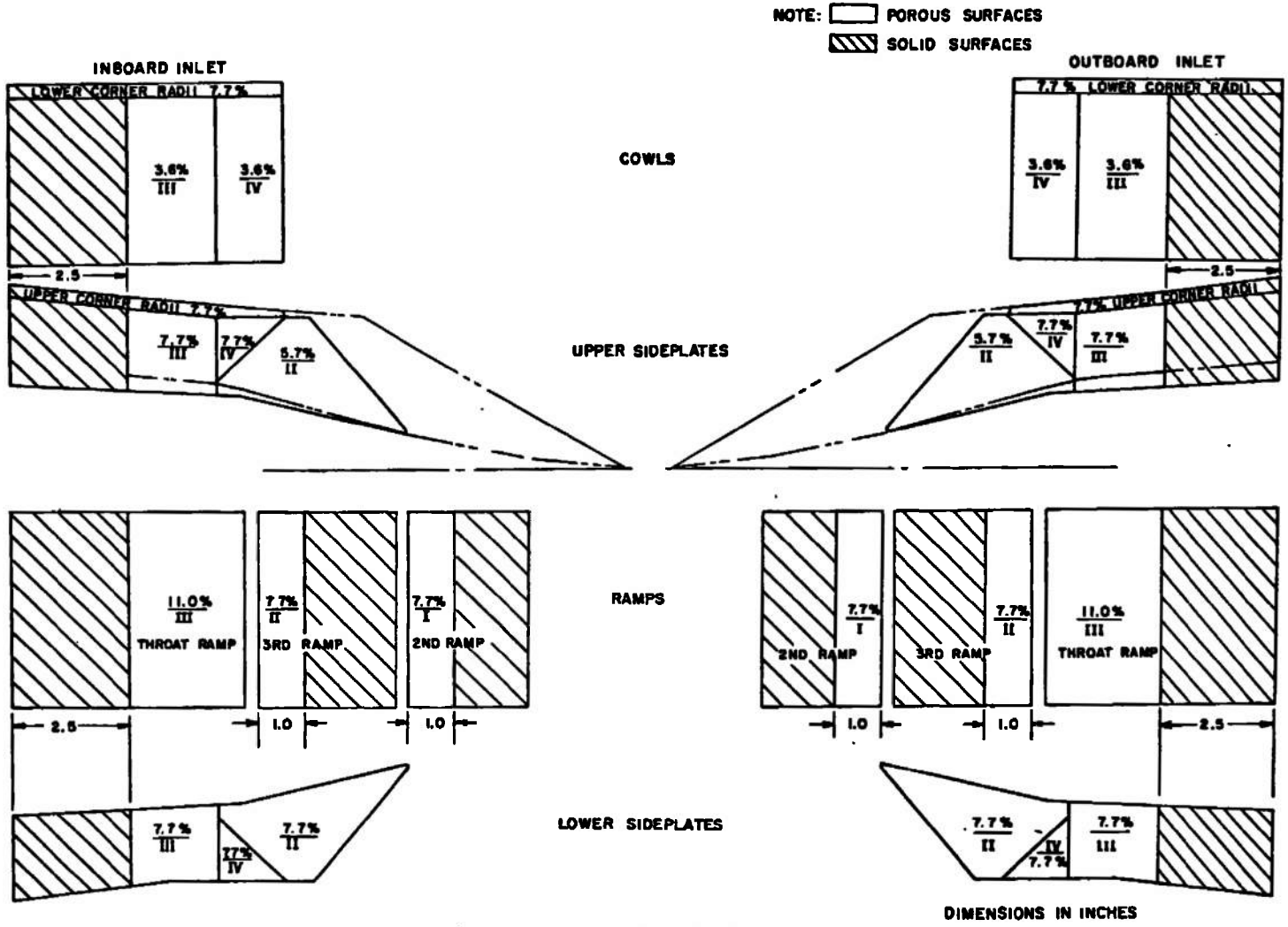

Fig. 6 Inlet Bleed Porosity Schematic

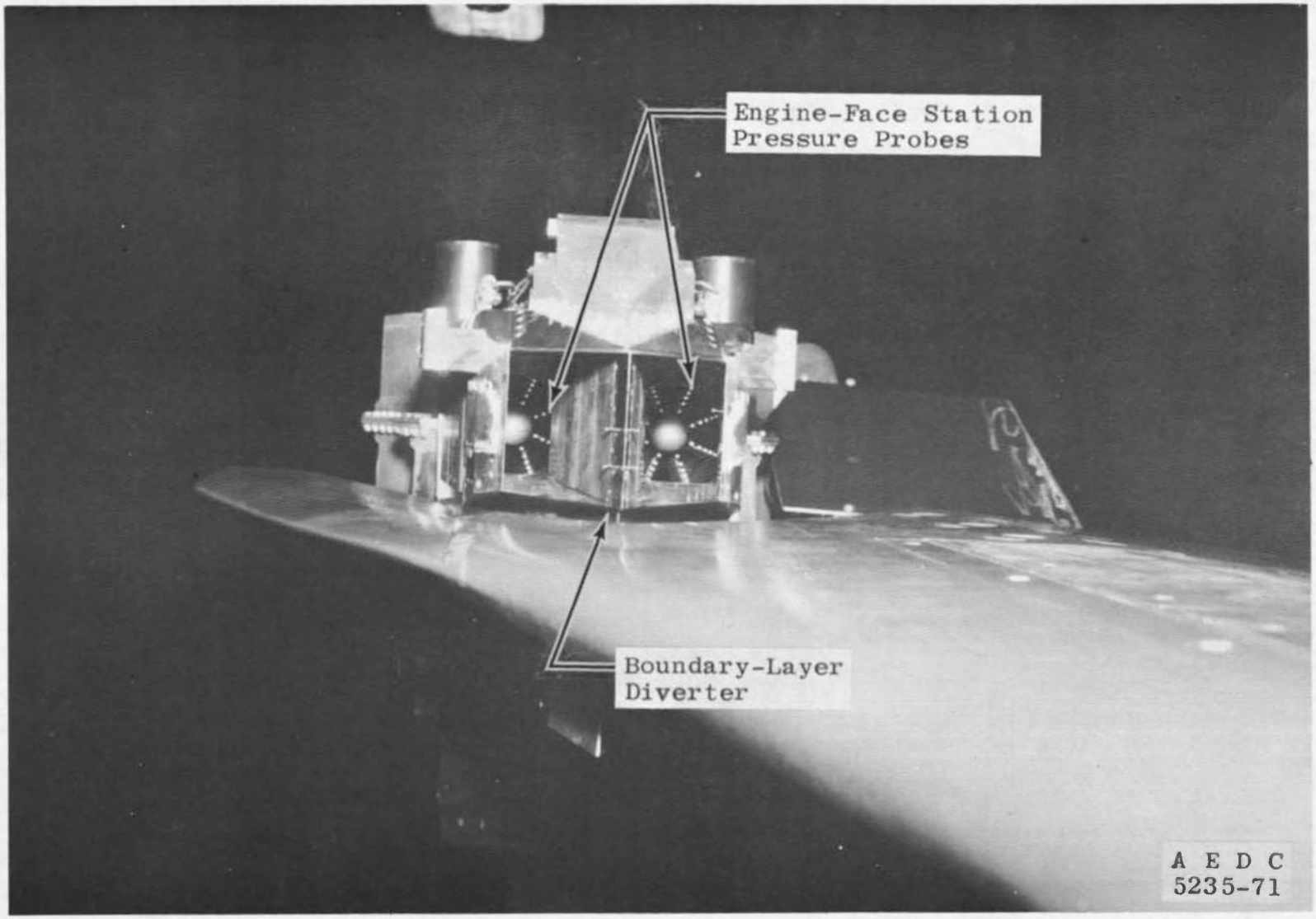

Fig. 7 Front View of Inlets

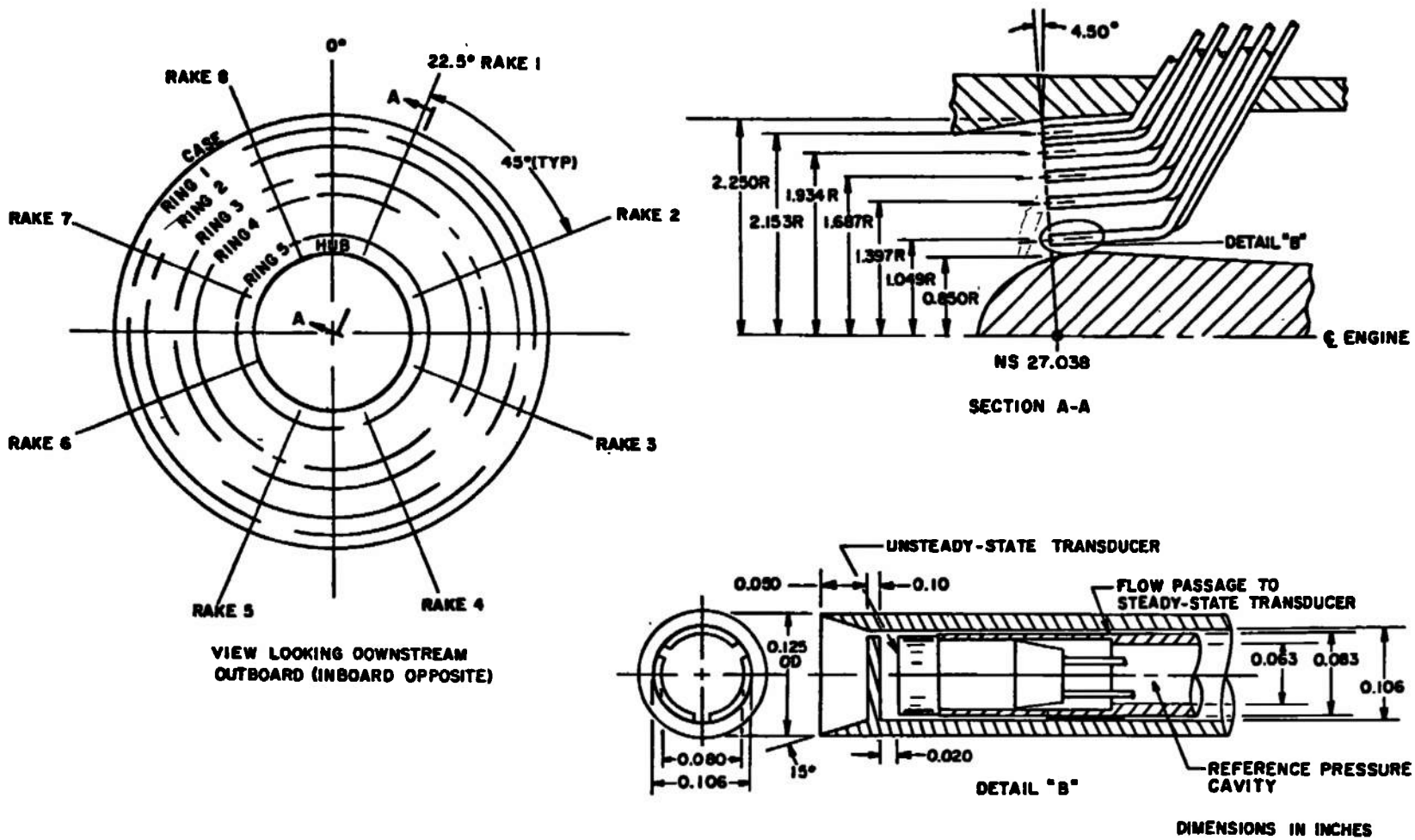

Fig. 8 Engine Face Instrumentation

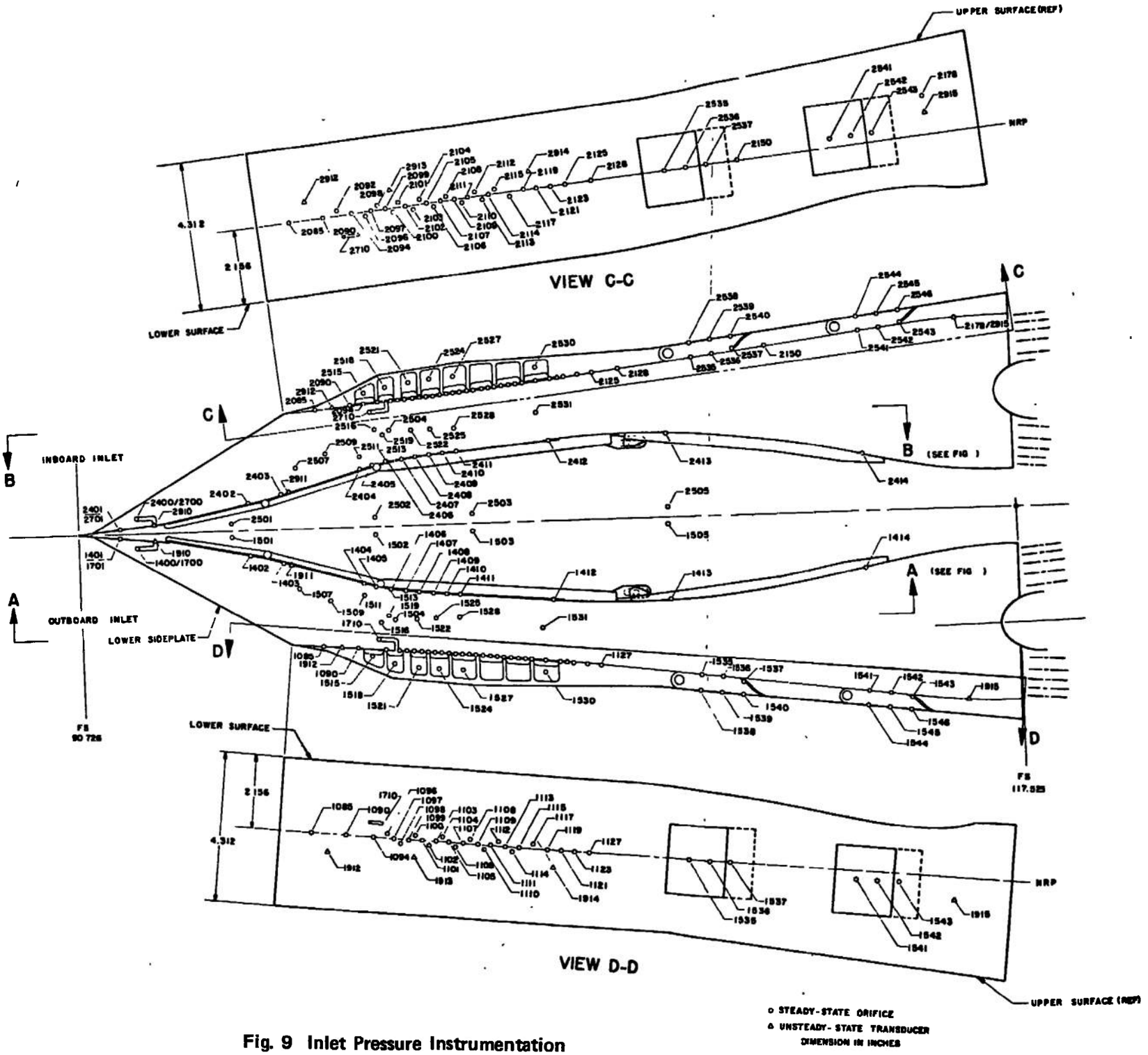

Fig. 9 Inlet Pressure Instrumentation

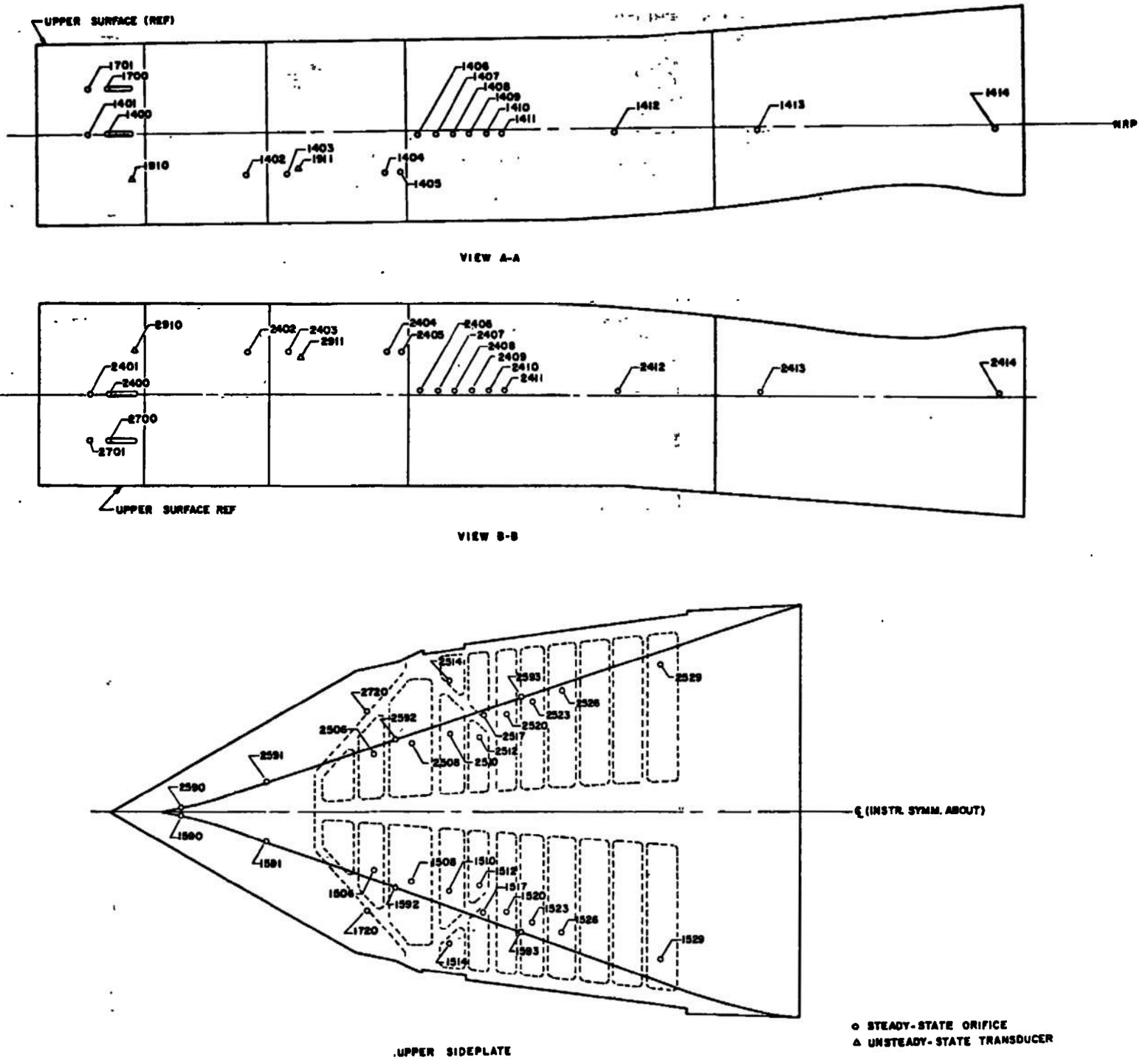

Fig. 9 Concluded

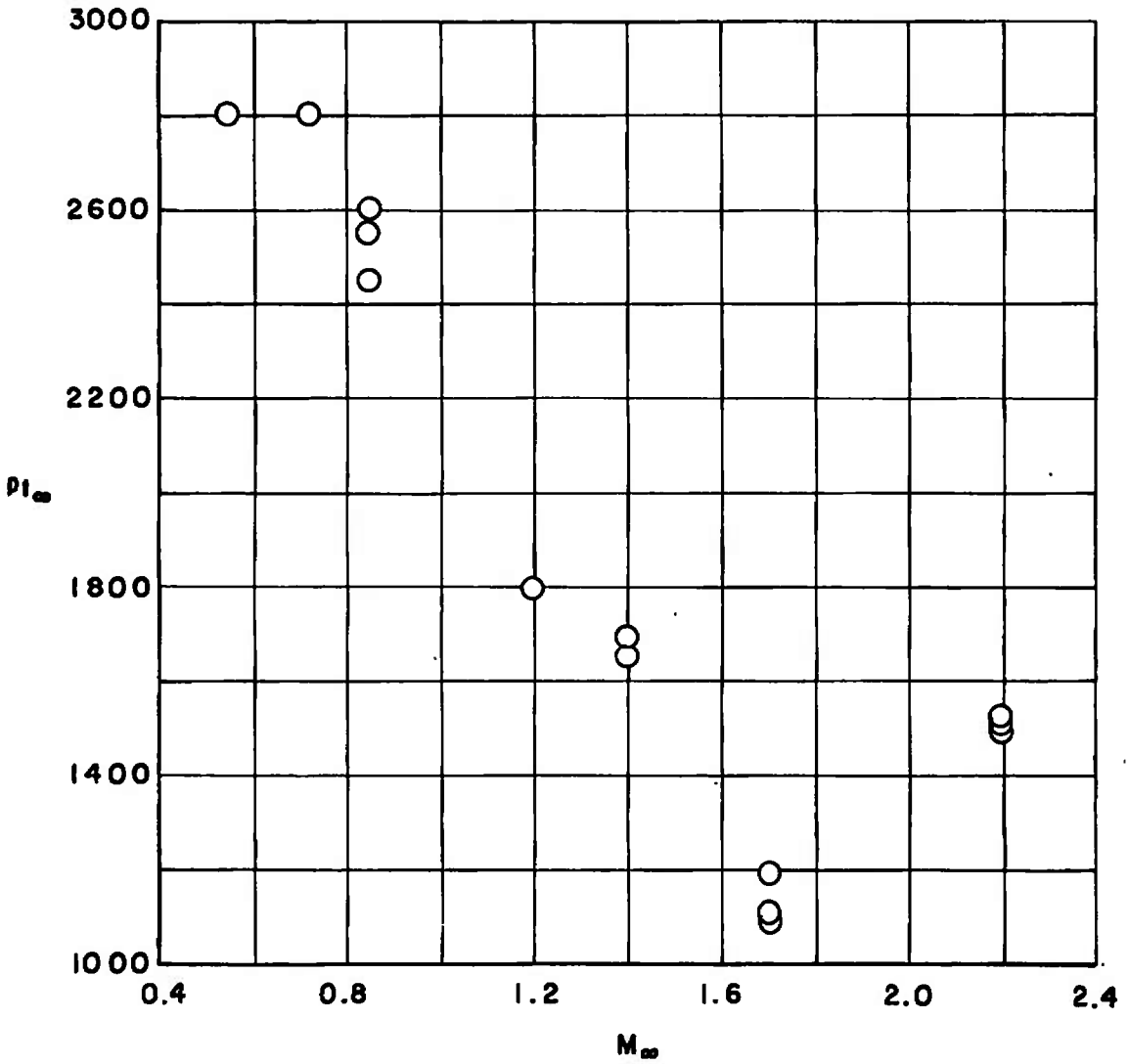

Fig. 10 Summary of Test Conditions

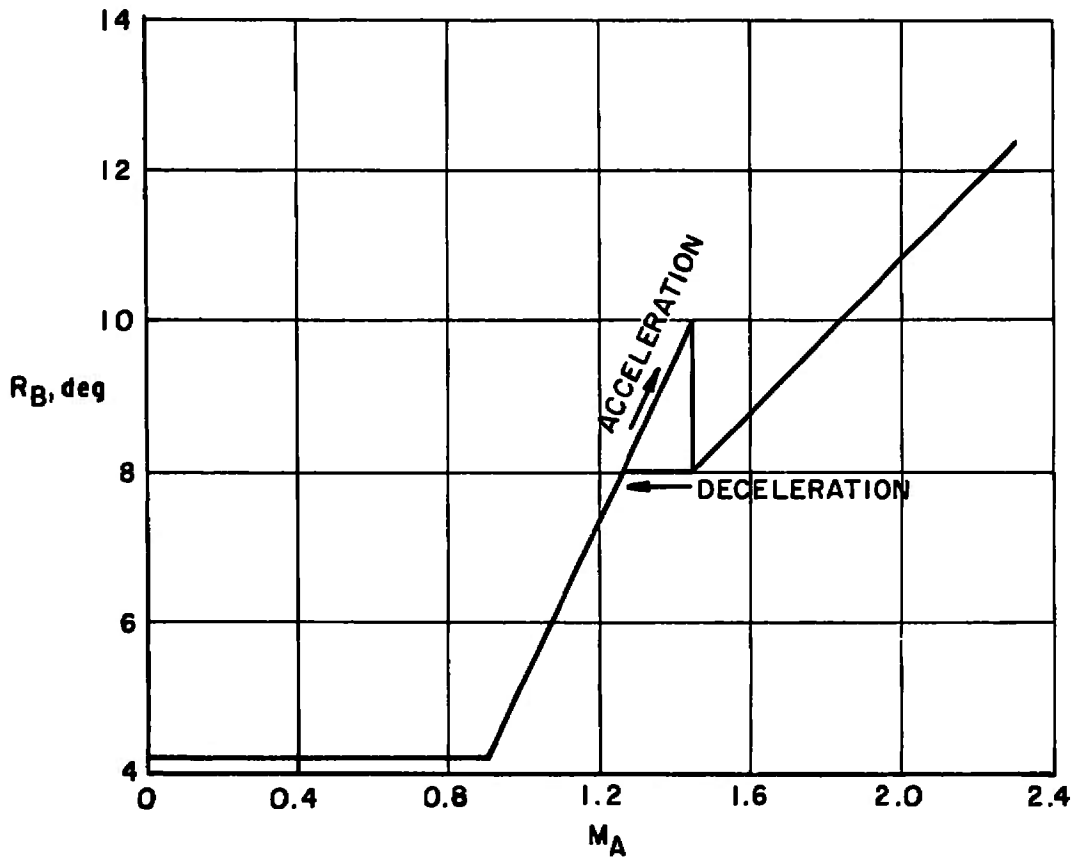

Fig. 11 Second-Ramp Schedule

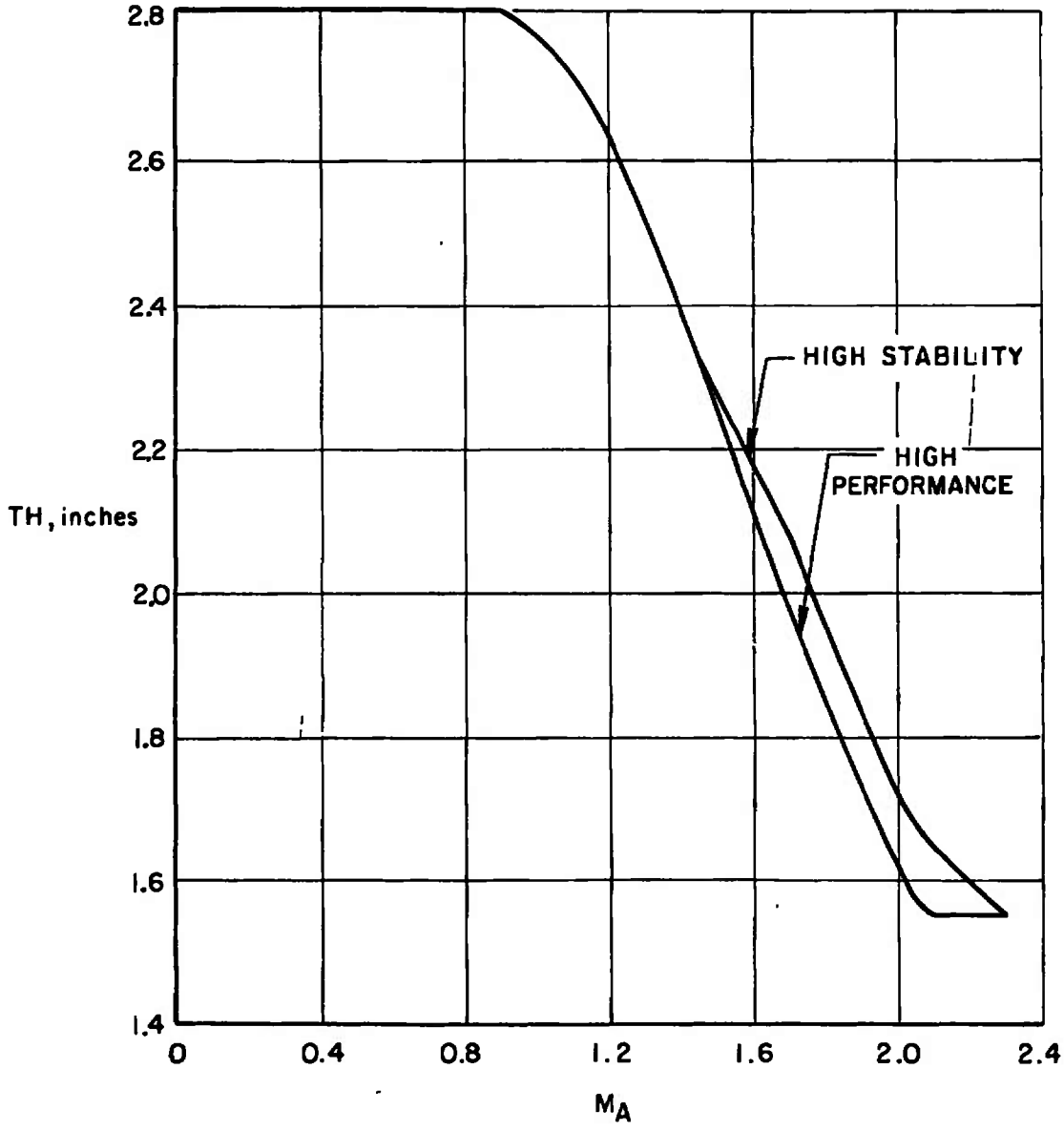

Fig. 12 Throat Height Schedule

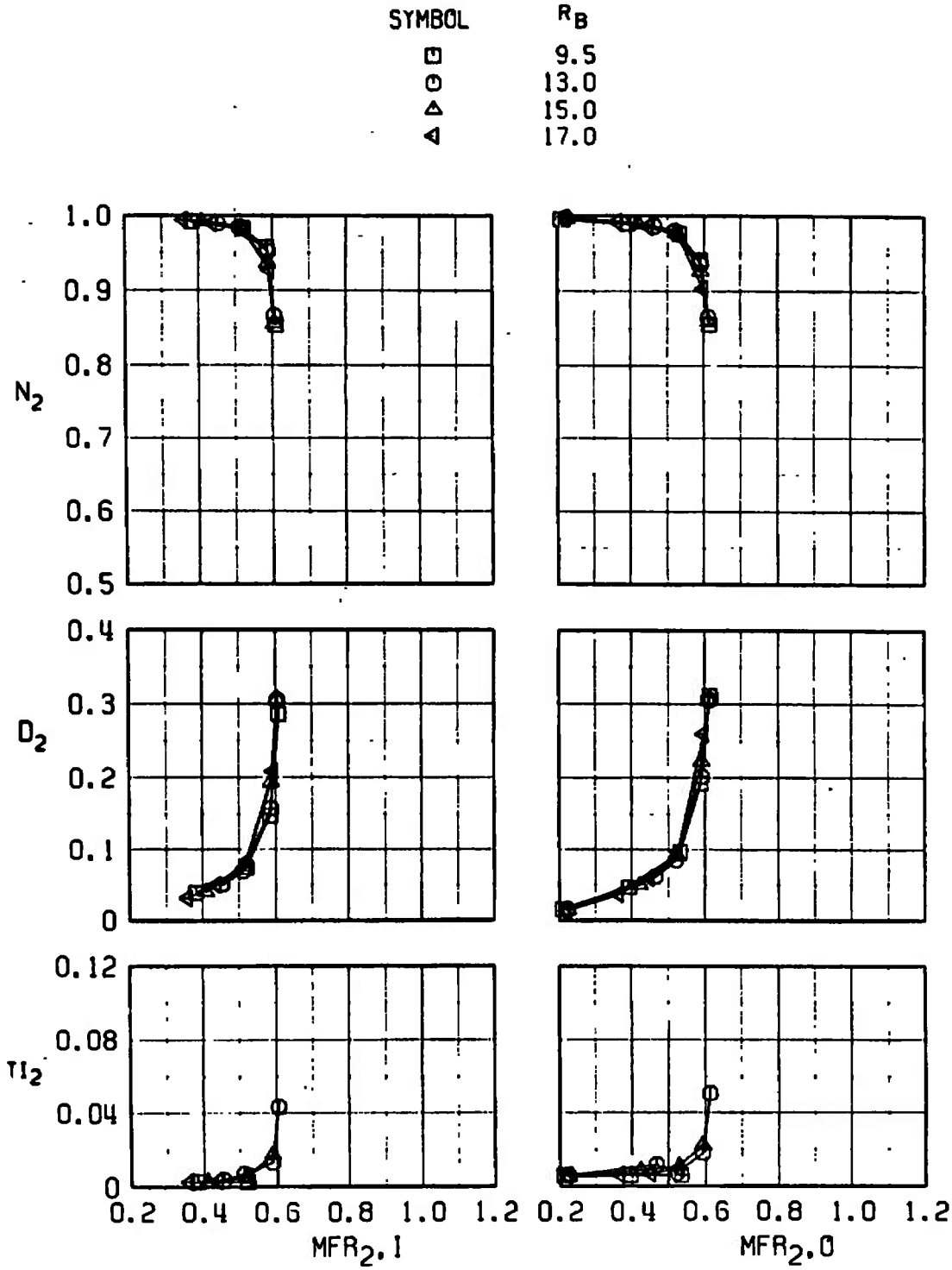

a. TH = 2.0 in.

Fig. 13 Effect of Second-Ramp Angle, M_∞ = 0.85, α = 3 deg, ψ = 0 deg

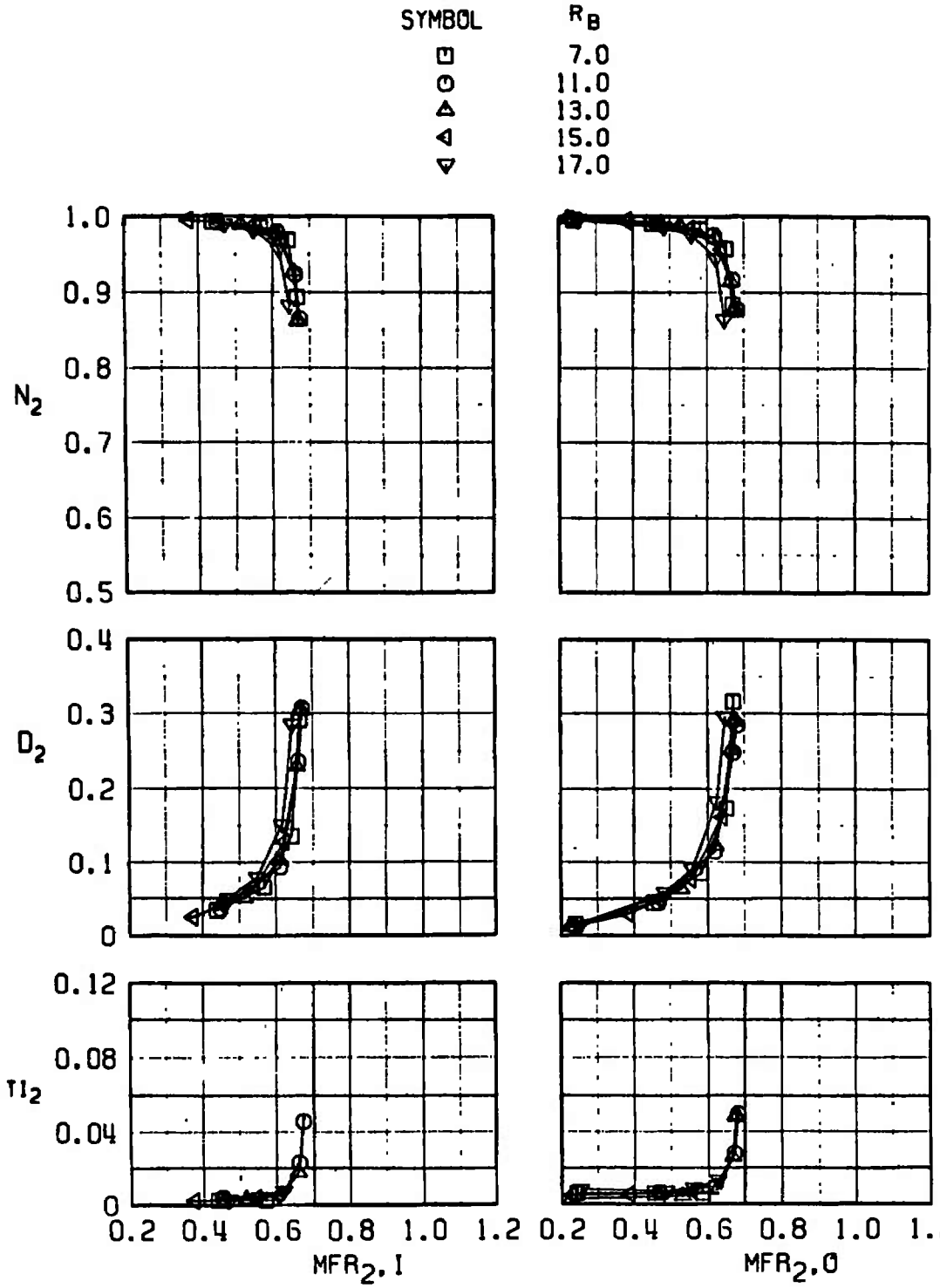

b. TH = 2.2 in.

Fig. 13 Continued

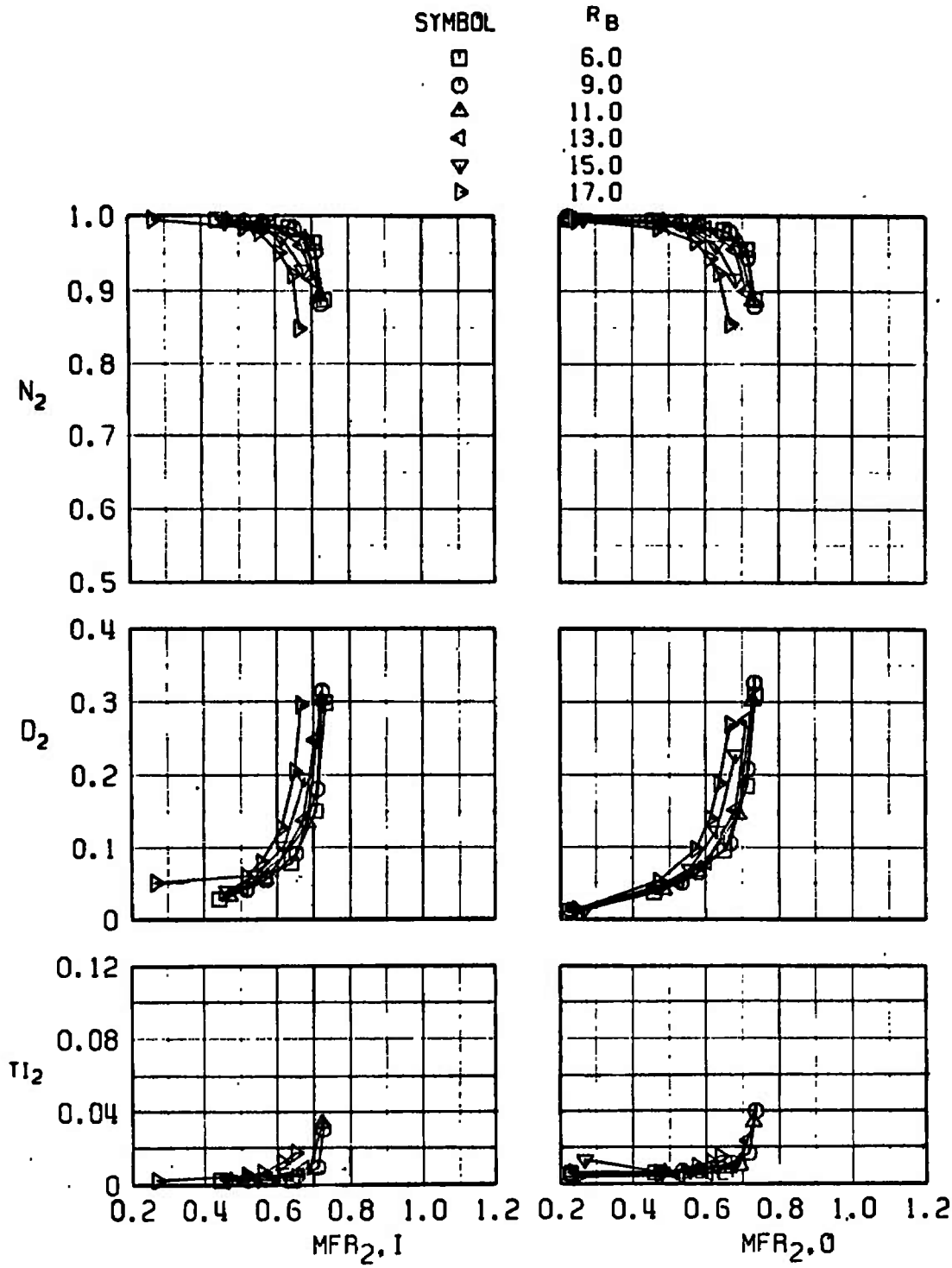

c. TH = 2.4 in.
Fig. 13 Continued

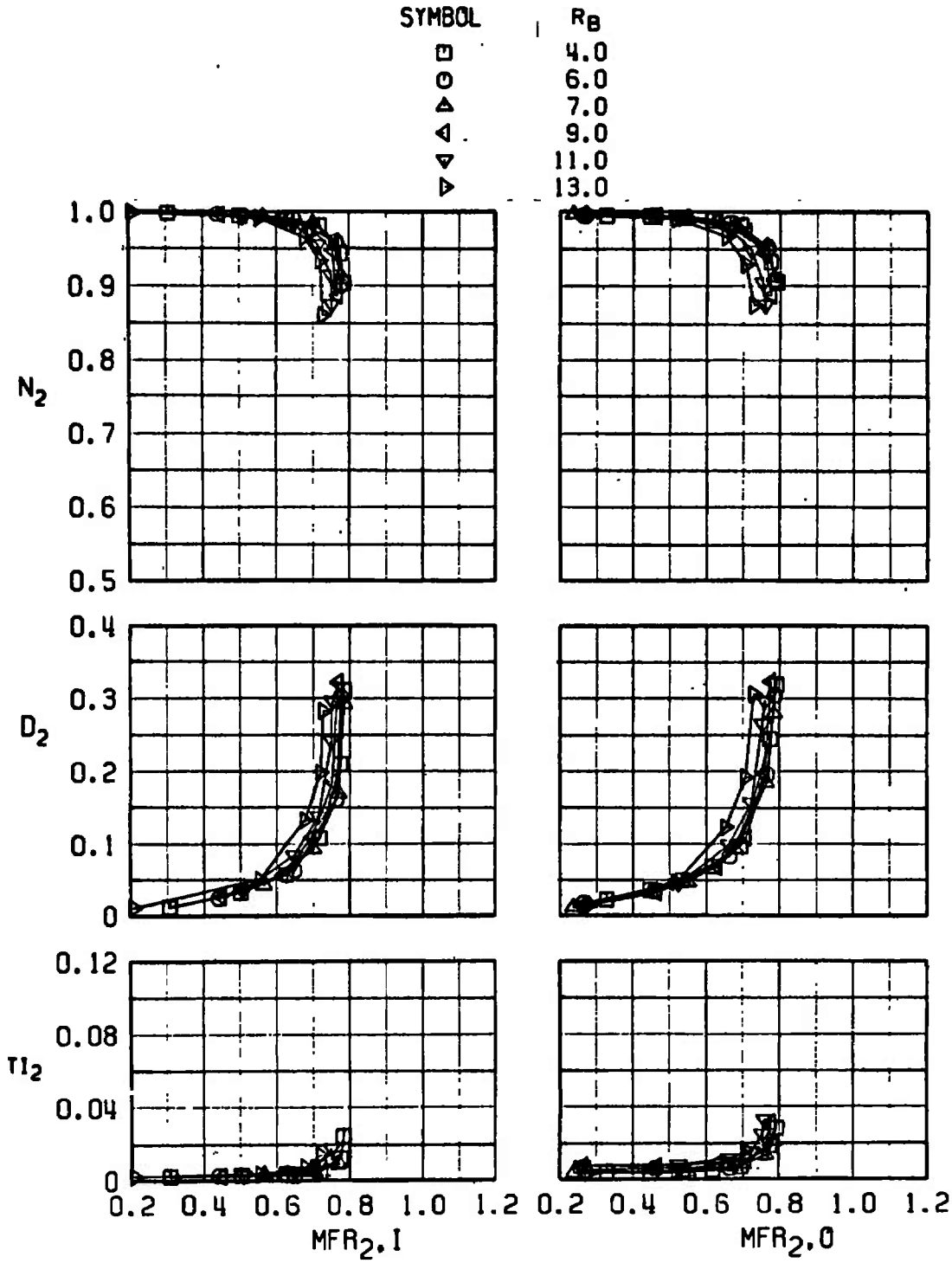

d. TH = 2.6 in.

Fig. 13 Continued

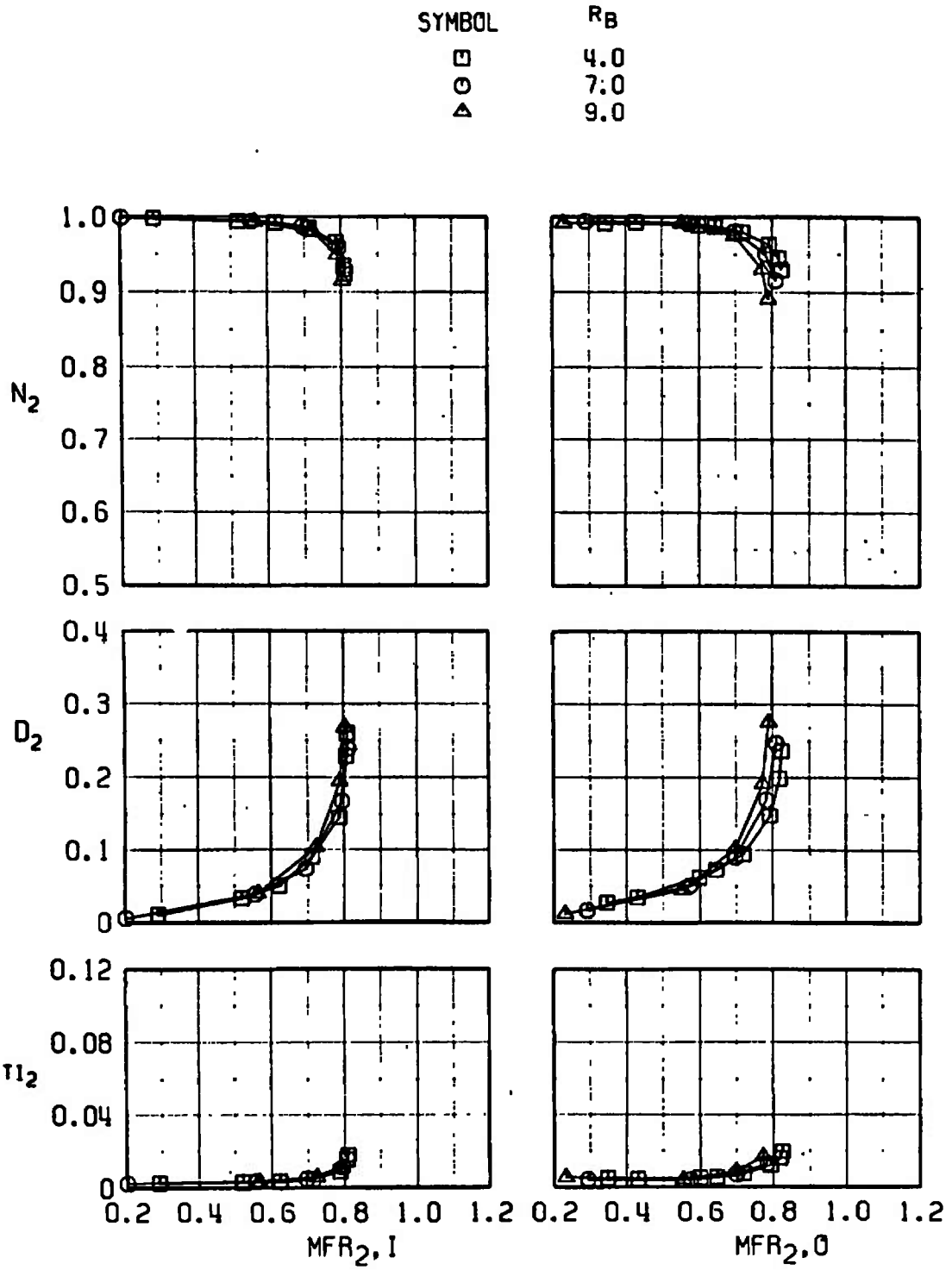

e. TH = 2.8 in.

Fig. 13 Concluded

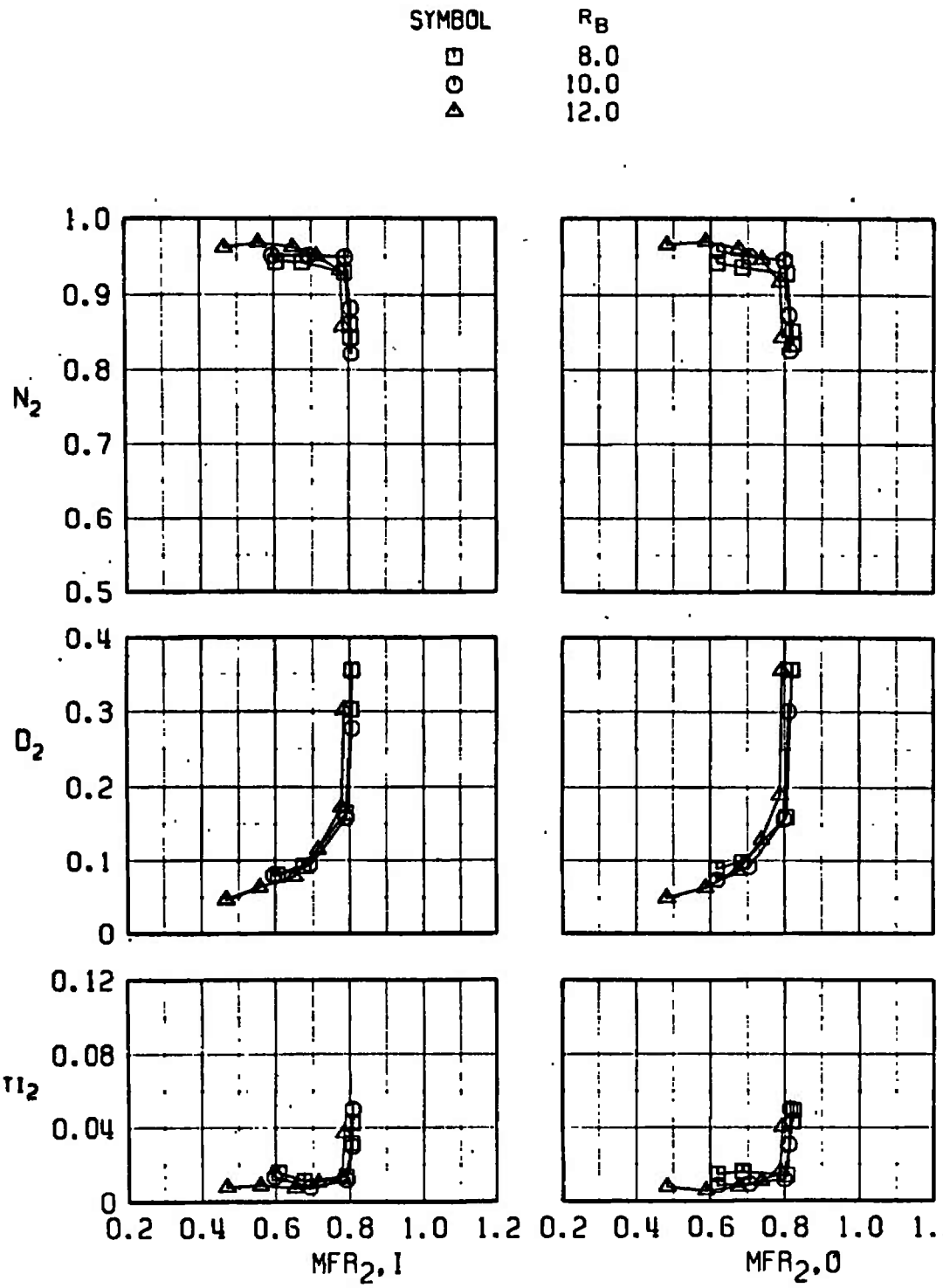

a. TH = 2.2 in.

Fig. 14 Effect of Second-Ramp Angle, M_∞ = 1.7, α = 2.5 deg, ψ = 0 deg

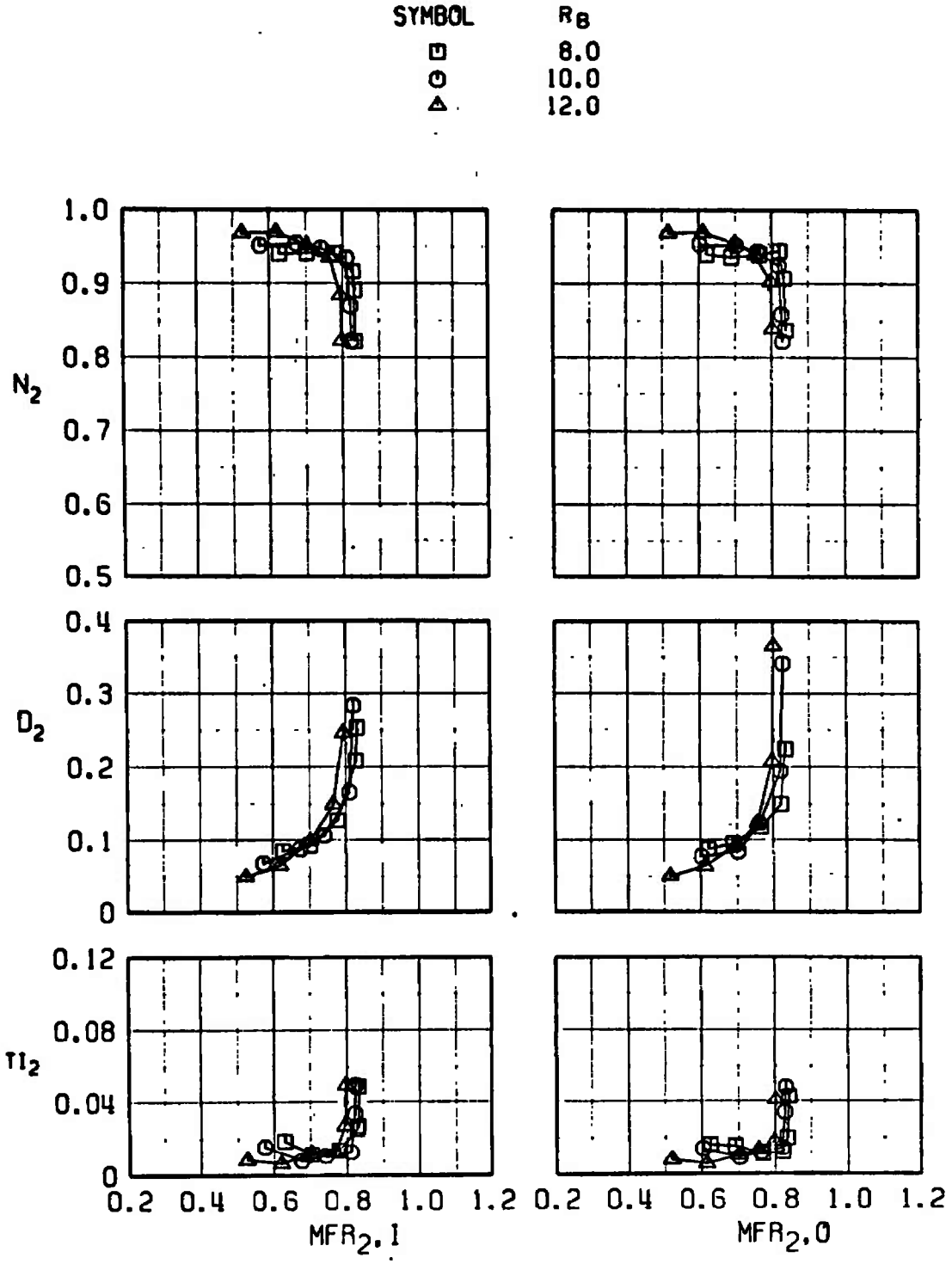

b. TH = 2.3 in.
Fig. 14 Continued

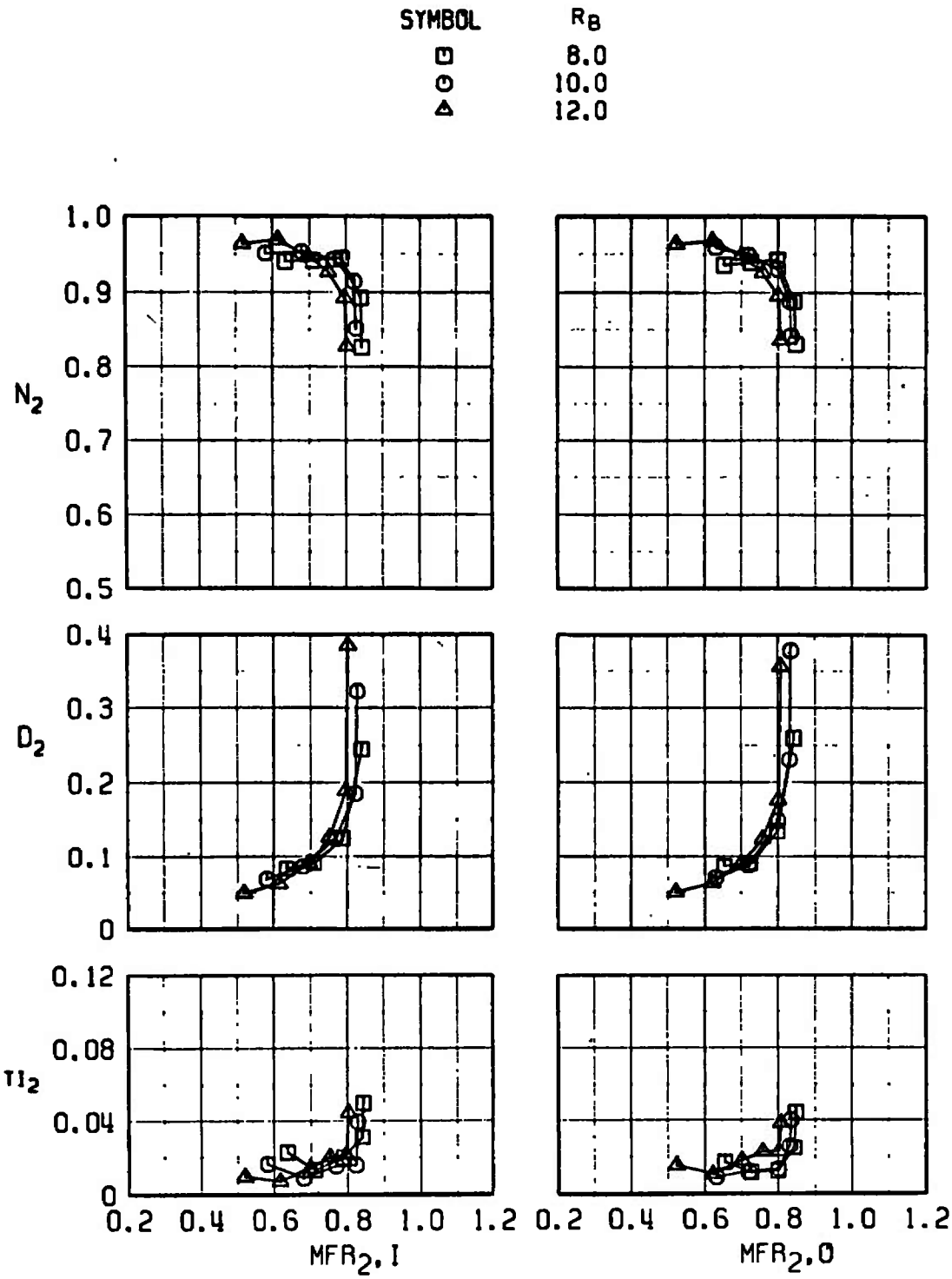

c. TH = 2.4 in.

Fig. 14 Concluded

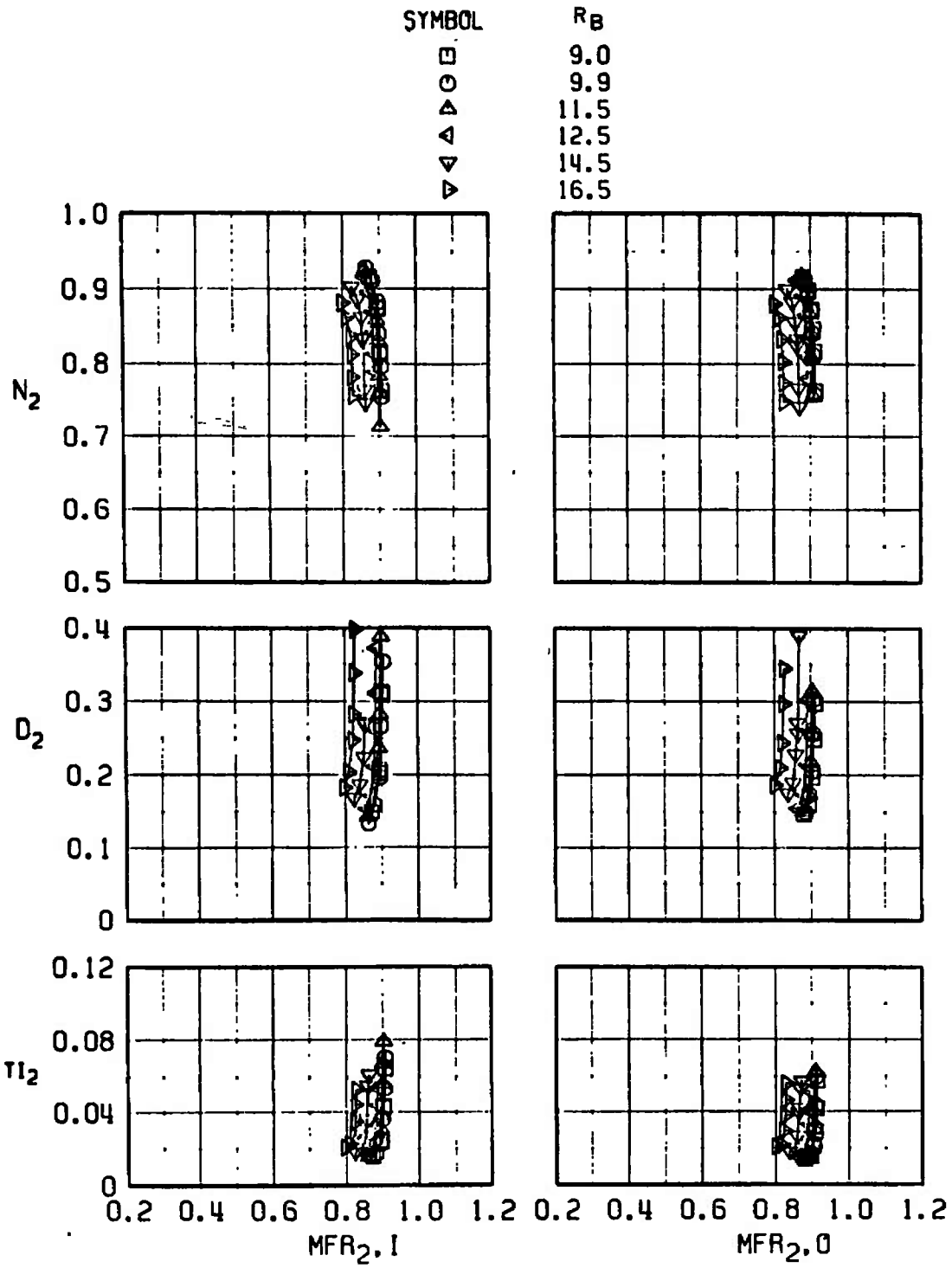

Fig. 15 Effect of Second-Ramp Angle, M_∞ = 2.2, α = 2.5 deg, ψ = 0 deg, TH/TU = 105 percent

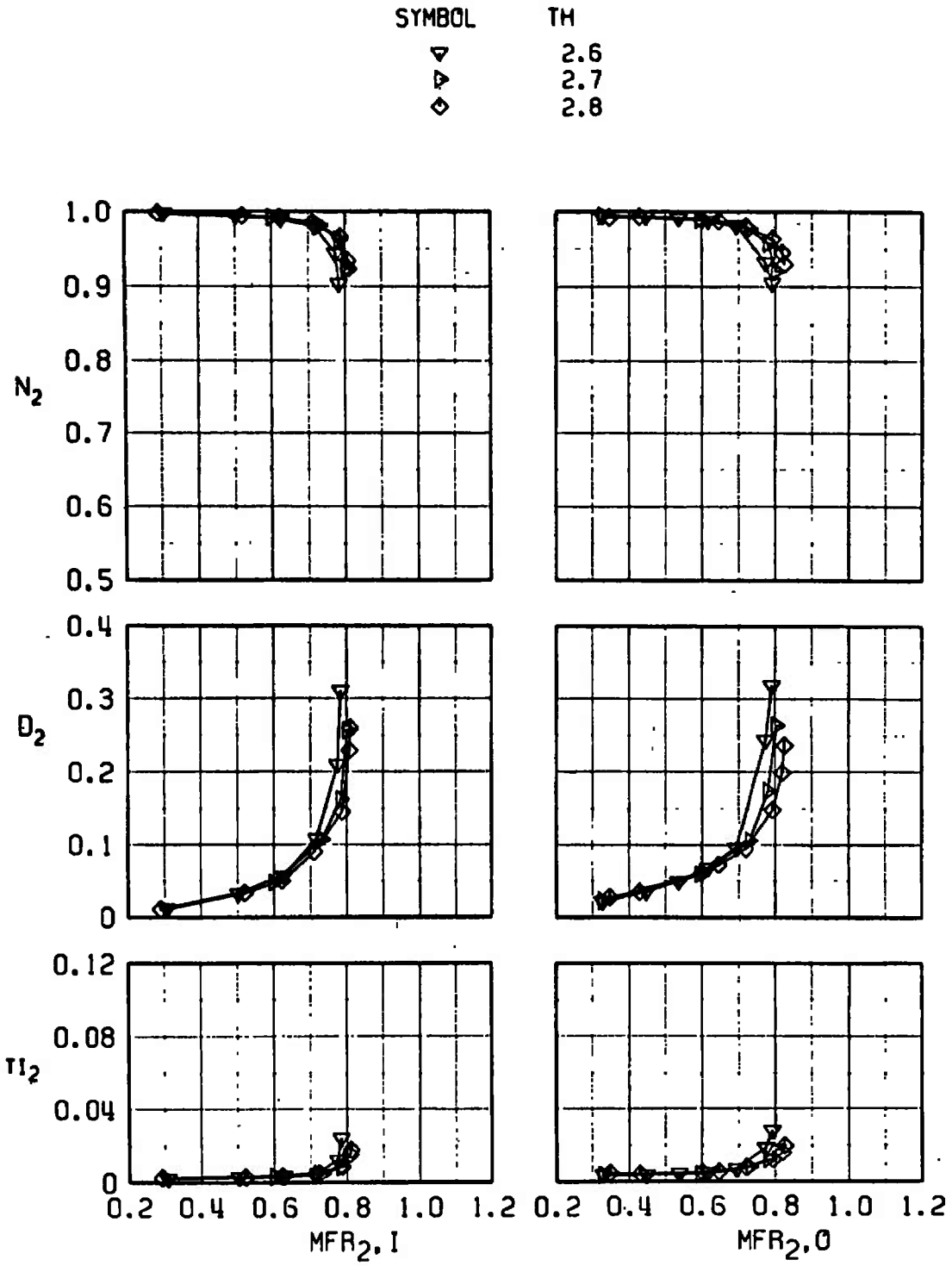

a. R_B = 4 deg

Fig. 16 Effect of Throat Height, M_∞ = 0.85, α = 3 deg, ψ = 0 deg

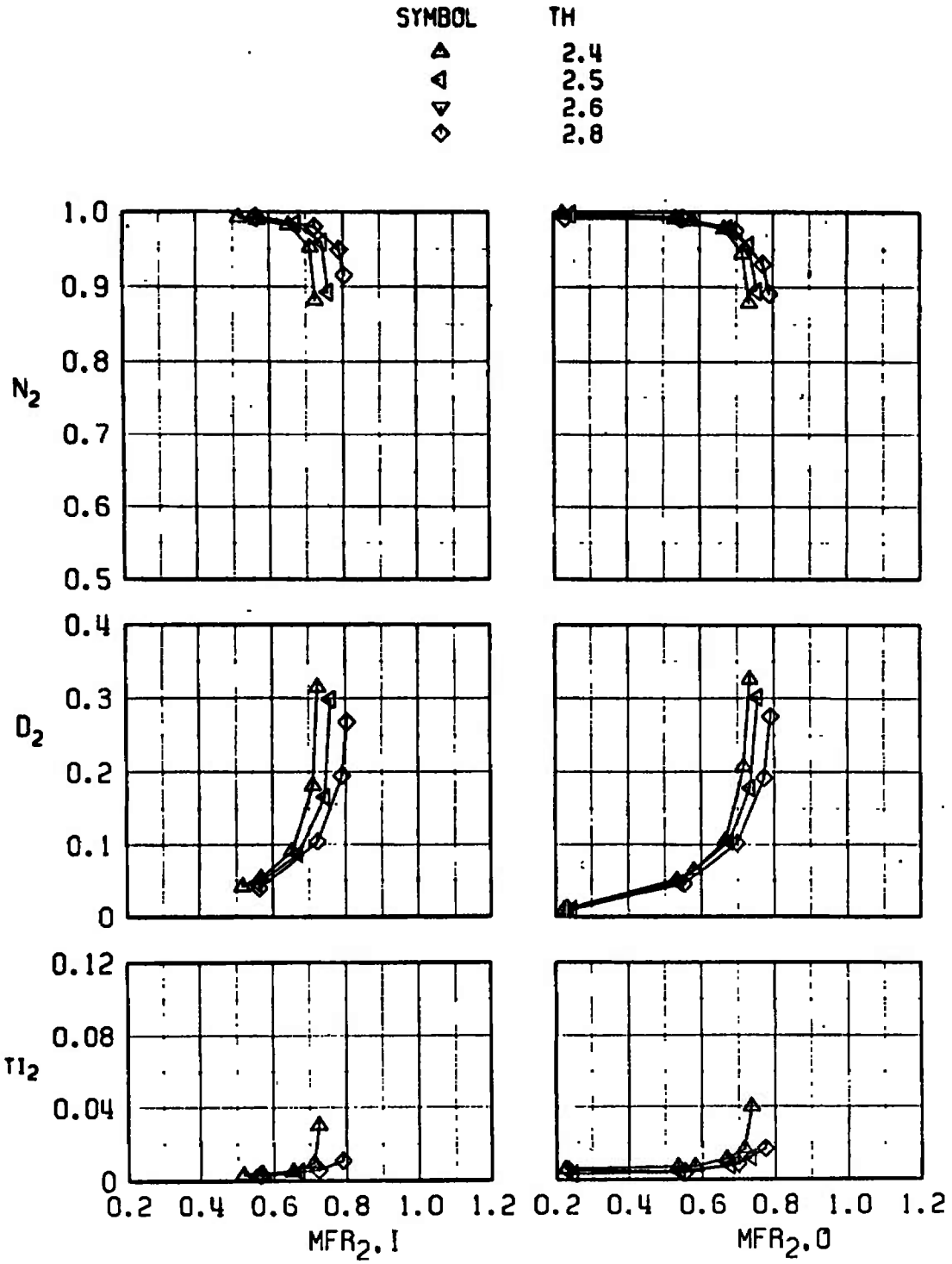

b. R_B = 9 deg
Fig. 16 Continued

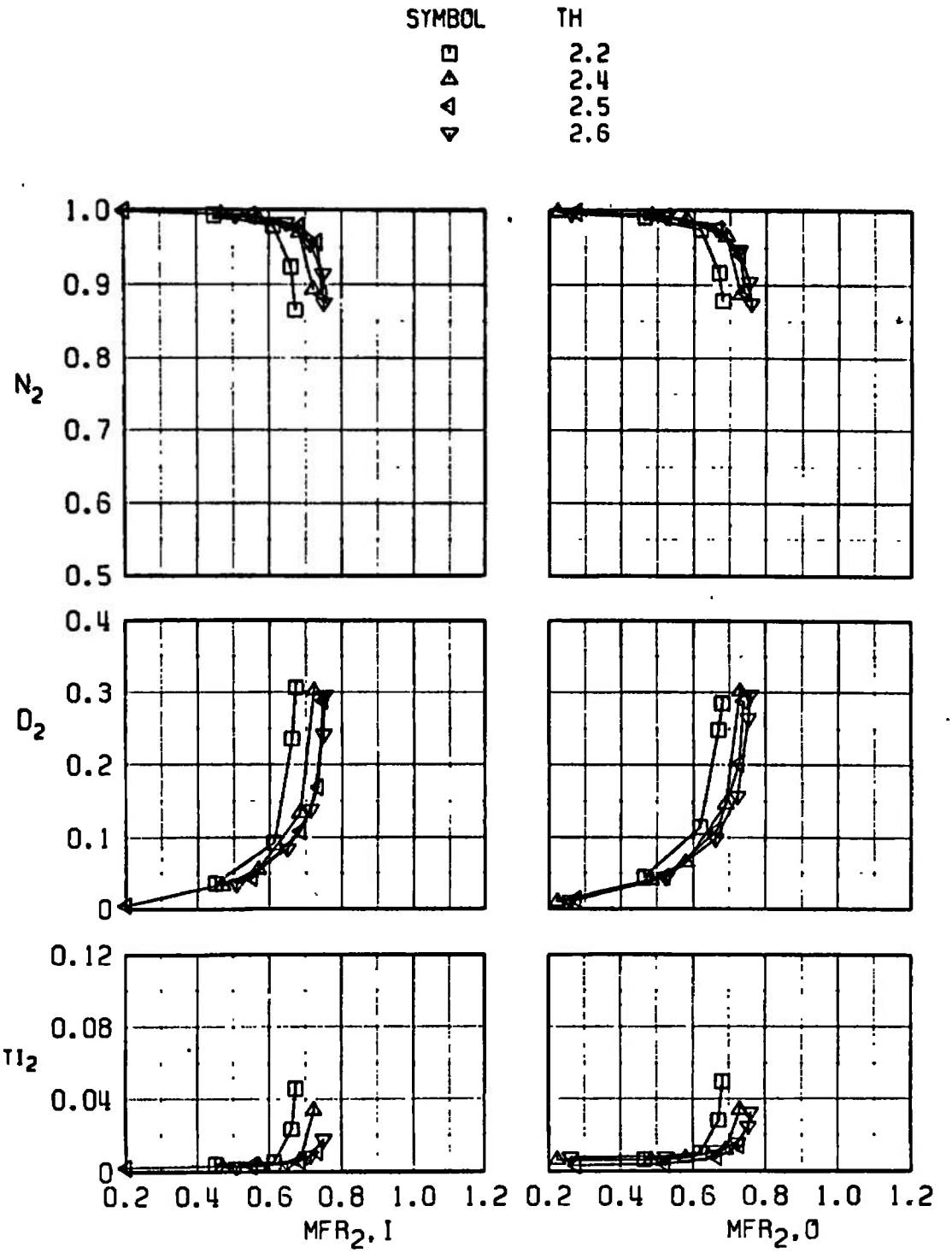

c. R_B = 11 deg
Fig. 16 Continued

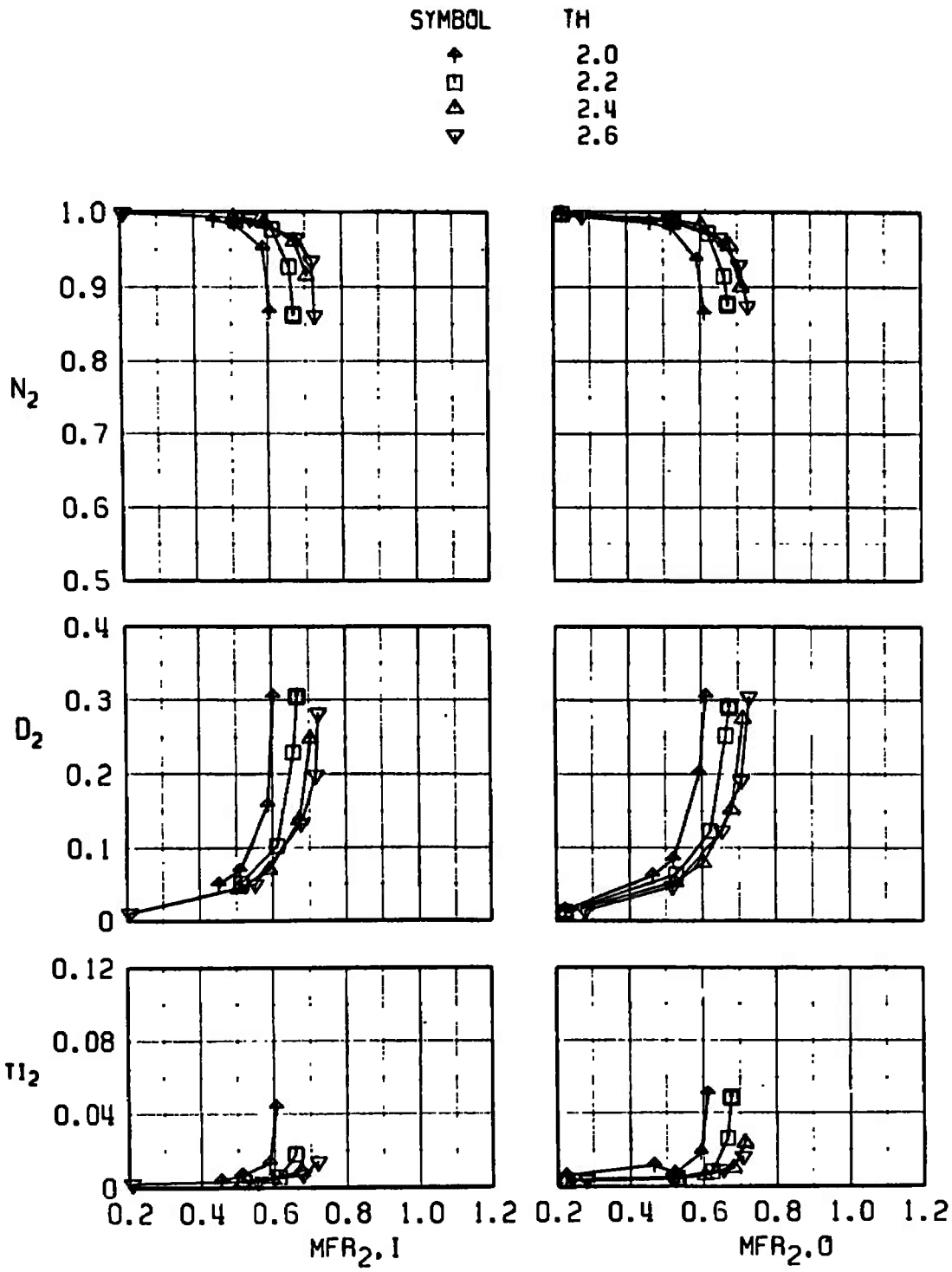

d. R_B = 13 deg
Fig. 16 Continued

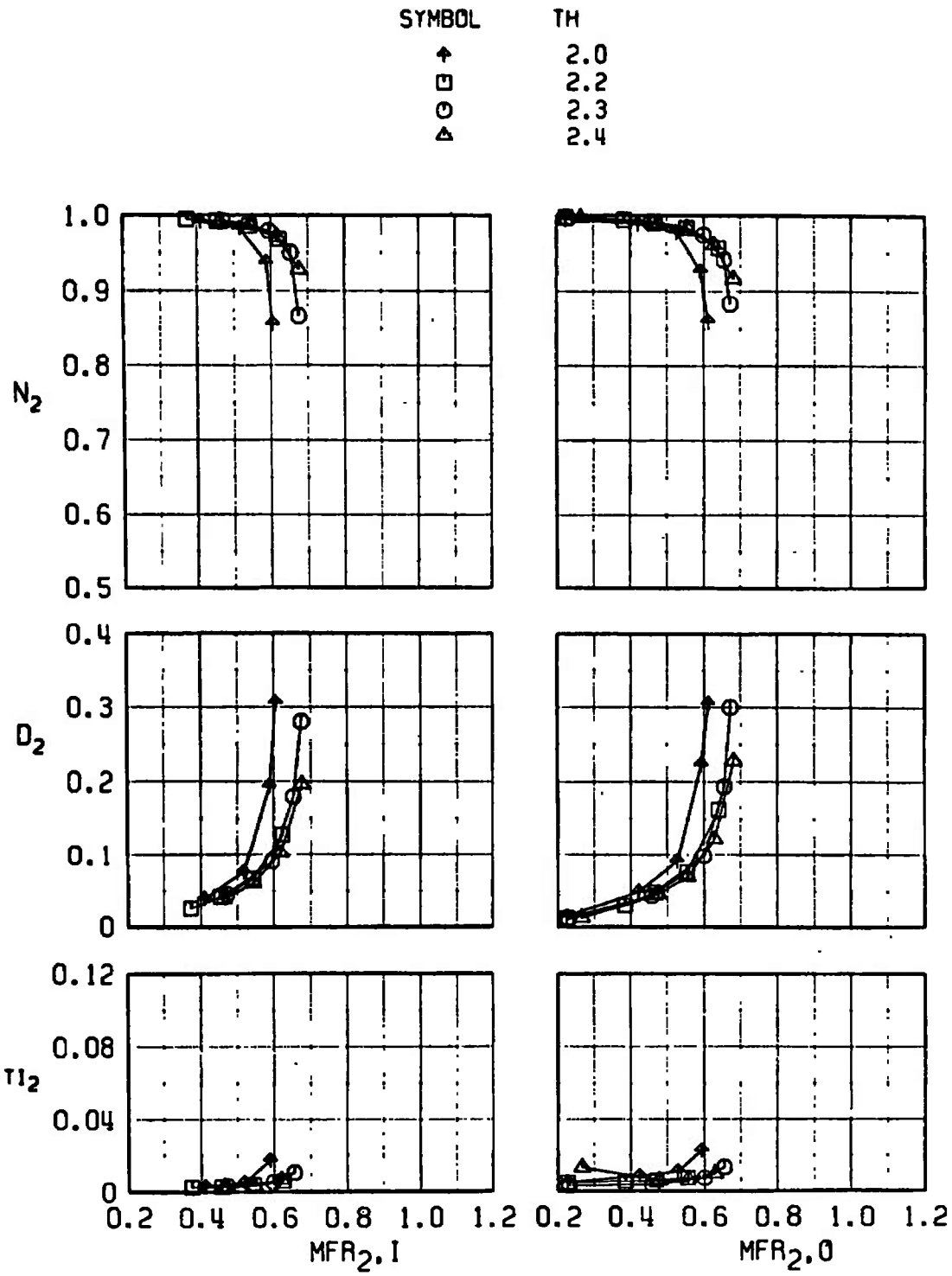

e. R_B = 15 deg

Fig. 16 Concluded

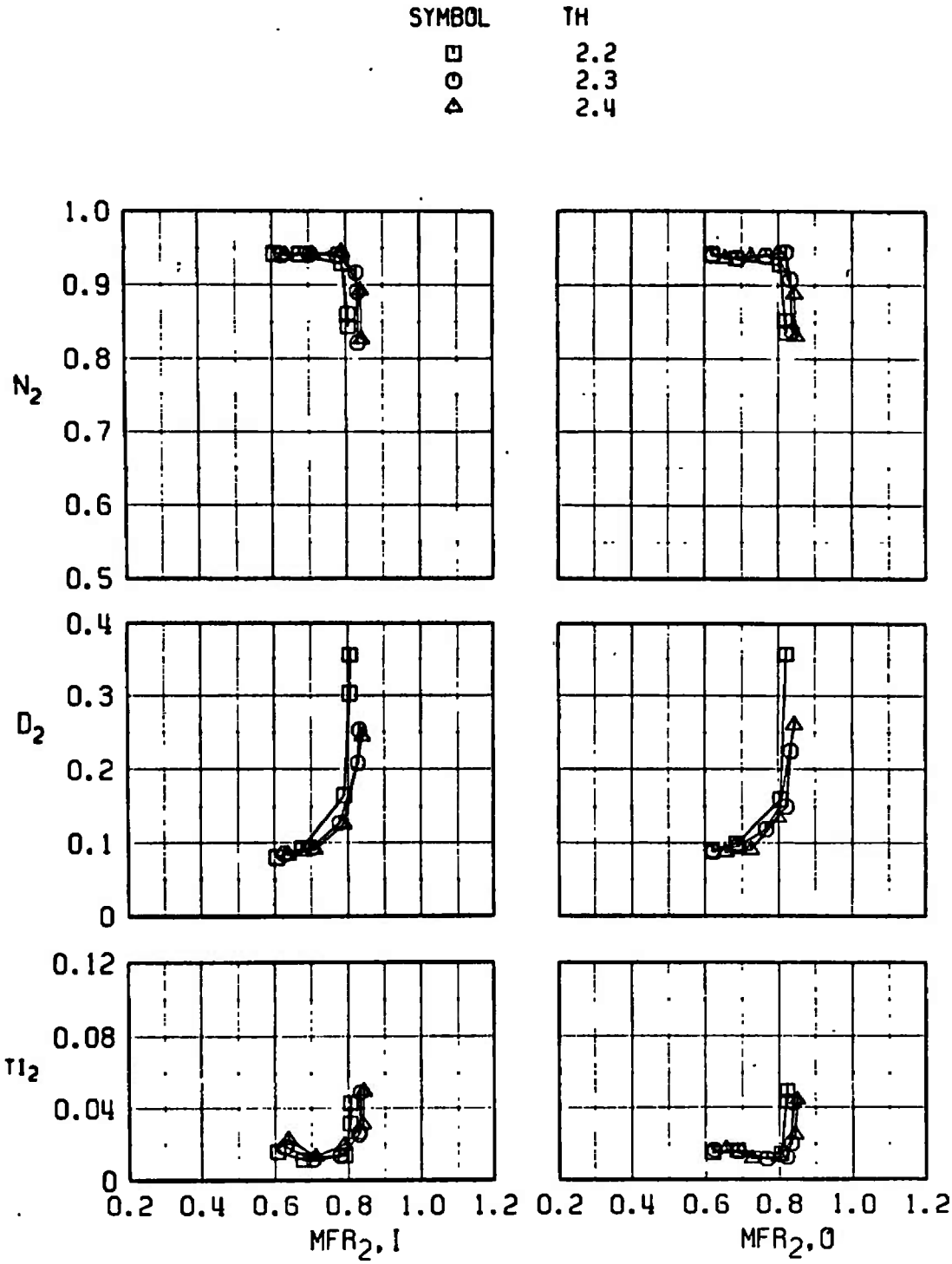

a. R_B = 8 deg

Fig. 17 Effect of Throat Height, M_∞ = 1.7, α = 2.5 deg, ψ = 0 deg

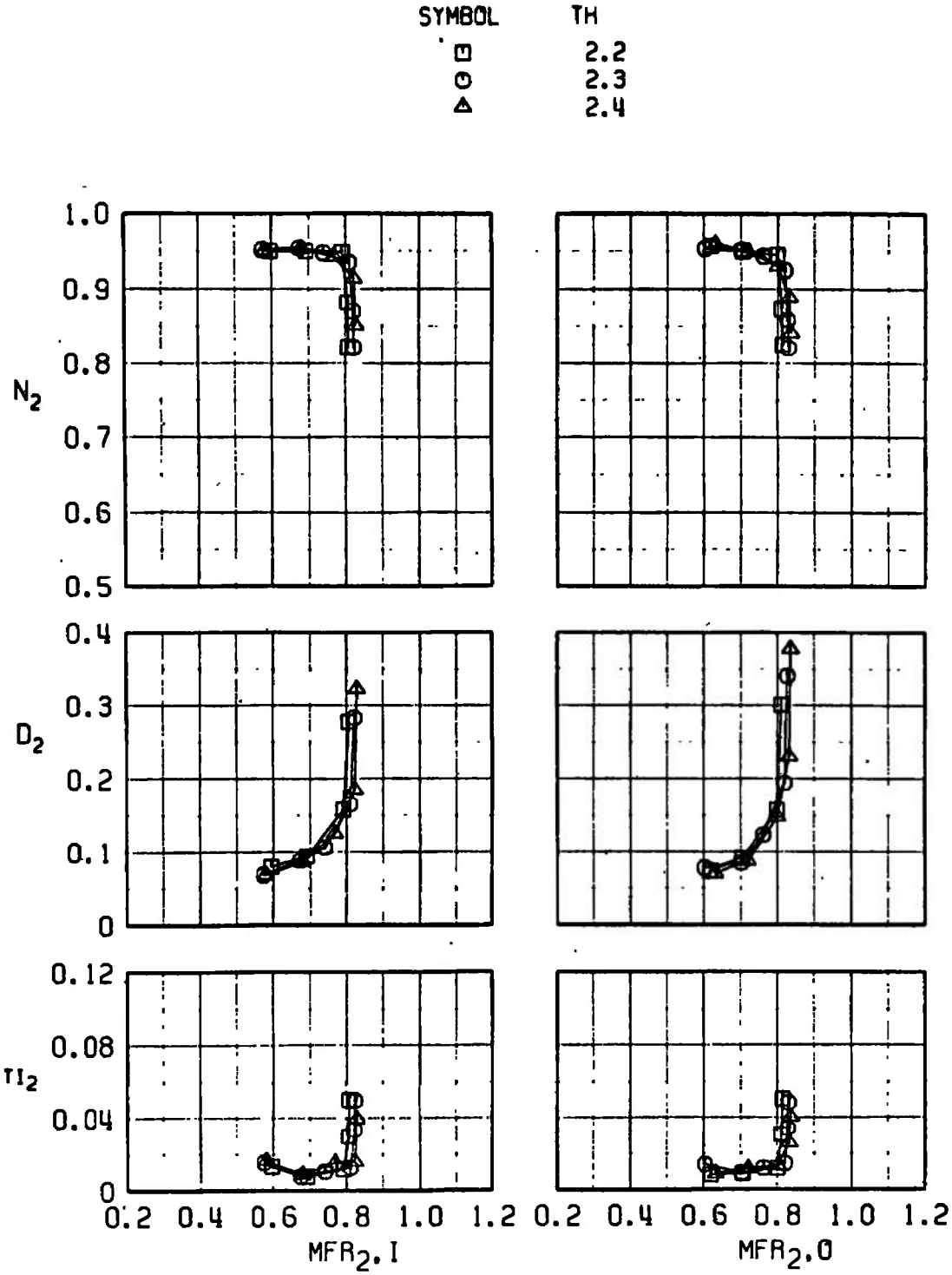

b. R_B = 10 deg
Fig. 17 Continued

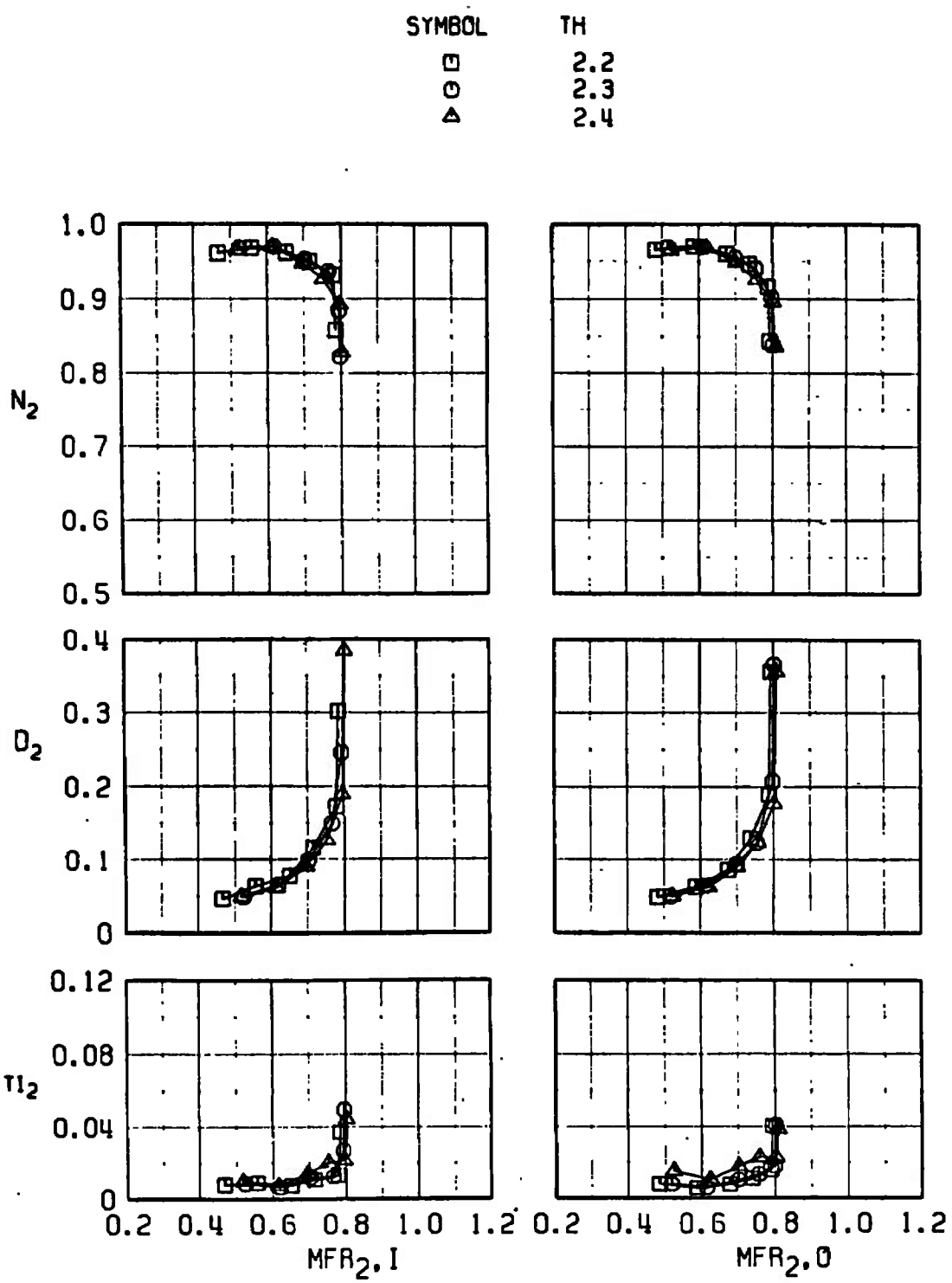

c. R_B = 12 deg

Fig. 17 Concluded

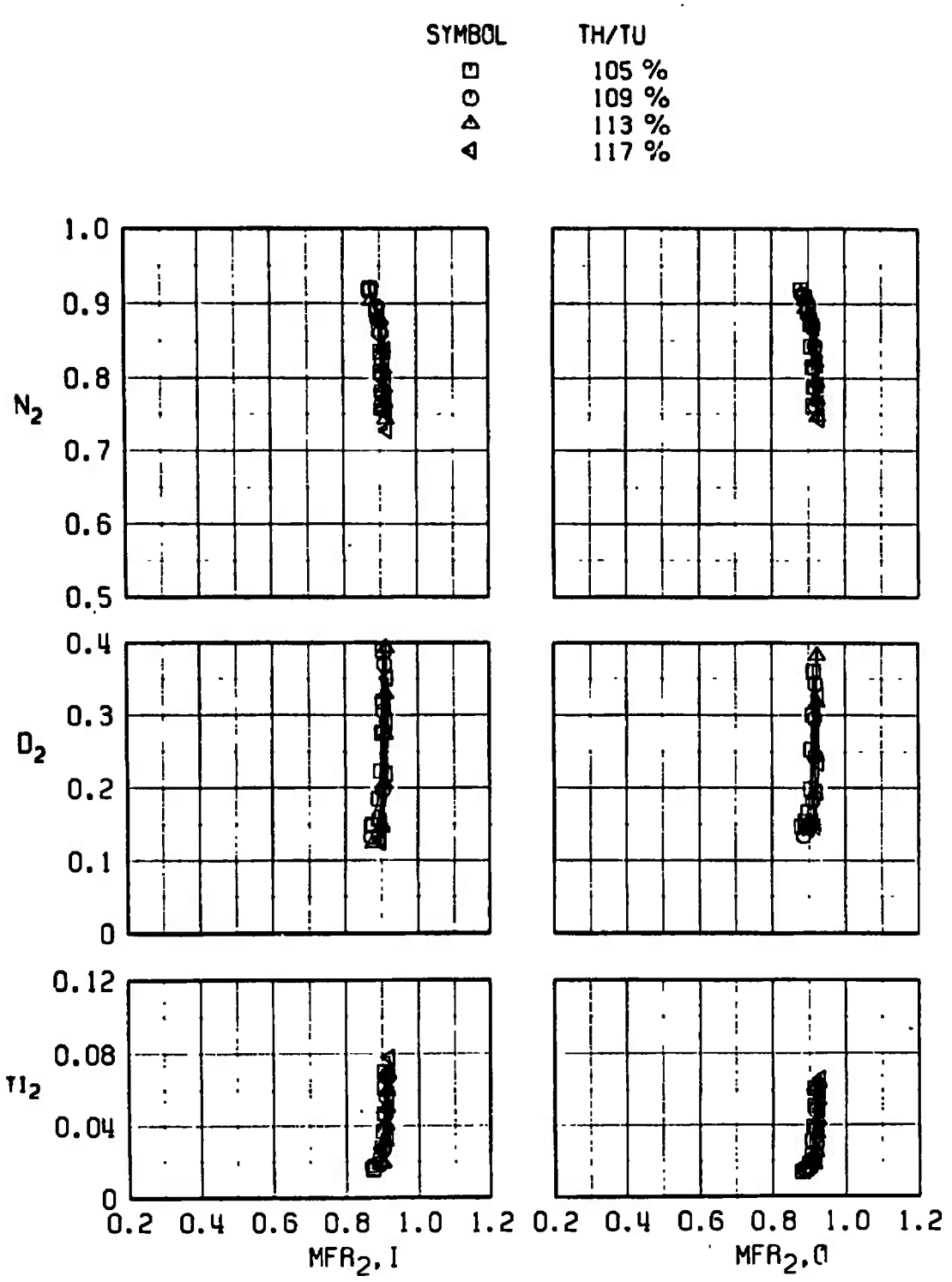

Fig. 18 Effect of Throat Height, M_∞ = 2.2, α = 2.5 deg, ψ = 0 deg, Scheduled R_B

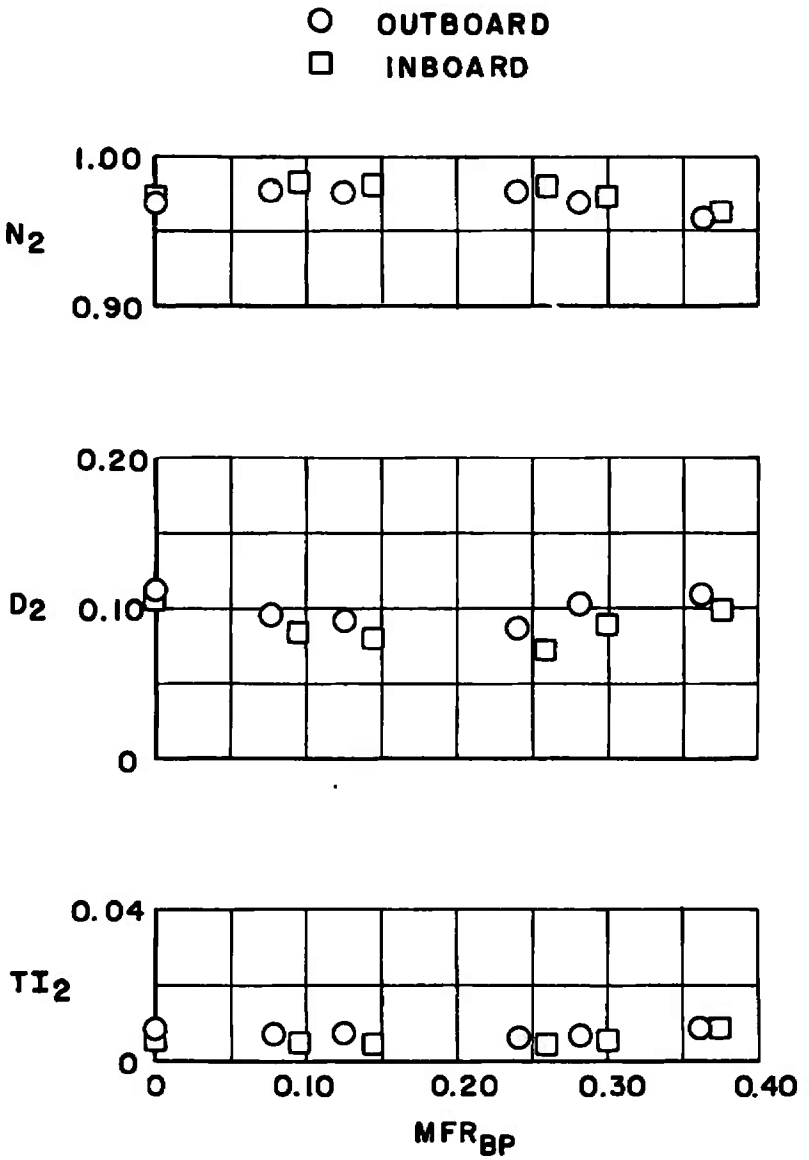

a. α = 3 deg

Fig. 19 Effect of Bypass Doors, M_∞ = 1.4, ψ = 0 deg, Scheduled R_B and TH

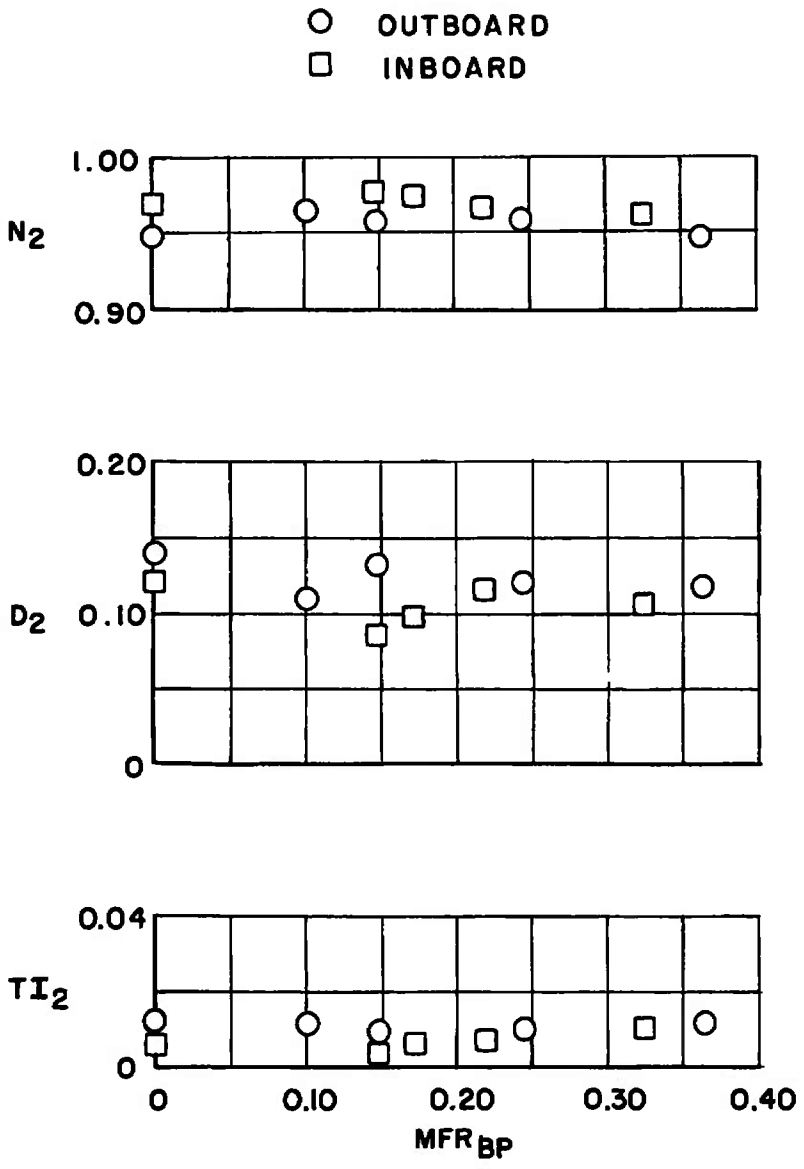

b. α = 9 deg
Fig. 19 Concluded

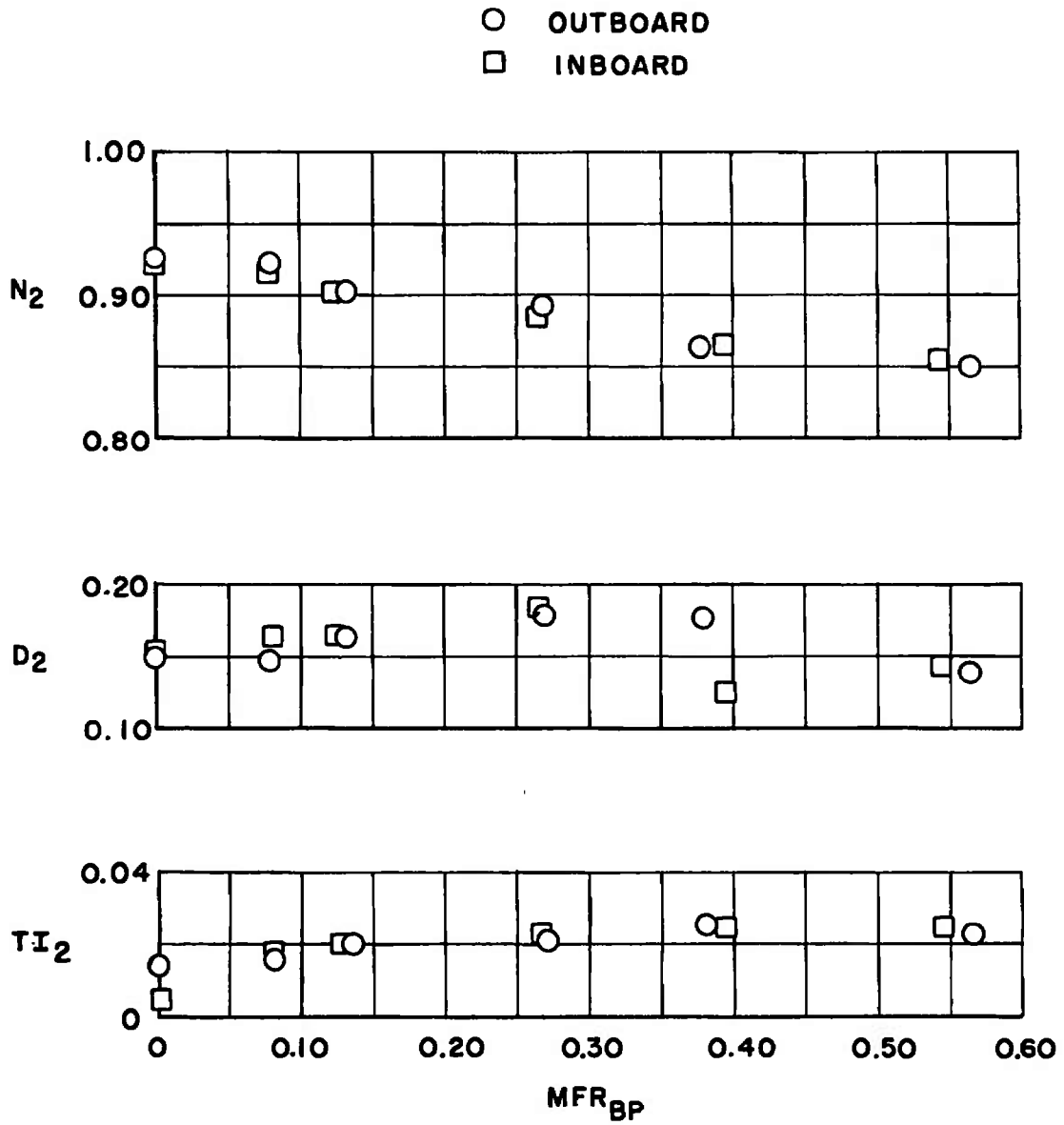

Fig. 20 Effect of Bypass Doors, M_∞ = 2.2, α = 2.5 deg, ψ = 0 deg, TH/TU = 105 percent, Scheduled R_B

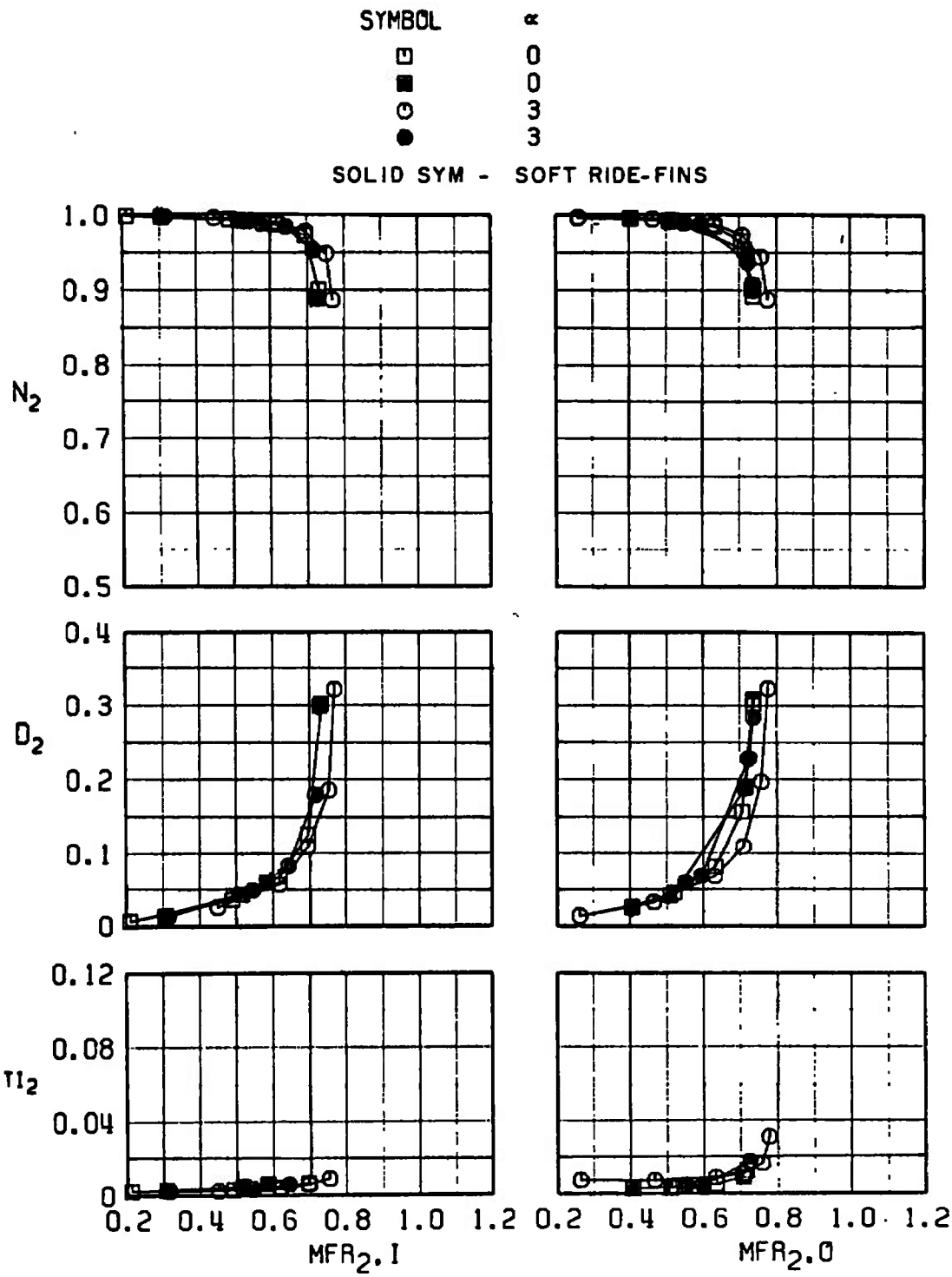

Fig. 21 Effect of Soft-Ride Fins, M_∞ = 0.85, ψ = 0 deg, R_B = 9 deg, TH = 2.4 in.

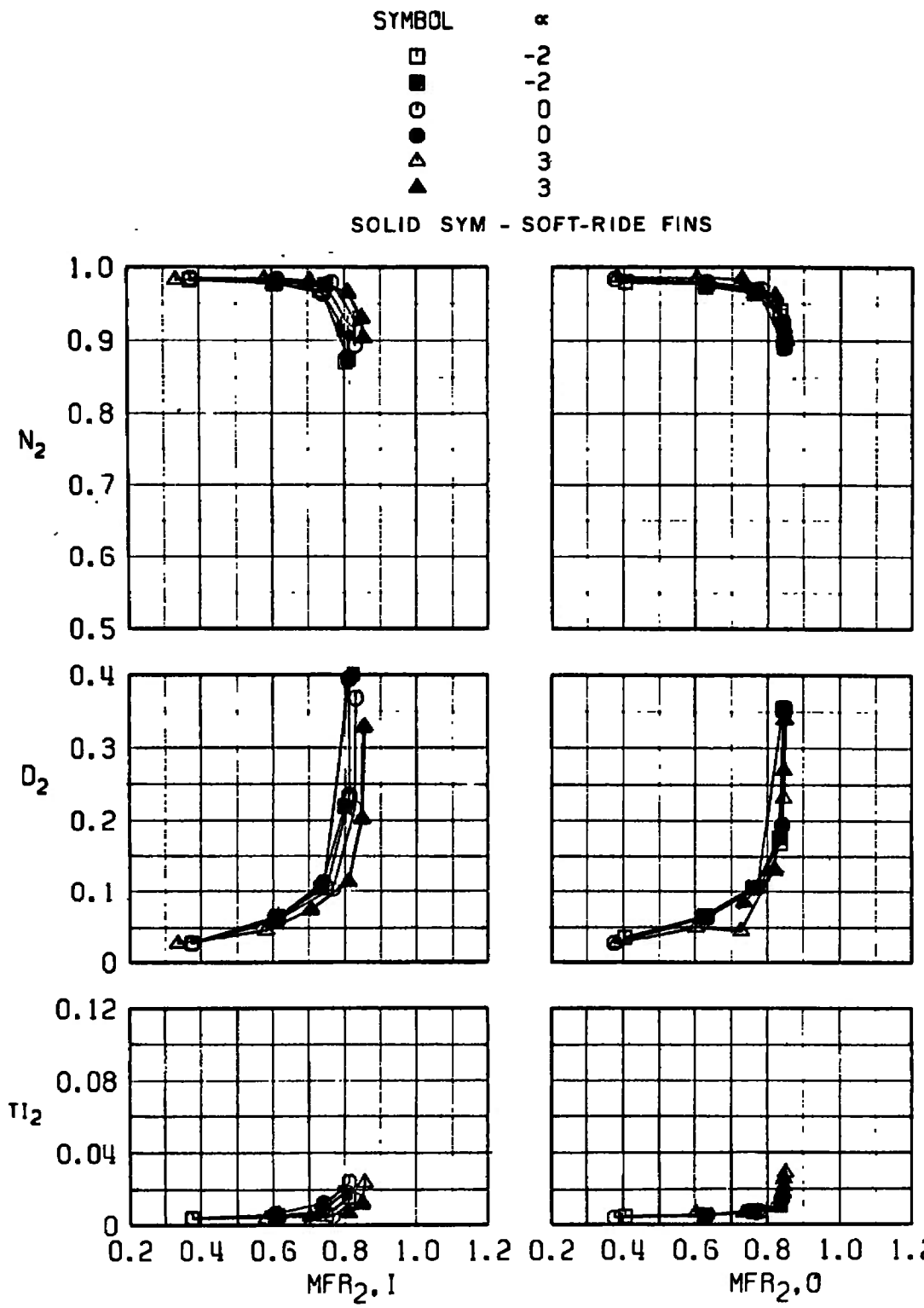

Fig. 22 Effect of Soft-Ride Fins, $M_\infty = 1.4$, $\psi = 0$ deg, Scheduled R_B and TH

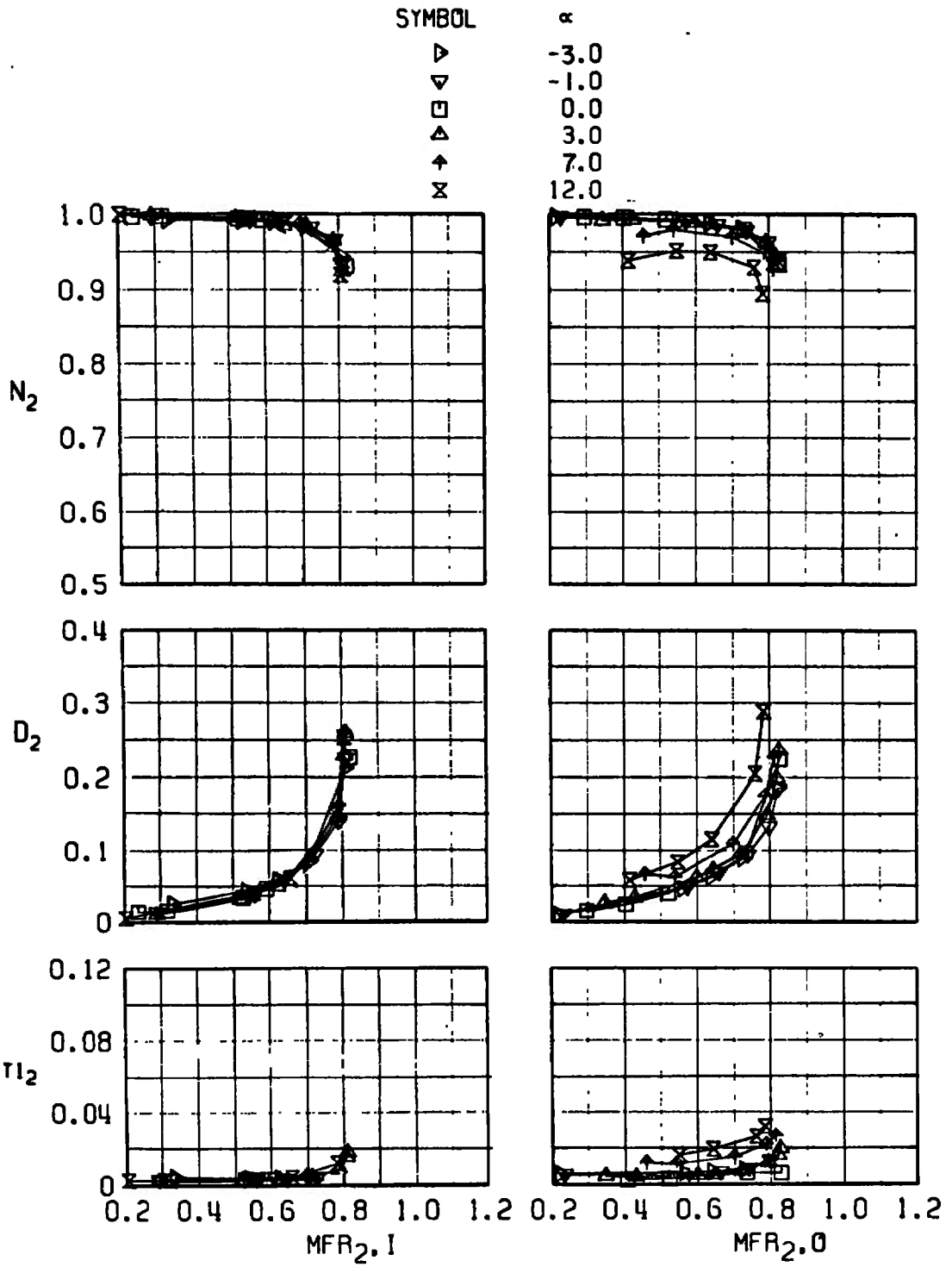

Fig. 23 Effect of Angles of Attack, $M_\infty = 0.85$, $\psi = 0$ deg, Scheduled R_B and TH

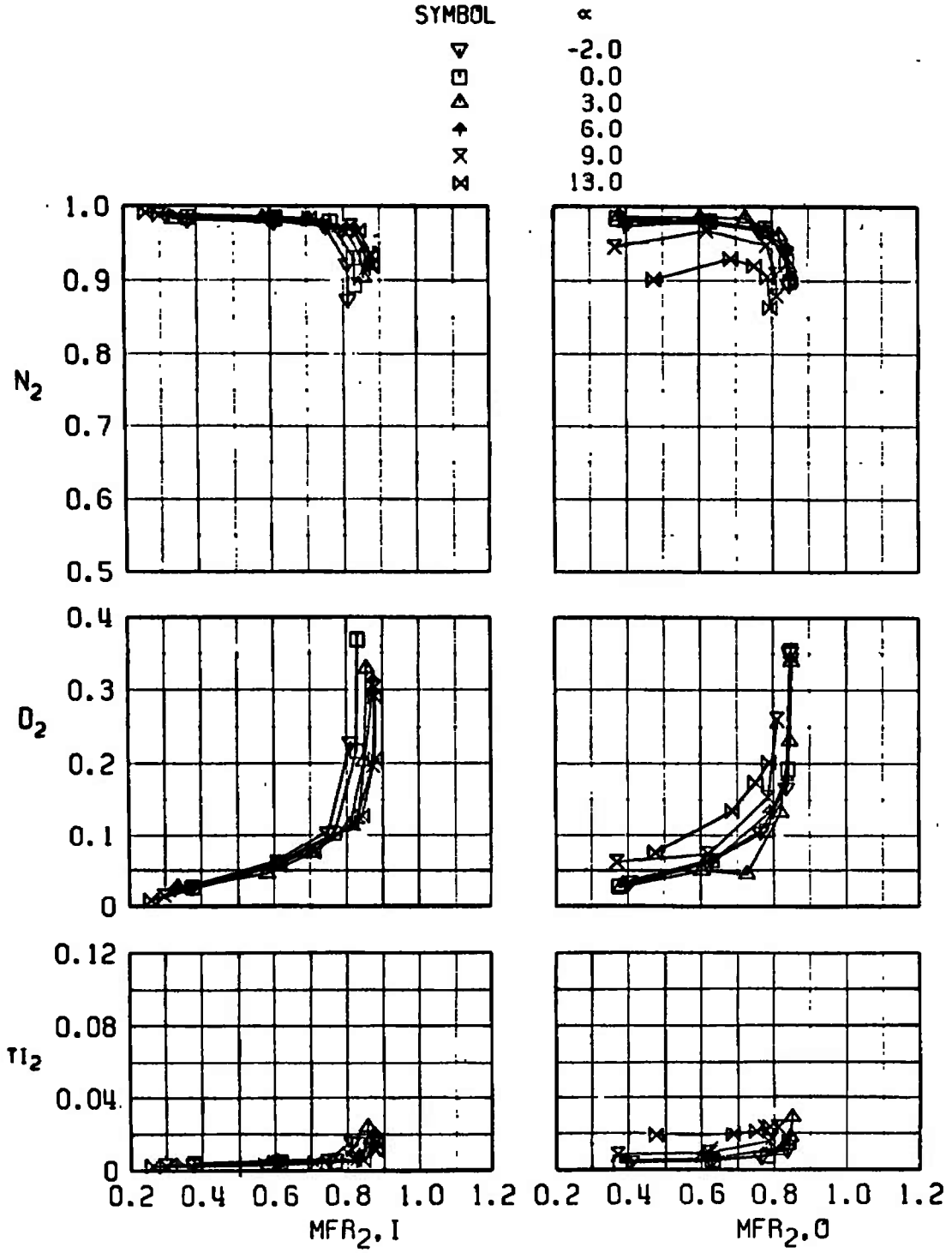

Fig. 24 Effect of Angle of Attack, M_∞ = 1.4, ψ = 0 deg, Scheduled R_B and TH

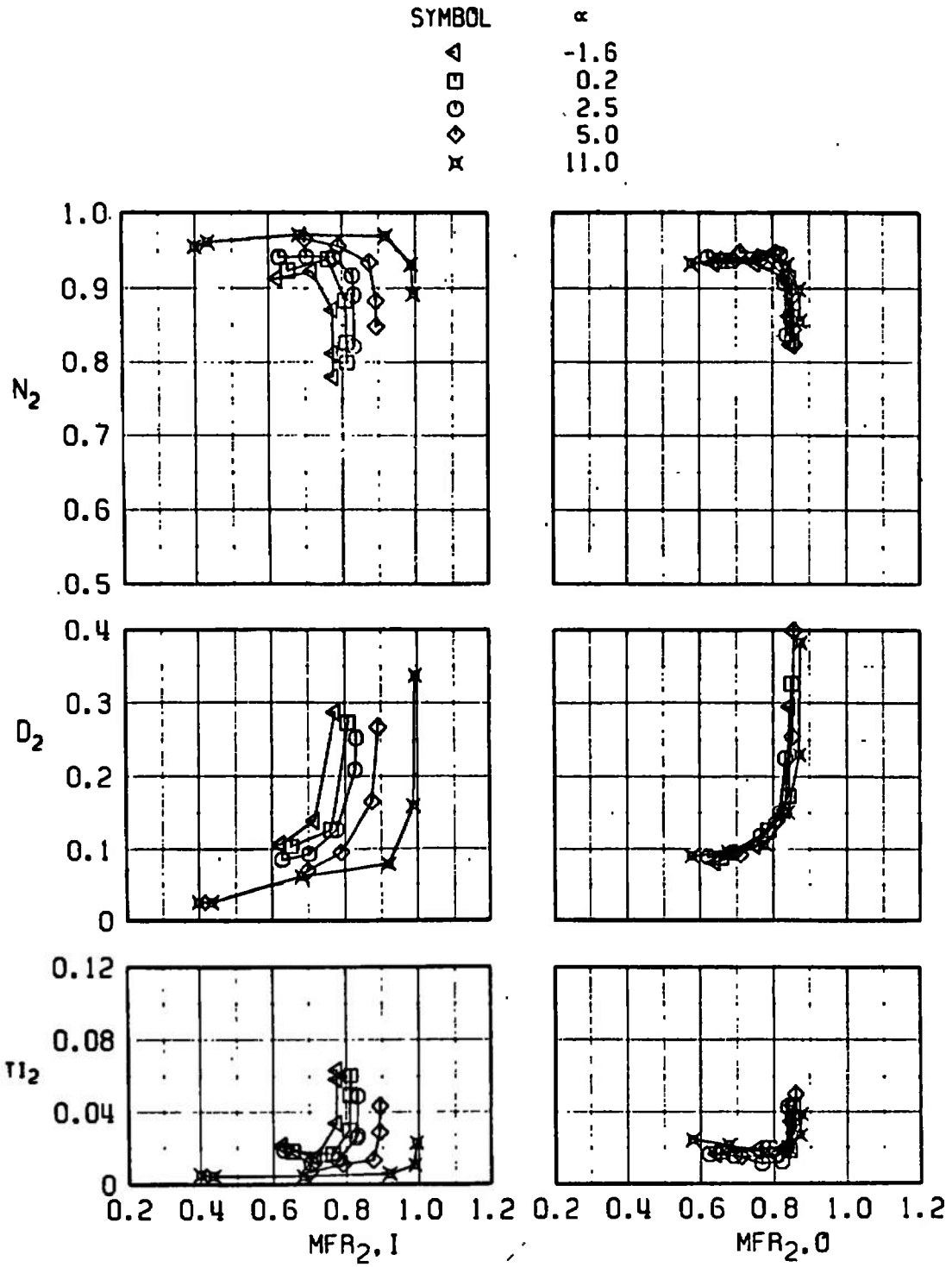

Fig. 25 Effect of Angle of Attack, $M_\infty = 1.7$, $\psi = 0$ deg, Scheduled R_B and TH

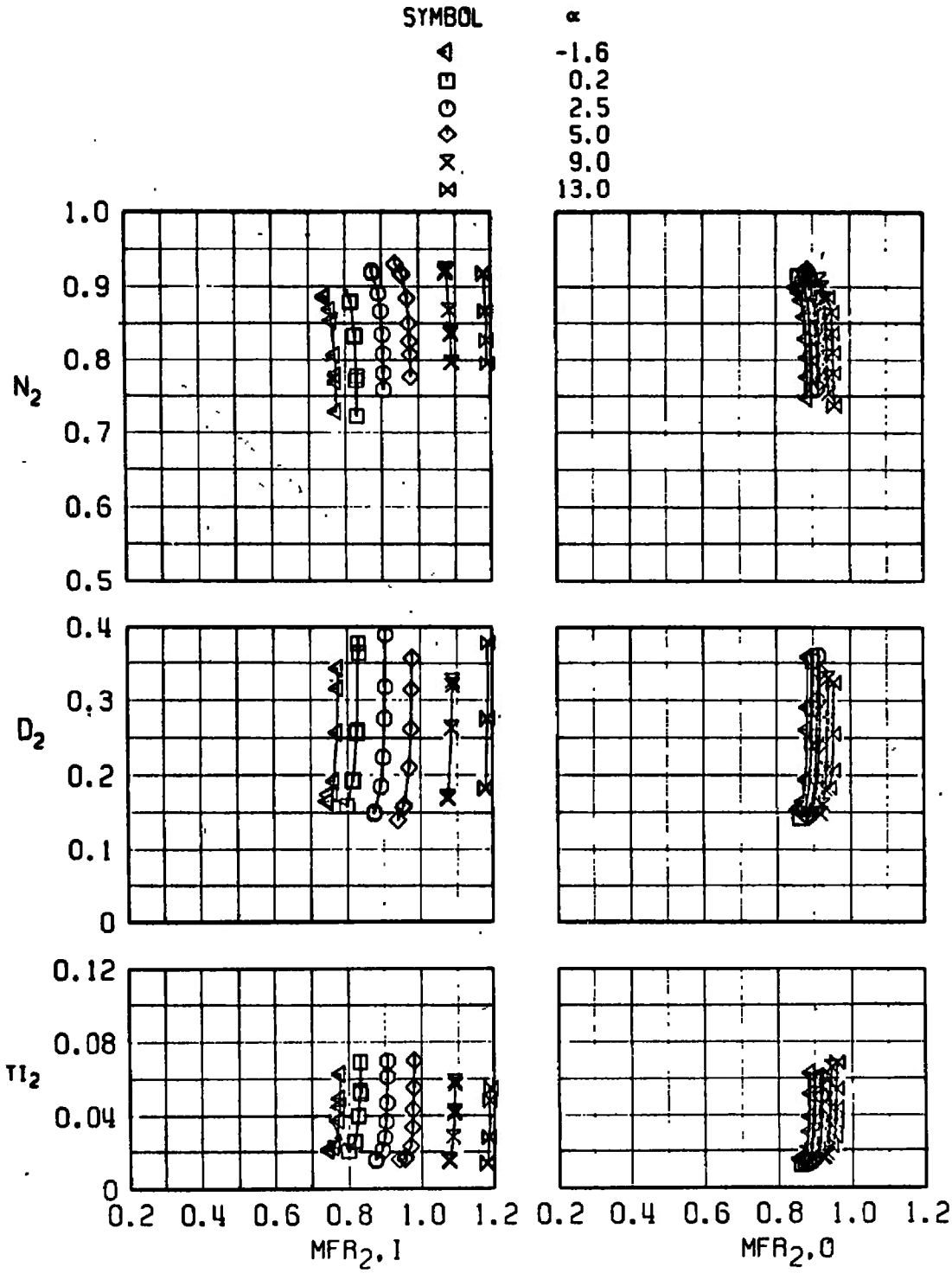

Fig. 26 Effect of Angle of Attack, M_∞ = 2.2, ψ = 0 deg, TH/TU = 105 percent, Scheduled R_B

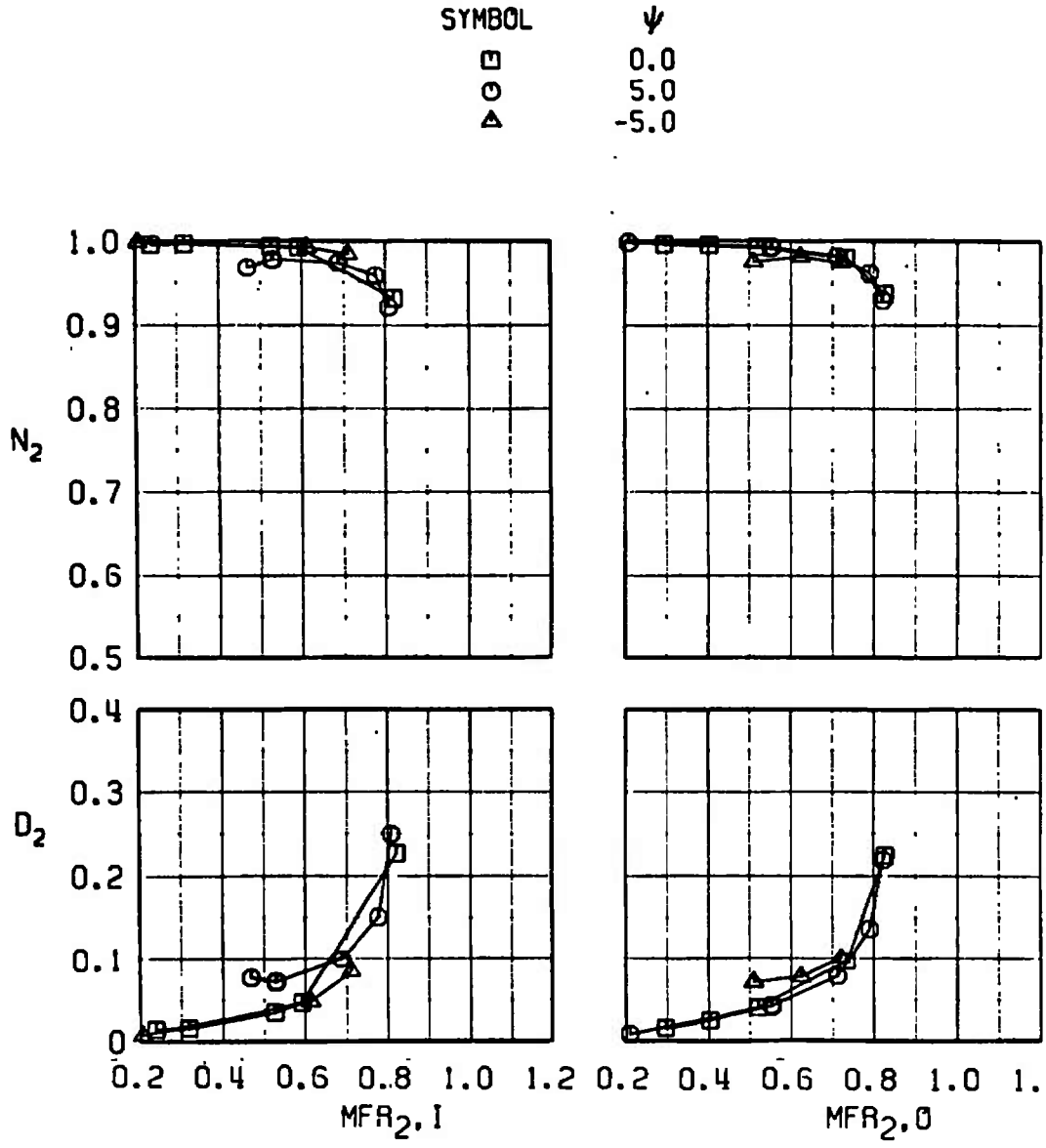

a. α = 0 deg

Fig. 27 Effect of Yaw Angle, M_∞ = 0.85, Scheduled R_B and TH

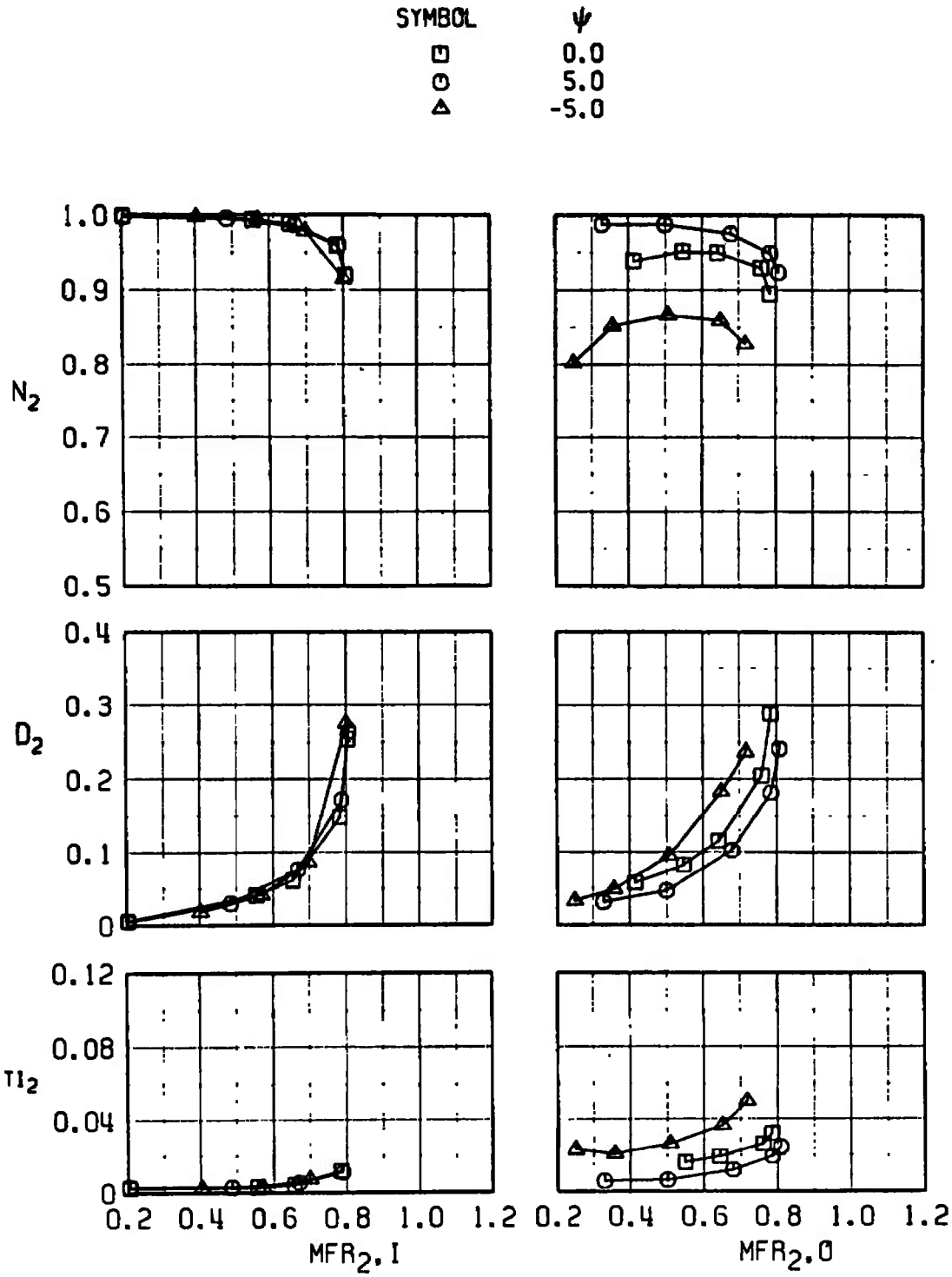

b. α = 12 deg

Fig. 27 Concluded

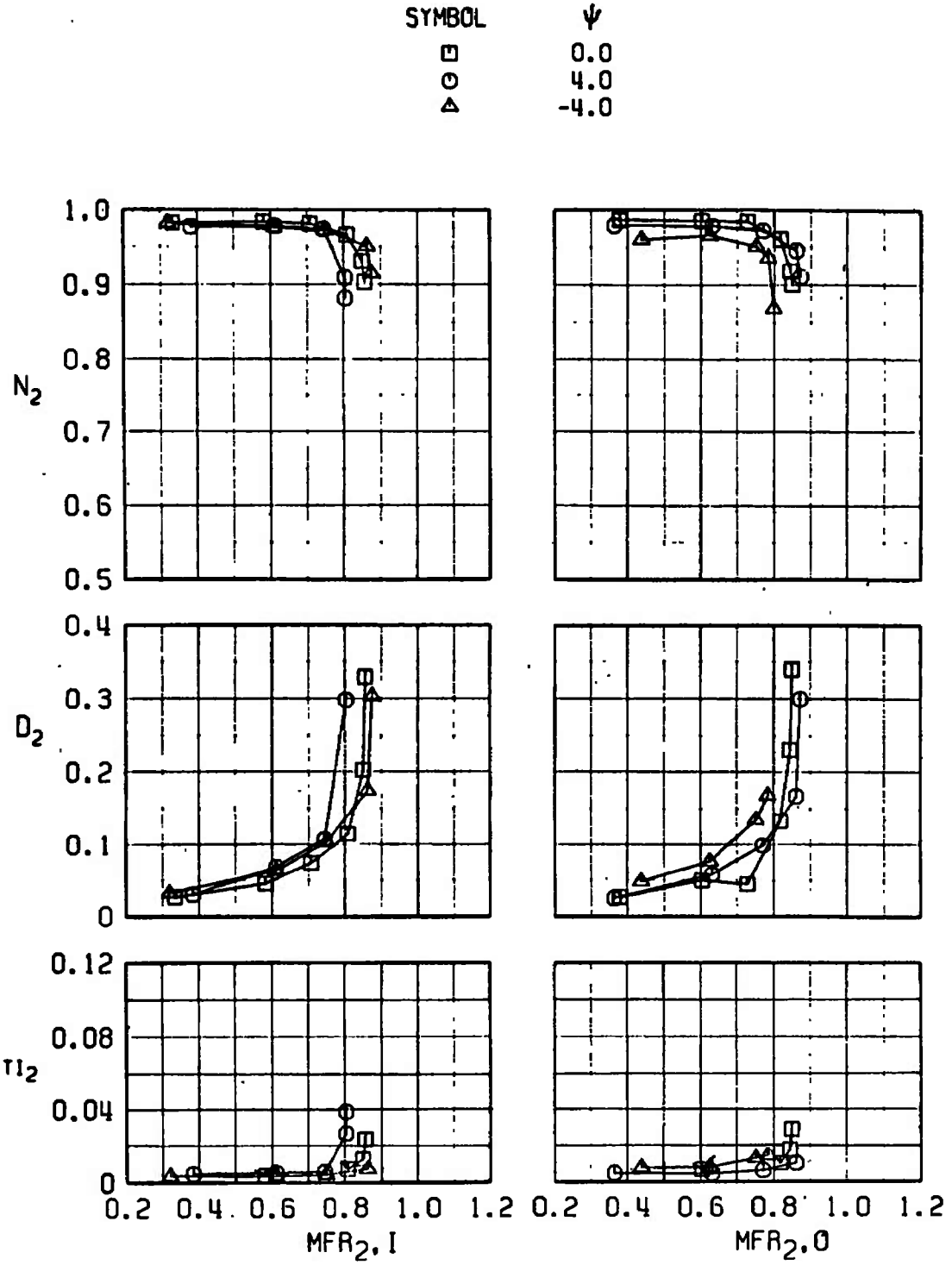

a. α = 3 deg

Fig. 28 Effect of Yaw Angle, M_∞ = 1.4, Scheduled R_B and TH

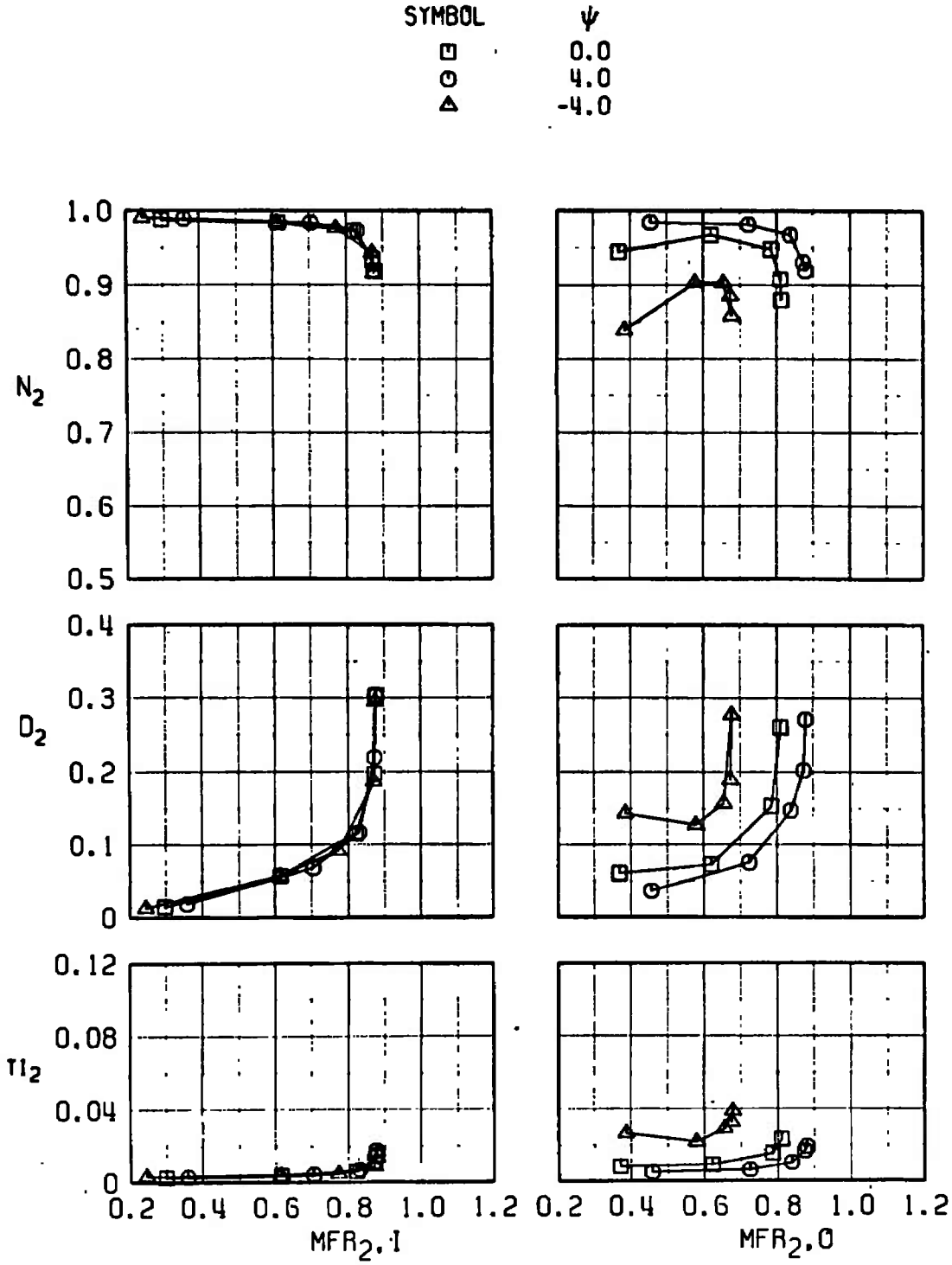

b. α = 9 deg
Fig. 28 Concluded

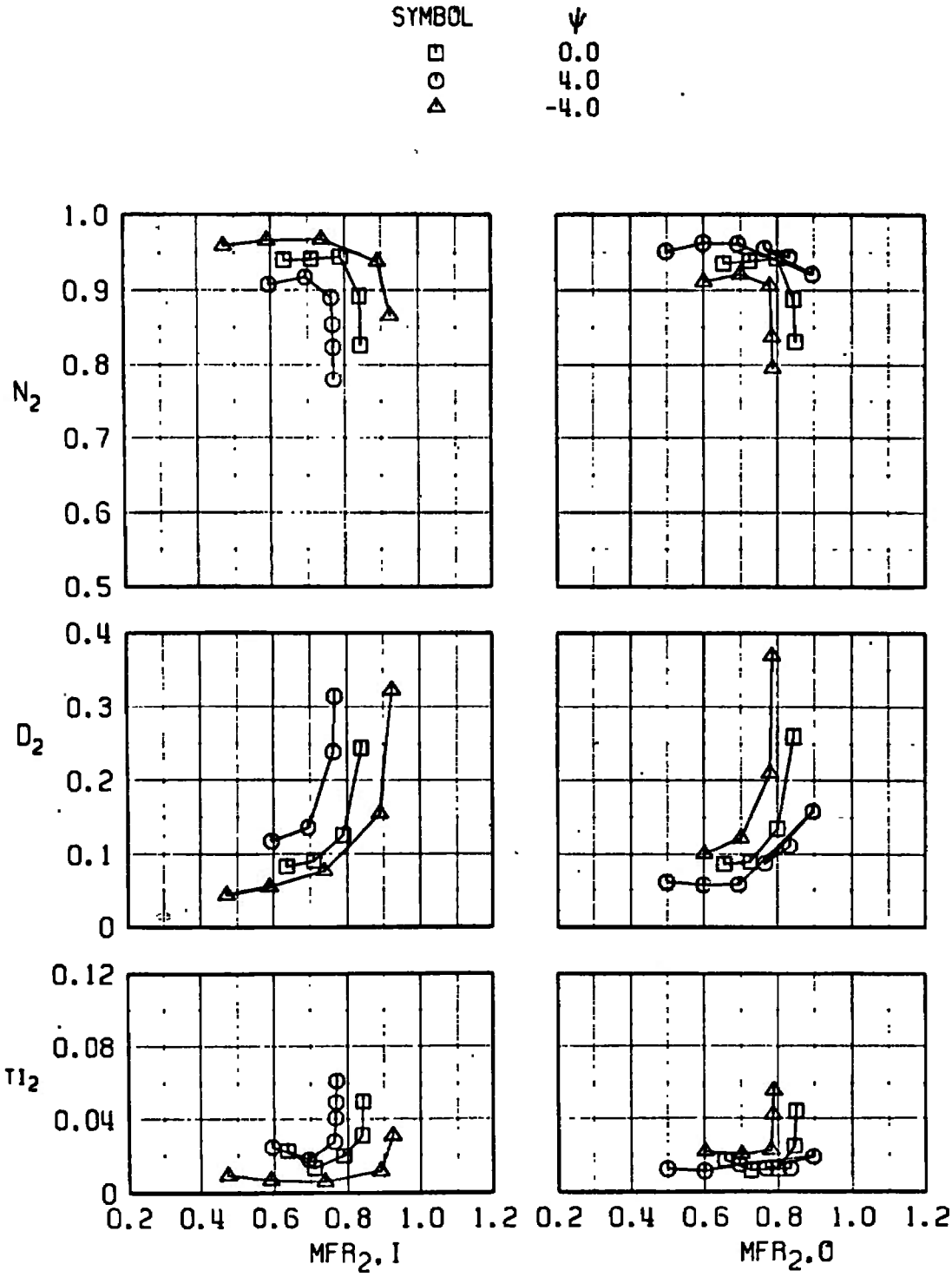

a. α = 2.5 deg

Fig. 29 Effect of Yaw Angle, M_∞ = 1.7, Scheduled R_B and TH

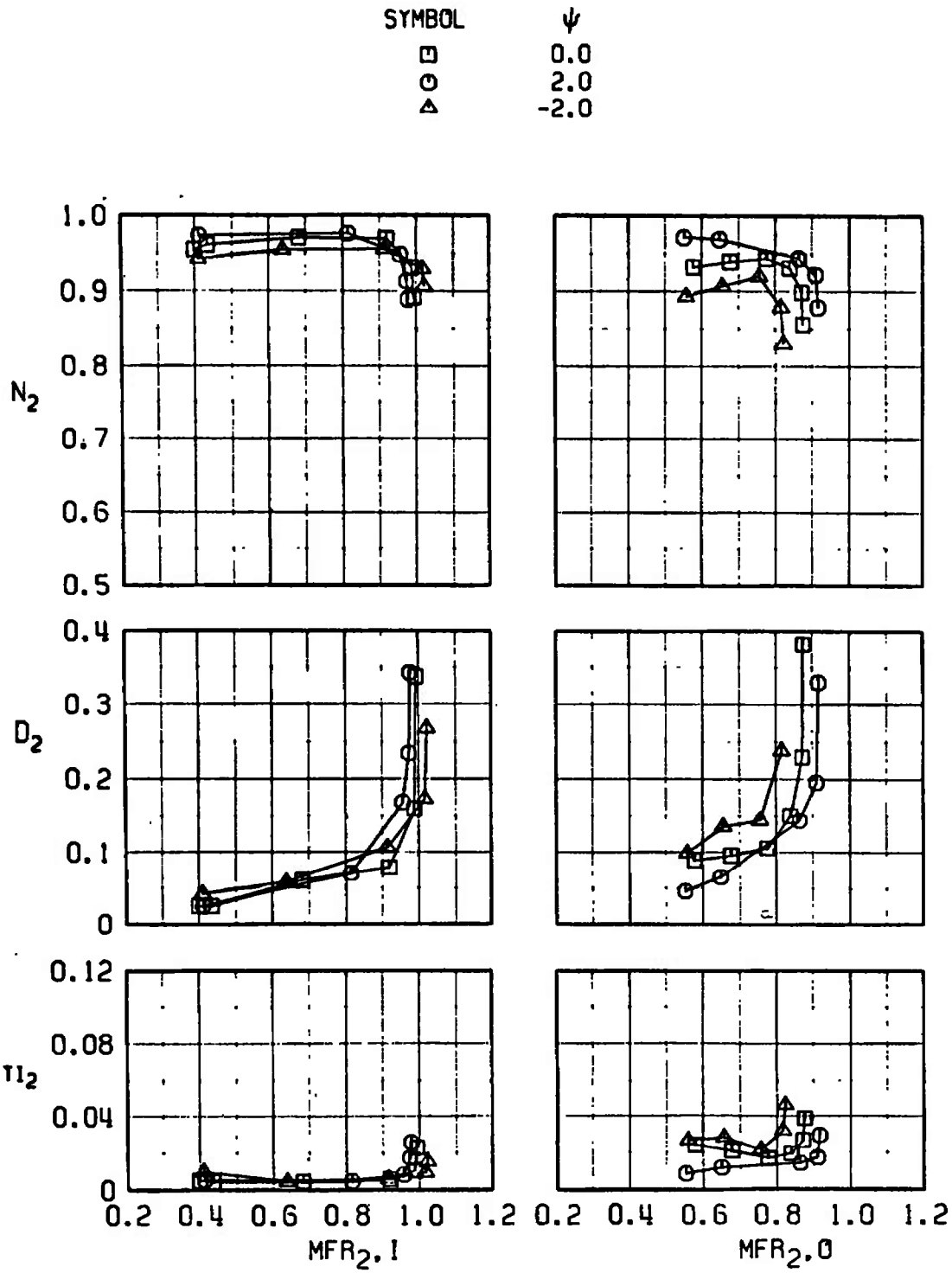

b. α = 11 deg

Fig. 29 Concluded

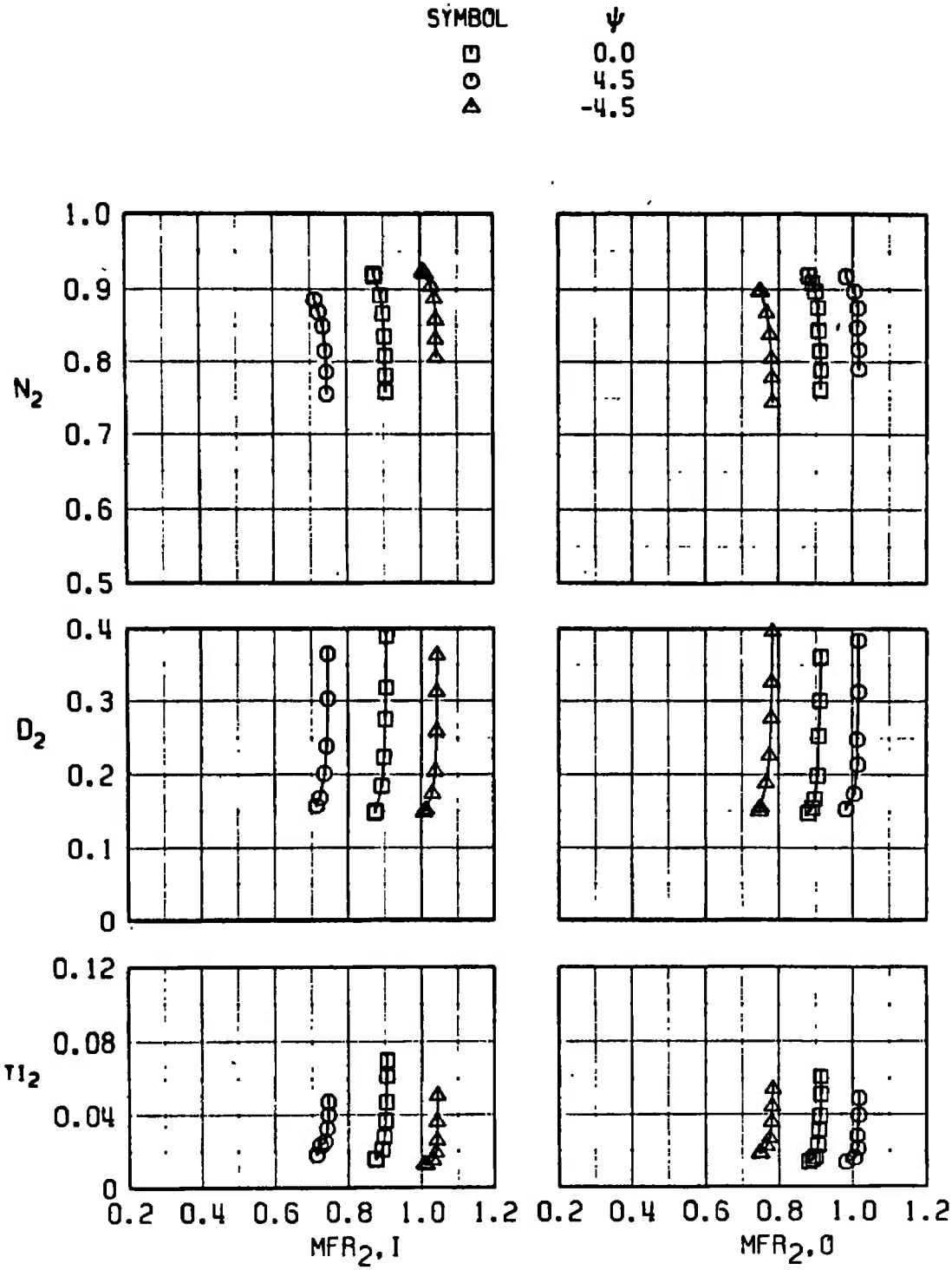

a. α = 2.5 deg

Fig. 30 Effect of Yaw Angle, M_∞ = 2.2, TH/TU = 105 percent, Scheduled R_B

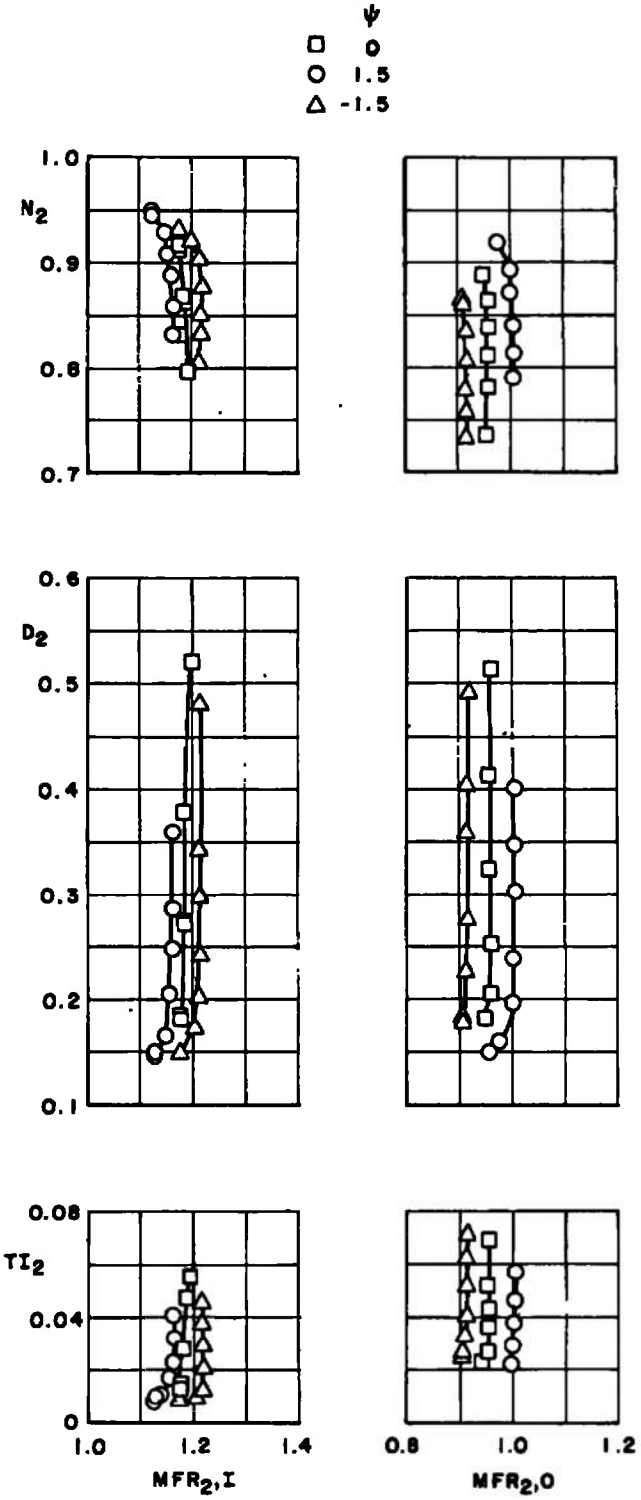

b. α = 13 deg

Fig. 30 Concluded

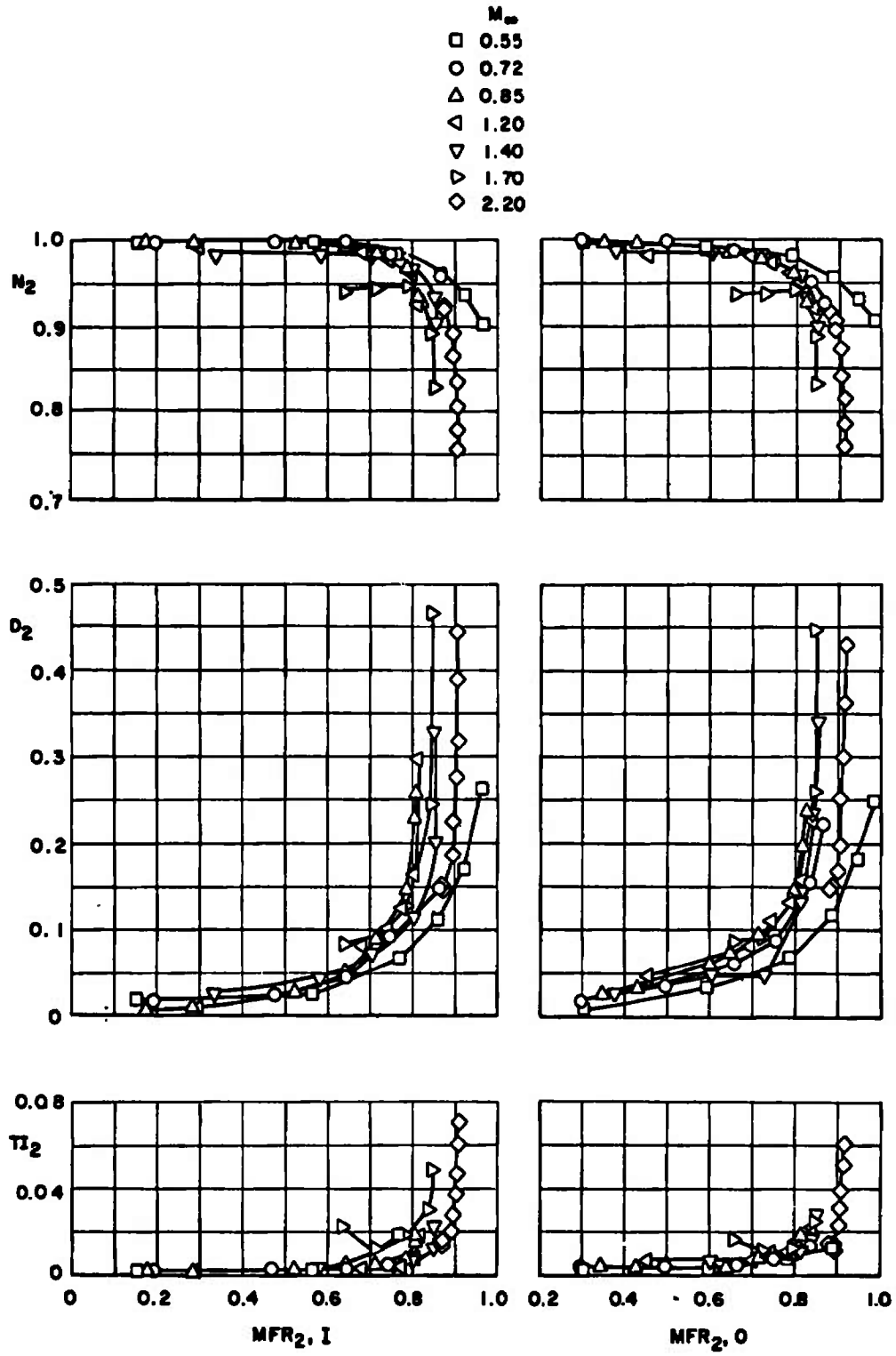

Fig. 31 Effect of Mach Number, α = 2.5 to 3 deg, ψ = 0 deg, Scheduled R_B and TH

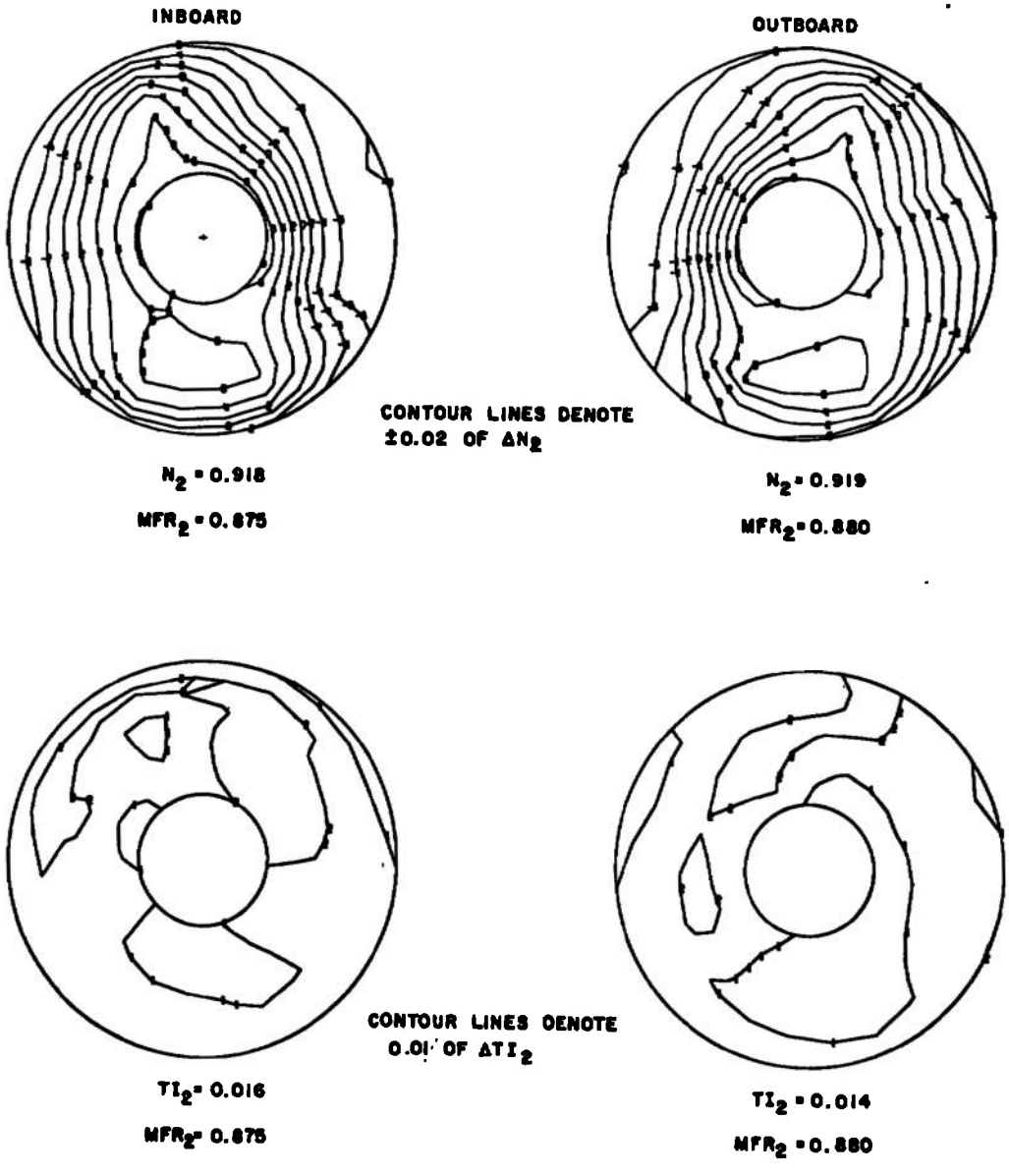

a. Critical

Fig. 32 Compressor-Face Pressure Profiles, M_∞ = 2.2, α = 2.5 deg, ψ = 0 deg, TH/TU = 105 percent, Scheduled R_B

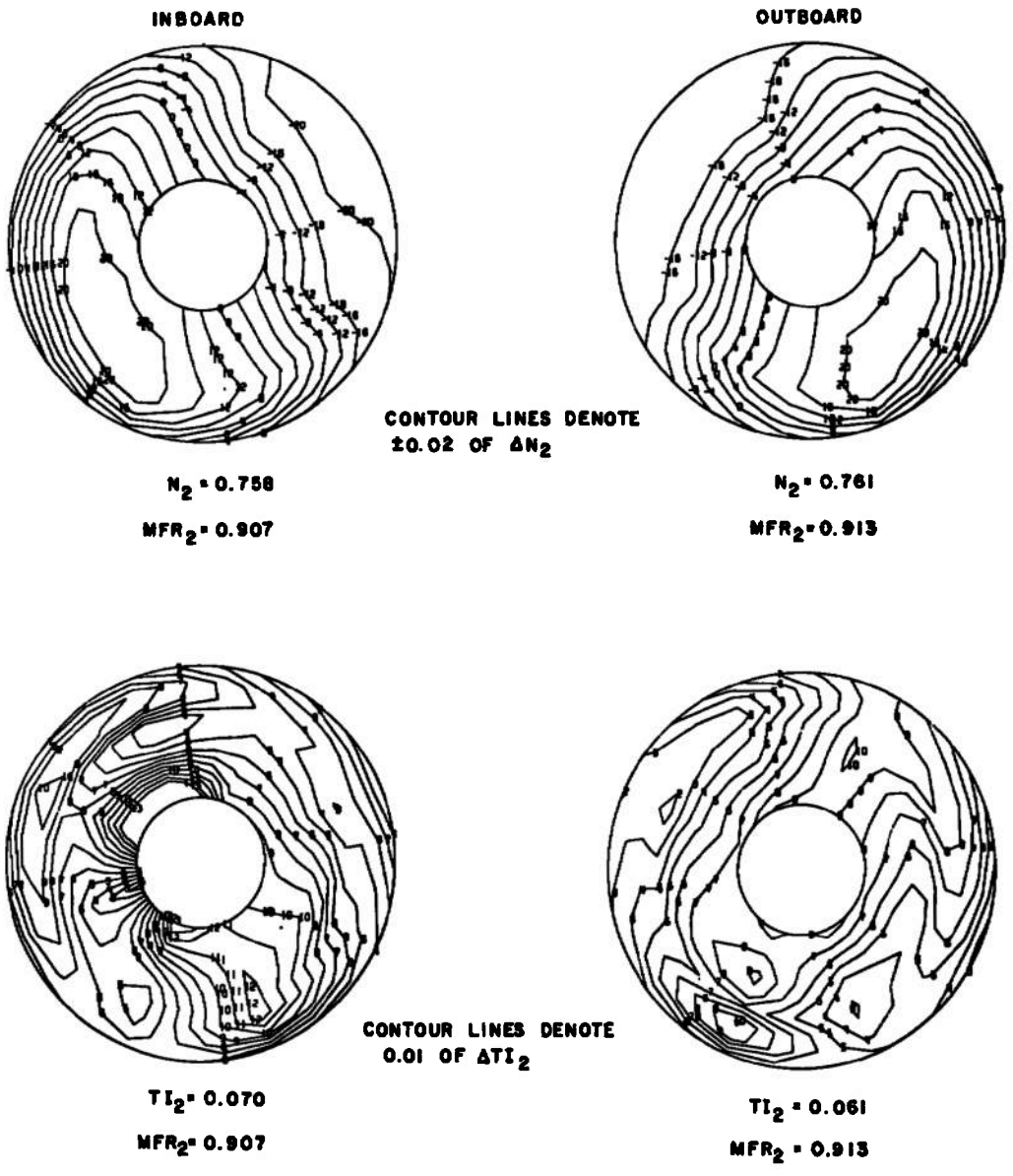

b. Supercritical
Fig. 32 Concluded

TABLE I
FIRST-RAMP MACH NUMBER SUMMARY

$M_\infty = 1.4$

ψ,deg/α,deg	-2	0	3	6	9	13	Outboard/Inboard
-4		1.234 1.000	1.297 0.847	1.400 0.769	1.524 0.704	1.705 --	O I
-2	1.144 1.179	1.165 1.133	1.198 0.920	1.285 0.809	1.421 0.739	1.617 --	O I
0	1.104 1.266	1.120 1.190	1.130 1.092	1.120 0.867	1.244 0.781	1.268 0.695	O I
2	1.056 1.344	1.072 1.267	1.092 1.162	1.086 0.946	0.943 0.822	0.863 0.726	O I
3	1.003 1.388						O I
4		0.943 1.347	0.973 1.232	0.946 1.130	0.891 0.871	0.848 0.762	O I

$M_\infty = 1.7$

ψ,deg/α,deg	-1.6	0	2.5	5	9	11	
-4			1.539 1.198	1.553 1.114	1.564 0.934		O I
-2		1.440 1.388	1.463 1.275	1.474 1.171	1.476 1.062	1.487 0.938	O I
0	1.336 1.555	1.360 1.490	1.376 1.380	1.392 1.256	1.388 1.120	1.394 1.072	O I
2		1.271 1.579	1.286 1.475	1.298 1.353	1.295 1.173	1.302 1.122	O I
4			1.200 1.565	1.210 1.449	1.205 1.249		O I

$M_\infty = 2.2$

ψ,deg/α,deg	-1.6	0	2.5	5	9	13	
-4.5			2.144 1.683	2.120 1.553	2.069 1.338		O I
-3		2.067 1.895	2.073 1.763	2.049 1.623	1.967 1.421		O I
-1.5	2.003 2.113	1.998 1.992	2.004 1.847	1.982 1.705	1.832 1.521	1.852 1.272	O I
0	1.929 2.182	1.929 2.092	1.933 1.933	1.912 1.781	1.870 1.556	1.833 1.343	O I
1.5	1.864 2.318	1.864 2.174	1.863 2.021	1.847 1.851	1.823 1.624	1.760 1.410	O I
3		1.798 2.237	1.798 2.117	1.770 1.920	1.746 1.694		O I
4.5			1.737 2.176	1.706 2.003	1.671 1.742		O I

UNCLASSIFIED

Security Classification

DOCUMENT CONTROL DATA - R & D

(Security classification of title, body of abstract and indexing annotation must be entered when the overall report is classified)

1. ORIGINATING ACTIVITY *(Corporate author)*
Arnold Engineering Development Center
Arnold Air Force Station, Tennessee 37389

2a. REPORT SECURITY CLASSIFICATION
UNCLASSIFIED

2b. GROUP
N/A

3 REPORT TITLE
RESULTS OF A 0.1-SCALE B-1 INLET MODEL TEST AT TRANSONIC AND SUPERSONIC MACH NUMBERS

4. DESCRIPTIVE NOTES *(Type of report and inclusive dates)*
Final Report - June 27 to July 20, 1971

5. AUTHOR(S) *(First name, middle initial, last name)*
F. J. Graham, ARO, Inc.

6. REPORT DATE	7a. TOTAL NO. OF PAGES	7b. NO OF REFS
October 1971	72	3

8a. CONTRACT OR GRANT NO.	9a. ORIGINATOR'S REPORT NUMBER(S)
b. PROJECT NO System 139A	AEDC-TR-71-219
c. Program Element 64215F	9b. OTHER REPORT NO(S) *(Any other numbers that may be assigned this report)*
d. Task 01A	ARO-PWT-TR-71-170

10. DISTRIBUTION STATEMENT Distribution limited to U.S. Government agencies only; this report contains information on test and evaluation of military hardware; October 1971; other requests for this document must be referred to Aeronautical Systems Division (YHT), Wright-Patterson AFB, OH 45433.

11. SUPPLEMENTARY NOTES	12. SPONSORING MILITARY ACTIVITY
Available in DDC	Aeronautical Systems Division (YHT) Wright-Patterson AFB, OH 45433

13 ABSTRACT

Results are presented of a wind tunnel investigation of a 0.1-scale model of the left-hand dual inlet air induction system of the B-1 aircraft. The test was conducted from Mach number 0.55 to 2.2 over an angle-of-attack range from -4 to 13 deg and yaw angles of -8 to 5 deg. Inlet performance in terms of compressor-face total-pressure recovery, total-pressure distortion, and turbulence index is presented as a function of inlet mass-flow ratios for various inlet geometries and model attitudes. The total-pressure recovery of the mixed-compression inlet was very good, but the total-pressure distortion at critical mass-flow ratios was higher than normally desired for satisfactory turbine engine operation. Best performance was realized with ramp and throat height schedules determined from previous testing. Effects of angle of attack and yaw were seen as general sidewash effects. The addition of canard-type fins had negligible effect on inlet performance.

Distribution limited to U. S. Government agencies only; this report contains information on test and evaluation of military hardware; October 1971; other requests for this document must be referred to Aeronautical Systems Division (YHT), Wright-Patterson AFB, OH 45433.

DD FORM 1 NOV 65 1473

UNCLASSIFIED

Security Classification

14. KEY WORDS	LINK A		LINK B		LINK C	
	ROLE	WT	ROLE	WT	ROLE	WT
B-1						
jet aircraft						
supersonic inlets						
jet engine inlets						
supersonic wind tunnels						
performance evaluation						

1. Air inlets -- Performance

AFSC
Arnold AFS Tenn